UNIVERSITÀ DI SIENA
1240

University of Siena - Department of Medical Biotechnologies
Doctorate in Genetics, Oncology and Clinical Medicine (GenOMec)
XXXIII cycle (2017-2020)
Coordinator: Prof. Francesca Ariani

CfDNA-NGS Liquid Biopsy for solid cancers and vascular malformations

Scientific disciplinary sector BIO/18 - Genetics

Tutor:

Dr. Frullanti Elisa

Ph.D. candidate:

Dr. Palmieri Maria

MARIA PALMIERI
18.11.2020
16:08:39
UTC

Academic Years: 2019/2020

Alla mia famiglia,
che mi indica la via da tutta una vita.

Al mio lui,
ormai il mio tutto.

Sistema Socio Sanitario
Ospedale Maggiore
Regione Lombardia
ASST Crema

Crema, li 10/10/2020

Dipartimento Cardiocerebrovascolare
Unità Operativa di Chirurgia Vascolare
Direttore Dr. Aldo Arzini

Largo Ugo Dossena, 2 – 26013 Crema
Telefono: 0373 280420
Mobile: 335 6060019
e-mail: aldo.arzini@asst-crema.it
e-mail: vaghim@yahoo.it

Sito Internet: www.asst-crema.it

Ufficio relazioni con il pubblico
ASST Crema

Corrections Chap 1.5

- 1According to the presence or absence of endothelial mitotic activity . Vascular malformation derive from errors in the first weeks of development of the embryo (angiogenesis) and in later phase of the vessel formation (vasculologenesis)
- 2According to the evolution of the therapy of vascular anomalies which is progressively becoming more endovascular than surgical we presumed that the examination of a blood specimen taken during vascular catheterism might give some information which could replace biopsies. In n cases of huge a-v shunts, intraosseous malformations , biopsies might be dangerous. But would it work? The most involved cells are endothelial cells and supportive cells which all are in contact with blood flow. We can assume that the death rate of these cell should be lower than that of neoplastic cells and for this reason we have chosen to take blood specimen as close as possible to the vascular lesion.

Vascular tumors classification

Tumor histological entity	Benign	Local aggressive and borderline	Malignant
Tumor type and subtype	infantile hemangioma congenital hemangioma rapidly involuting hemangioma (RICH) partly involuting hemangioma (PICH) non-involuting (NICH) spindle cell hemangioma epitheloid cell hemangioma lobular capillary hemangioma tufted angioma	kaposiform hemangioendothelioma retiform hemangioendothelioma papillary intralymphatic angioendothelioma composite hemangioendothelioma kaposi sarcoma	angiosarcoma epitheloid hemangioendothelioma

Vascular malformation classification

Flow component	Vascular component	Clinical malformation
Slow flow	Capillary malformation	CM cutaneous/mucosal ("port wine stain") ▪ CM with soft tissue and/or bone overgrowth ▪ CM with central nervous system and/or ocular anomalies (sturge-weber syndrome) ▪ CM with arterio-venous malformation (CM-AVM) ▪ teleangiectasia in hereditary hemorrhagic teleangiectasia (HHT) ▪ cutis marmorata telangiectatica congenita (CMTC) ▪ naevus simplex (stork bite, angel kiss)
Slow flow	Lymphatic malformation	CM cutaneous/mucosal ("port wine stain") ▪ CM with soft tissue and/or bone overgrowth ▪ CM with central nervous system and/or ocular anomalies (sturge-weber syndrome) ▪ CM with arterio-venous malformation (CM-AVM) ▪ teleangiectasia in hereditary hemorrhagic teleangiectasia (HHT) ▪ cutis marmorata telangiectatica congenita (CMTC) ▪ naevus simplex (stork bite, angel kiss)
Slow flow	Venous malformation	common VM ▪ glomovenous malformation (GVM) ▪ blue rubber bleb naevus VM syndrome ▪ cutaneo-mucosal VM (VMCM)
Fast flow	Arterio venous malformation	sporadic AVM ▪ AVM in HHT
Fast flow	Arteriovenous fistula	sporadic AVF ▪ AVF in HHT
Combined vascular malformation		
slow flow	CM VM	Capillary venous malformation
Slow flow	CM LM	Capillary lymphatic malformation
Fast flow	CM AVM	Capillary artero venous malformation
Slow flow	LM VM	Lymphatic venous malformation
Slow flow	CM LM VM	Capillary lymphatic venous malformation
Fast flow	CM LM AVM	Capillary lymphatic arterio venous malformation
Fast flow	CM VM AVM	Capillary venous arterio venous malformation
Fast flow	CM LM VM AVM	Capillary lymphatic venous arterio venous malformation

Vascular malformation associated with other anomalies

Slow flow	CM VM LM	With limb overgrowth Klippel Trenaunay syndrome
Fast flow	CM AVF	With limb overgrowth Parkes weber syndrome
Slow flow	Limb VM	With limb overgrowth Servelle Martorell syndrome
Slow flow	Limb VM	With congenital limb hypertrophy
Slow flow	VM	With /without spindle cell hemangioma and encondroma (maffucci syndrome)
Slow and fast flow	LM VM CM. AVM	With lipomatous overgrowth Sindrome di Cloves
Slow flow	CM VM LM	With asymmetric somatic overgrowth (Proteus)
Fast Flow	AVM VM	With macrocephaly and lipomatous overgrowth (PTEN hamartoma syndrome

ISSVA genetic classification of vascular anomalies (2014)

"Vascular anomaly	Gene/locus	Location	Inheritance
Capillary/venulocapillary malformation			
Sturge-Weber syndrome (leptomeningeal and cutaneous venulocapillary malformation, aka "port-wine stain")			
	a. GNAQ	9q21	Somatic
Non-syndromic port-wine stain			
	b. GNAQ	9q21	Somatic
Arteriovenous malformations			
Capillary malformation-arteriovenous malformation (CM-AVM)			
	*RASA1	5q14.3	AD
Parkes Weber syndrome			
	*RASA1 (in subset)	5q14.3	AD
Hereditary hemorrhagic telangiectasia			
HHT1	*ENG	9q34.11	AD
HHT2	ACVRL1/ALK1	12q13.13	AD
HHT3	Unknown	5q31.3-q32	AD
HHT4	Unknow	7p14	AD
Juvenile polyposis/HHT syndrome (JP/HHT)			
	*SMAD4	18q21.2	AD
HHT5/atypical HTT	*BMP9/GDF2	10q11.22	Association only
HBT	Unknown	CMC1/5q14	Association only
Angiokeratoma			
Fabry disease	*GLA	Xq22.1	XD
Progressive patchy capillary malformations			
Angioma serpiginosum	Unknown	Xp11.3-Xq12	Association only
Familial cerebral cavernous malformations (CCM)			
CCM1	*KRIT1	7q21.2	AD
CCM2	*Malcavernin/CCM2	7p13	AD
CCM3	*PDCD10	3q26.1	AD
CCM4	Unknown	3q26.3-27.2	

Venous malformations

Sporadic Venous malformations (VM)

	*TEK/TIE2	9p21.2	Somatic

Familial venous malformations cutaneous-mucosal (VMCM)

c.	TEK/TIE2	9p21.2	AD

Glomuvenous malformation (GVM)

	*Glomulin/GLMN	1p22.1	AD

Verrucous venous malformation (VVM)/verrucous hemangioma

	MAP3K3	17q23.3	Somatic

Lymphatic malformations, lymphedemas, and complex syndromes

CLOVES	*PIK3CA	3q26.32	Somatic

Klippel-Trenaunay syndrome (KTS)

d.	PIK3CA	3q26.32	Somatic

Fibro-adipose vascular anomaly (FAVA)

	*PIK3CA	3q26.32	Somatic

Macrocephaly-capillary malformation

	PIK3CA	3q26.32	Somatic

“Microcephaly-capillary malformation (MICCAP)

	*STAMBP	2p13.1	AR

Nonne-Milroy syndrome

	*FLT4/VEGFR3	5q34-35	AD/AR

Primary hereditary lymphedema (Nonne-Milroy-like syndrome)

	*VEGFC	4q34	AD

“Hypotrichosis lymphedema telangiectasia (HLT)

e.	SOX18	20q13.33	AD/AR

Primary hereditary lymphedema

f.	GJC2/Connexin 47	1q41-42, 4q34	AD

Lymphedema distichiasis

g.	FOXC2	16q24.1	AD

Primary lymphedema with myelodysplasia (Emberger syndrome)

h.	GATA2	3q21.3	AD

Primary generalized lymphatic anomaly (Hennekam syndrome)

i.	CCBE1	18q21.32	AR

Microcephaly with or without chorioretinopathy, lymphedema, or mental retardation syndrome

j.	KIF11	10q23.33	AD

Lymphedema-choanal atresia

k.	PTPN14	1q41	AR

Proteus syndrome

l.	AKT1	14q32.3	Somatic

PTEN hamartoma tumor syndrome (PHTS)

Bannayan-Riley-Ruvalcaba syndrome (BRRS)

m.	PTEN	10q23.3	AD

Cowden syndrome (CS)/Cowden-like syndrome			
	*PTEN, *SDHB, *SDHD, KLLN	10q23.3	AD
“Proteus-like” syndrome			
	*PTEN	10q23.3	AD
PTEN-related Proteus syndrome (PS)			
	*PTEN	10q23.3	AD

”

Massimo Vaghi

VAGHI
MASSIMO
10.10.2020
16:03:30
UTC

DBM
Dipartimento
Biotecnologie Mediche

Maria Palmieri <maria.palmieri@dbm.unisi.it>

Re: thesis review

4 messaggi

Jose Luis Costa <jcosta@ipatimup.pt> 5 ottobre 2020 15:12
A: Maria Palmieri <maria.palmieri@dbm.unisi.it>
Cc: Elisa Frullanti <elisa.frullanti@dbm.unisi.it>

Dear Maria,

Here you have my comments. It needs language correction on the abstract and discussion. You might want to ask a collegue to review the english.
Concerning the thesis document, what is the title?
Overall I do understand the focus on liquid biopsy. I must say your work was the first I saw on the use of liquid biopsy for somatic muations detection in genetic malformation syndormes. You should highlight this. It is highly novel. In contrast, the work on cancer patients is thin compared to the large works already published.
It is the first time I see a thesis in this format, there are formating aspect that you may want to check.

I hope this is what you were expecting from my side.

Kind regards,

Jose

Jose Luis Costa, PhD

UNIVERSITÀ
DI SIENA
1240

Dipartimento di Biotecnologie Mediche

Siena,12th November 2020

To Whom It May Concern,

In accordance of what required by Prof. Costa I corrected the grammatical errors and I highlighted the novel aspects about the use of liquid biopsy in vascular malformations.

In accordance of what required by Dr. Vaghi I expanded the introduction with major focus on angiodysplasias and I added the entire classification of vascular malformations provided by the ISSVA.

The thesis has been sanded back to the reviewers after the corrections in the current version.

Maria Palmieri

PhD Student
DOCTORATE in
GENETICS, ONCOLOGY and CLINICAL MEDICINE (GenOMec)

Dipartimento di Biotecnologie Mediche
Genetica Medica
Policlinico Santa Maria alle Scotte (I piano III lotto), V.le Bracci, 2 – 53100 Siena (Italia)
Tel. +39 0577 233303 Fax +39 0577 233325 – http://www.biotecnologie.unisi.it/sezione.php?sez=5
CF 80002070524 P.IVA 00273530527

INDEX

Abstract **1**

1 Introduction **2**

1.1 Liquid biopsy 2

1.2 Circulating cell-free DNA 3

1.3 Clinical Application of liquid biopsy in cancers 6

1.4 Tumor heterogeneity and therapy selection 9

1.5 Vascular malformations and liquid biopsy 10

1.6 Aim's project 17

2 Materials and methods **18**

2.1 Patient samples collection 18

2.2 Cell-free Plasma Isolation 18

2.3 Cell-free Nucleic Acid Isolation 19

2.4 cfDNA quantity check 20

2.5 cfDNA quality check 20

2.6 Library preparation 21

2.7 Library quality check 22

2.8 Library qPCR quantification 22

2.9 Ion Proton™ Sequencing 23

2.10 Sequencing Analysis 25

2.11 Cell-free Nucleic Acid Isolation 27

2.12 Preparation of sequencing libraries 27

2.13 Illumina NextSeq 550 Sequencing 28

2.14 Sequencing Analysis 29

3 Results **30**

3.2 PIK3CA-CDKN2A clonal evolution in metastatic breast cancer and multiple points cell-free DNA analysis 30

3.3 Two-point-NGS analysis of cancer genes in cell-free DNA of metastatic cancer patients 34

3.4 A pilot study of next generation sequencing-liquid biopsy on cell-free DNA as a novel non-invasive diagnostic tool for Klippel-Trenaunay syndrome 44

3.5 MET somatic activating mutations are responsible for lymphovenous malformation and can be identified using cell-free DNA next generation sequencing liquid biopsy 51

3.6 Cell-free DNA next-generation sequencing liquid biopsy as a new revolutionary approach for arteriovenous malformation 56

4 Discussion and Conclusion **61**

4.1 Discussion 61

4.2 Conclusion 63

5 Bibliography **64**

Abstract

The liquid biopsy is a new emerging and repeatable low risky approach able to detect drive mutations that characterize the tumor, to monitor cancer evolution over time, and to overcome the standard tissue biopsy limits. The biomarker par excellence is the circulating cell-free DNA (cfDNA) that was the principal leading actor of this study.

The scope of this study was to perform different liquid biopsy analysis both in metastatic cancer and in vascular malformations patients to detect, from a precision medicine perspective, the sniper clone responsible for the tumor evolution or the vascular malformations.

The cfDNA was extracted from plasma coming from peripheral and/or efferent vein of vascular malformation. The obtained cfDNA was used to perform the libraries using two different genes panel of 52 and 77 cancer-driver genes, respectively the Oncomine™ Pan-Cancer Cell-Free Assay and AVENIO ctDNA Expanded Kit.

The most frequent mutations that we found in metastatic patients were the SNV in *TP53*, follow by *PIK3CA*, *KRAS*, and CNV in *FGFR3*. In the majority of cases, the mutations found at first liquid biopsy were confirmed by an increased allele frequency at the second one.

In vascular anomalies affected patients, the *PIK3CA*, *MET*, and *KRAS* mutated genes were found in Klippel-Trenaunay syndrome, in lymphovenous malformations, and in artero-venous malformations respectively, with a very low allele frequency percentage.

In conclusion, repeated analysis of liquid biopsy lead to the identification of key cancer genes and the following of clonal evolution over time. Moreover, the liquid biopsy is suitable not only for cancer patients but also for the diagnosis of vascular malformation. Our data prove that in the new era of precision medicine, this novel approach, based on the combination of NGS and liquid biopsy from the efferent vein at the vascular malformation site, allows to detect even low-grade somatic mosaicism responsible for the vascular phenotype. This approach let to bypassing the need for a highly risky tissue biopsy and lead to a tailored personalized treatment.

1 Introduction

1.1 ***Liquid biopsy***

It has long been known that the conventional setting of "one size fits all" cancer treatment is not beneficial in most patients due to inter and intra-tumor heterogeneity. For this reason, the emerging precision medicine for cancer treatment able to provide "the right treatment for the right patient at the right time" is needed. In this scenario, thanks to Next-Generation Sequencing (NGS) technology, a new technique is gaining importance and could make possible to achieve the goal of precision cancer medicine: the liquid biopsy [1].

In the last decades, it has been studied that during the tumor progression, an active or passive intratumoral escape of cellular components occurs [2]. The liquid biopsy refers to isolation and analysis of this material derived from the tumor. It begins to be increasingly applied as it represents a minimally invasive tool that offers the possibility of capturing the tumor molecular characteristics and its evolution in real-time [3].

These tumoral components include intact circulating tumor cells (CTCs) that intravasate into the bloodstream at low frequency and can be isolated from a background of healthy blood cells. Tumor cells also release subcellular particles, the exosomes, or extracellular membrane-encased vesicles that contain tumor-specific proteins and nucleic acids. Moreover, it is possible to isolate circulating cell-free nucleic acid derived from tumor cells, including microRNAs (miRNAs), non-coding RNA, cfRNA (less stable), and cfDNA [4] *Figure 1*.

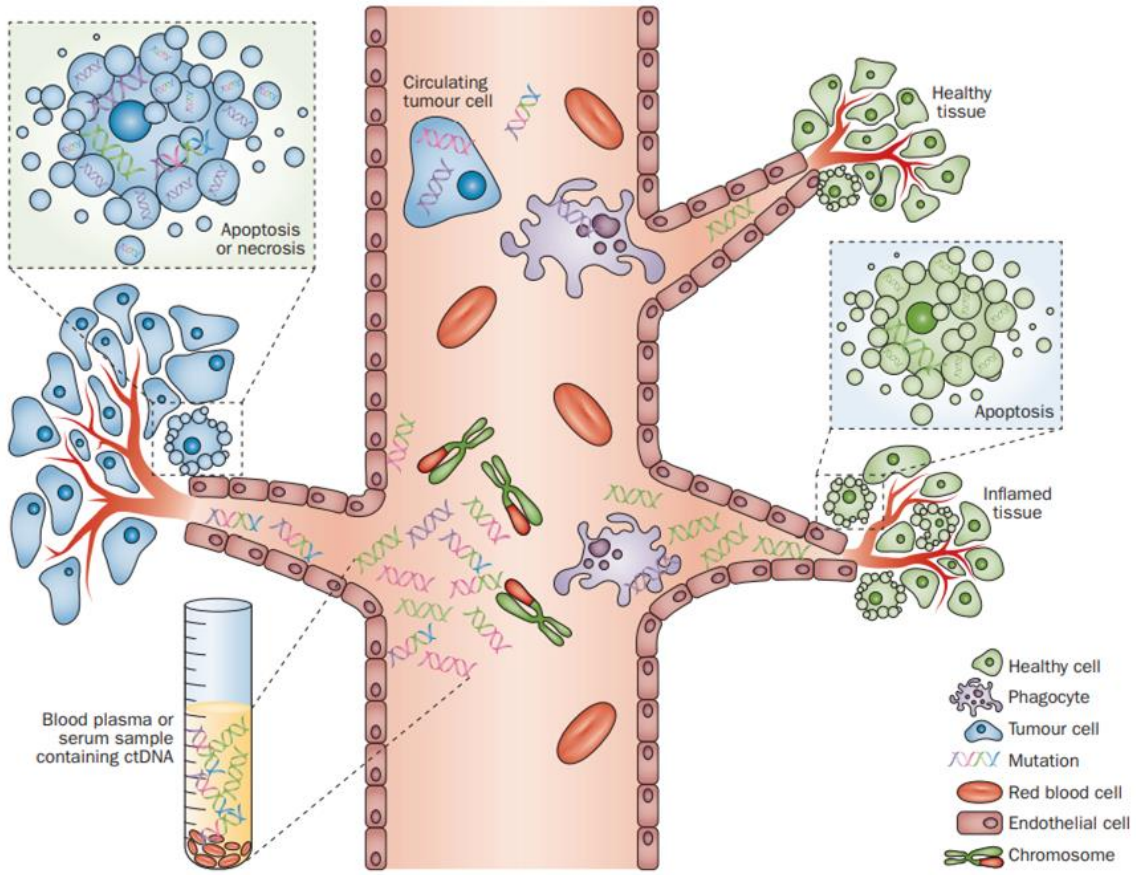

Figure 1. Release and extraction of cfDNA from the blood. cfDNA is released from healthy, inflamed or diseased (cancerous) tissue from cells undergoing apoptosis or necrosis [5].

During my Ph.D research work, I focused on the analysis of tumoral cfDNA, which is the most studied and relevant biomarker analyzed through liquid biopsy approach. The cfDNA can come from several different fluids for specific tumor types such as blood, saliva, urine, stool, cerebrospinal fluid (CSF), pleural fluid, and ascites [6]. Among them, blood is the most utilized one [7].

1.2 ***Circulating cell-free DNA***

First reported by Mandel and Metais in 1948, the cfDNA represented the fragmented DNA found in the non-cellular component of the blood [8]. The discovery of circulating cell-free DNA (cfDNA) remained obscure for several years until scientists observed differences between the characteristics of cfDNA from healthy and diseased individuals. Several studies have reported increased concentrations and cancer-associated mutations of cfDNA in cancer patients [9], [10], [11].

In 1997 was found out the presence of circulating fetal DNA in maternal plasma and serum in pregnant women, and this discovery had important clinical implications for the non-invasive prenatal test [12].

CfDNA is generally found in the bloodstream as double-stranded fragments of about 150 to 200 base pairs in length. The fragments are often associated with histone proteins; this explains the typical cfDNA length, which is rapidly cleared, having a half-life of an hour or less [13]. In healthy persons, the cfDNA released from cells in the blood is very low (~10 to 15 ng per mL), while it ranges between 0-5 and >1000 ng/ml in patients with cancer. However, a high level of cfDNA is not always specific to tumor presence *Figure 2.*

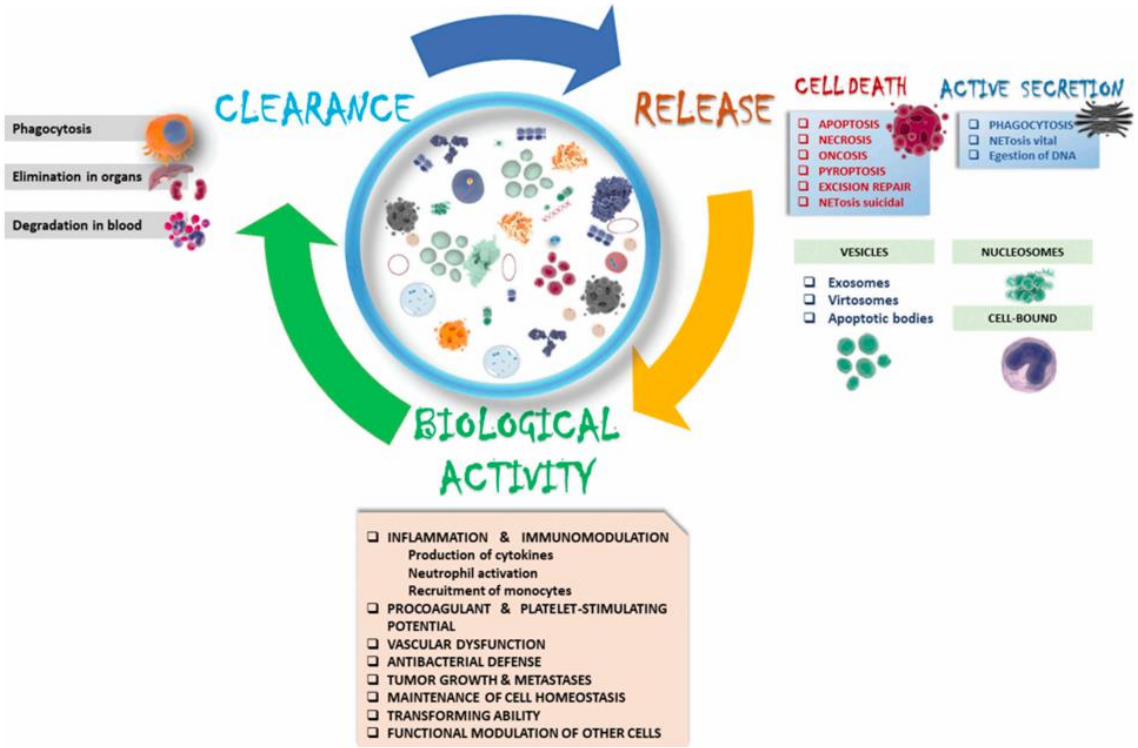

Figure 2. The figure lists the three main fases of cfDNA life cycle [13].

The cfDNA high concentration in the blood is frequently due to detected under tissue stress, pregnancy, inflammation, diabetes, injury conditions, or sepsis [6]. Other mechanisms, including phagocytosis, pyroptosis, and active secretion, may contribute to cfDNA release. Although the exact mechanism responsible for the active release of cfDNA remains not clear, it could be a consequence of genomic instability [13].

In cancer patients, the cfDNA is released from tumor cells as circulating tumor DNA (ctDNA); it is highly fragmented DNA with a short half-life in the blood (~ 2.5 h) and

represents the only 0.1% of the overall cfDNA [6]. The ctDNA can be specially distinguished from cfDNA by specific molecular characteristics such as variants, copy number variations, methylation, and amplifications or deletions associated with tumor [14].

Of course, the ctDNA can come from both primary and metastatic sites since cancer cells closely interact with vascular cells and release DNA into the bloodstream. ctDNA can also be released through other mechanisms, such as that implemented by migrant cancer cells called CTC. These cancer cells can enter into the bloodstream directly, but they are not the only ones, as there are cancer cell exosomes [15] that contribute to the release of ctDNA [13]. The origin and process by which tumor DNA is released and enters circulation have been extensively studied, and to date, we are aware of several mechanisms [16].

Growing tumors have been shown to experience periods of apoptosis or heightened necrosis that is responsible for ctDNA release. Apoptosis seems to produce shorter cfDNA fragments with lengths of approximately 150-200 bps, while necrosis seems to produce larger cfDNA fragments, up to thousands of base pairs [17].

Furthermore, it has also been shown that the ctDNA released by cultured cancer cells is related to the percentage of cells in phase G1. An increase in the release of ctDNA by differentiated cells suggests the hypothesis of an active release of nucleic acid enclosed within exosomes, which well protects it from blood degradation [18].

In healthy people, the release of cfDNA from the normal apoptotic process is well controlled, and the rapid elimination of nucleic acid explains the low amount of cfDNA detectable in the blood. On the other hand, in patients suffering from tumors, chronic inflammation, and excessive cell death, the clearance is overloaded and not sufficient, resulting in an accumulation of cfDNA in pathological conditions [19].

Besides the elimination of ctDNA from the bloodstream through clearance mechanisms, it has been reported that other cells in the body might uptake cfDNA circulating in blood performing horizontal gene transfer that can result in alterations in the recipient host cells. This process could be a key event in the initiation of molecular metastasis of the tumor [20].

Moreover, ctDNA amount is notably variable among patients depending on the type and the stage of the tumor [21] suggesting a correlation with tumor burden (primary tumor and all metastasis), biological features [6], and cancers aggressivity [7]. Notably, cfDNA levels have also been correlated with the outcome and survival of cancer patients: increased amount seems to associate with a poorer prognosis [22].

However, in some cases, the release of ctDNA may be limited by the presence of physiological barriers such as the blood-brain barrier or capsules surrounding some organs, and this affects the distribution of cell-free DNA derived from the tumor [23].

1.3 ***Clinical Application of liquid biopsy in cancers***

So far, tissue biopsy represents the gold standard for tumor analysis and the histological features are the basis for conventional pathological diagnosis of cancer; Nevertheless, the morphological classification, immunohistochemical subclassification, and microscopic tissue pattern are not sufficient to predict the treatment response and the development of the disease.

Nowadays, for patient management and treatment decisions, the analysis of cancer genetic alterations is crucial also in the advancements of precision medicine genotype-directed therapy that is becoming a standard approach. Notwithstanding, knowledge of cancer and its mutational profile assessment performed using a primary tumor fragment or metastases have several limitations [24].

First, tissue biopsies oblige an invasive surgical intervention, which may not always be feasible, determined by tumor localization and the accessibility of tumor tissue. Furthermore, the analysis of a single tissue biopsy might not be representative of the malignancy due to intra and inter-tumor heterogeneity, the clonal evolution of the disease over time, and in response to therapy.

A further limitation of the tissue biopsy is the almost impossibility of obtaining tissue samples repeated over time, especially for those tumors that are housed in anatomical areas, which are difficult to reach. Furthermore, the recurrence and the appearance of drug resistance are also difficult to cope with the only tissue biopsy [2], [4]. Whereas liquid biopsy is considered a minimally invasive repeatable test that represents a fitting approach to following the tumor evolution. Serial blood withdrawal can be easily obtained, providing a dynamic assessment of cfDNA and its variations [6], [25].

In particular, it has been shown that ctDNA analysis allows dynamic monitoring (real-time) of cancer evolution, response to therapy, resistance appearance, minimal residual disease (MRD), and relapse. Indeed, some studies highlighted that ctDNA levels upturn immediately after treatment, as tumor cell death leads to increased release of ctDNA and decreases within some weeks to months in patients responding to therapy [26].

Moreover, relevant findings reveal that liquid biopsy can find alterations of resistance not captured by the single lesion tissue biopsy also while the patient is still responding to the

therapy, predicting in this way the timing and the cause of the treatment failure [27], [28]. Following this evidences, the liquid biopsy gives the possibility of earlier therapeutic intervention and improved clinical outcomes [29].

Several studies illustrate how the analysis of ctDNA could identify the minimal residual disease (MRD) in breast, lung, and colon cancer patients after the surgery or the local therapy indicating that the postoperative ctDNA detection might be a valid biomarker to select patients who need to receive adjuvant therapy and spare patients who have been completely cured [30], [31].

Potentially, another appealing application of liquid biopsy could be early cancer detection using a simple blood test for screening a healthy, asymptomatic population [4]. However, a highly sensitive method, able to detect trace amounts of cfDNA released by precancerous lesions or early-stage cancers, and high specificity would be required to screen the unaffected population [6].

In this new revolutionary approach liquid biopsy is an emerging, non-invasive technique that provides more accurate and easy representations of disease biology, giving the possibility to overcome tissue biopsy and imaging limitations [25] as summarized in *Table 1* [32].

Table 1. Advantages of liquid biopsy over tissue biopsy

	Liquid biopsy	Tissue biopsy
Clinical sample	Blood	Affected tissue
Risk	Minimal risk/pain	Risk depends on the location of tumor
Ease of collecting sample	Quick	Depends on the location of the tumor. Some tumors are hard to reach.
Ease of monitoring patients	Simple blood test	No repeatable surgeon. Surgeon may not know where to look for metastatic tumor
Invasive	Minimally invasive	Invasive
Time for patient recovery	Quick; does not require hospitalization	Time intensive; it requires hospitalization of patients

Liquid biopsy represents an attractive and essential alternative method aiming to overcome the limits of the typical tissue biopsy and imaging detection methods providing a more accurate representation of the disease. The liquid biopsy approach can show the total heterogeneity of the tumor mass(es) and the clonal selection process, to intercept the onset of disease relapse or resistance to therapy, possibly predicting treatment response and prognosis and managing therapy decisions [4], [7].

In particular, the analysis of the circulating tumor DNA demonstrates massive potential as a biomarker in oncology representing a new point towards the use of molecular methods for the development of inclusive clinical tests based on the concept of non-invasive personal and precision medicine for cancer treatment [16]. Its validity has been demonstrated by numerous studies that showed high concordance rates of 80% to 90% between the mutational profile established through cfDNA testing and the mutational profile resulting from a tumor biopsy,

which remains the normality of care, making liquid biopsy, particularly cfDNA analysis, an attractive implement [6].

To achieve efficient clinical treatment, it would be crucial to work on the standardization of both pre-analytical and analytical procedures for all liquid biopsies components. These procedures include the choice of blood collection tubes, the time allowed between blood draw and plasma processing, the isolation/extraction of liquid biopsy components, and also their characterization and quantification [4].

Moreover, the small fraction of ctDNA within the background of non-tumoral cfDNA in cancer patients and the short half-life of tumor-derived DNA represent challenging issues [6]. However, recently improved technologies such as NGS and ddPCR facilitated the liquid biopsy analysis approach [19]. Additionally, there are still numerous open questions concerning cfDNA subtypes, mechanism of release, and its clearance in patients with cancer.

1.4 ***Tumor heterogeneity and therapy selection***

The mutational profile and the behavior of cancer change in time and space: tumor tissues reveal significant variation in morphology, cellular composition, and genetic features within different regions of the same tumor. Additionally, in the case of metastatic cancer, metastases present further differences. Moreover, the tumor develops dynamically, showing additional or completely deviant features during its clinical progress [33].

Generally, studies associated to the ctDNA analysis have demonstrated that the generated mutational profile reflects the same somatic alterations found in patient cancers' and it is possible to capture mutations absent in the first tissue biopsy [34], [35]. The evaluation of the mutational status is strongly necessary for targeted therapies valid only when specific pathways are altered in the tumor cells. Tissue biopsies do not consider tumor heterogeneity, bias, and errors that can affect the selection and efficacy of personalized treatment.

The release of ctDNA from all tumor cells reflects the heterogeneity of the tumor, leading to the use of these therapies, which represent an excellent diagnostic tool and allow for a strong stratification of therapy [16].

Levels of cfDNA have been shown to vary greatly between patients with different types of cancer and between patients with benign lesions or with early-stage cancer, who show lower amounts of cfDNA than patients with advanced or metastatic cancer [21]. The variability is also given by its interactions with the microenvironment as well as by the rate of cell death and proliferation [13]. High cell proliferation rates are often associated with local overgrowth and,

consequently, elevated oxygen and nutrient consumption that leads to hypoxia and tissue necrosis *Figure 3*.

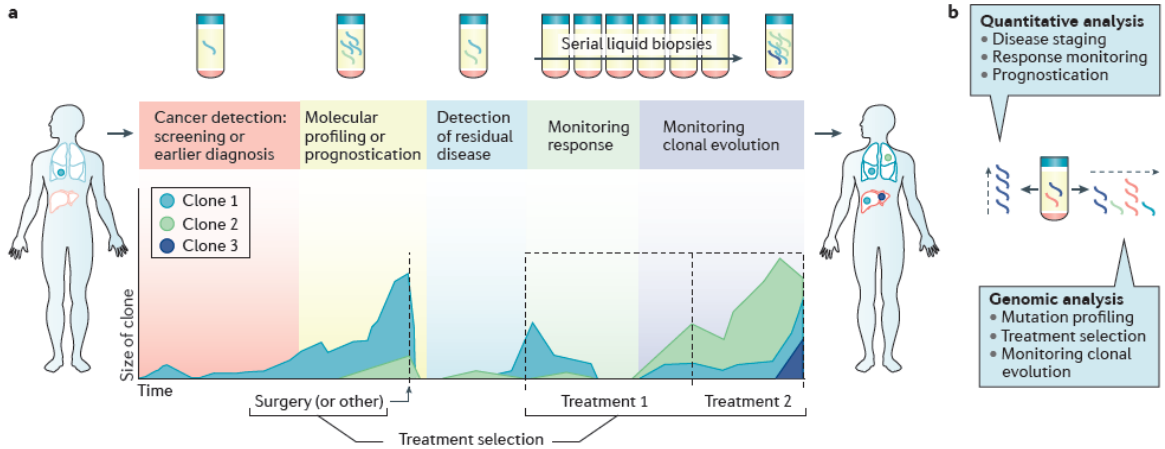

Figure 3. Application of circulating tumor DNA analysis during the course of disease and treatment administration.
a. In the image are indicated the potential applications of liquid biopsies during care of a patient who undergoes surgery (or other initial treatment), has a disease relapse and consequently receives systemic therapy: the patient starts with one single clone, but multiple metastases and distinct clones (depicted in different colors) emerge following treatment.
b. ctDNA give both quantitative information (that is, relating to tumor burden and allow disease staging and prognosis) and genomic information that is useful for the selection of therapies. Therefore, longitudinal analysis allows to monitor treatment response and by comparing genomic profiles over time, clonal evolution may be monitored [20].

Moreover, most tumor tissues are preserved in formalin-fixed, paraffin-embedded (FFPE) blocks for pathological interpretation and staining. However, this process crosslinks and fragments DNA, putting at risk their structural integrity, thus, introducing challenges for sequencing and interrogating genomic alterations [29].

1.5 ***Vascular malformations and liquid biopsy***

The vascular malformations are due to errors that occur at the embryological level. They are very complex and the first classification was made by Glowacki and Mulliken in 1982 based on biological features such as histology and histochemistry [36]. In 1988, a classification on the morphological basis was accepted and subsequently, in 1996, accepted by the International Society for the Study of Vascular Anomalies (ISSVA) in Rome in which the malformations were divided into tumors and vascular malformations.

The classification system was further expanded in 2014 at the congress held in Melbourne. This classification also maintains the subdivision of vascular anomalies into tumors and malformations but provides further details such as the addition of mutated genes and clinical associations such as coagulopathies [37] *Table 2-5*.

Table 2. Vascular tumors classification

Tumor histological entity	Benign	Local aggressive and borderline	Malignant
Tumor type and subtype	infantile hemangioma congenital hemangioma rapidly involuting hemangioma (RICH) partly involuting hemangioma (PICH) non-involuting (NICH) spindle cell hemangioma epitheloid cell hemangioma lobular capillary hemangioma tufted angioma	kaposiform hemangioendothelioma retiform hemangioendothelioma papillary intralymphatic angioendothelioma composite hemangioendothelioma kaposi sarcoma	angiosarcoma epitheloid hemangioendothelioma

Table 3. Vascular malformation classification

Flow component	Vascular component	Clinical malformation
Slow flow	Capillary malformation	CM cutaneous/mucosal (“port wine stain”) ▪ CM with soft tissue and/or bone overgrowth ▪ CM with central nervous system and/or ocular anomalies (sturge-weber syndrome) ▪ CM with arterio-venous malformation (CM-AVM) ▪ teleangiectasia in hereditary hemorrhagic teleangiectasia (HHT) ▪ cutis marmorata telangiectatica congenita (CMTC) ▪ naevus simplex (stork bite, angel kiss)
Slow flow	Lymphatic malformation	CM cutaneous/mucosal (“port wine stain”)

		▪ CM with soft tissue and/or bone overgrowth ▪ CM with central nervous system and/or ocular anomalies (sturge-weber syndrome) ▪ CM with arterio-venous malformation (CM-AVM) ▪ teleangiectasia in hereditary hemorrhagic teleangiectasia (HHT) ▪ cutis marmorata telangiectatica congenita (CMTC) ▪ naevus simplex (stork bite, angel kiss)
Slow flow	Venous malformation	common VM ▪ glomovenous malformation (GVM) ▪ blue rubber bleb naevus VM syndrome ▪ cutaneo-mucosal VM (VMCM)
Fast flow	Arterio venous malformation	sporadic AVM ▪ AVM in HHT
Fast flow	Arteriovenous fistula	sporadic AVF ▪ AVF in HHT
Combined vascular malformation		
slow flow	CM VM	Capillary venous malformation
Slow flow	CM LM	Capillary lymphatic malformation
Fast flow	CM AVM	Capillary artero venous malformation
Slow flow	LM VM	Lymphatic venous malformation
Slow flow	CM LM VM	Capillary lymphatic venous malformation
Fast flow	CM LM AVM	Capillary lymphatic arterio venous malformation
Fast flow	CM VM AVM	Capillary venous arterio venous malformation
Fast flow	CM LM VM AVM	Capillary lymphatic venous arterio venous malformation

Table 4. Vascular malformation associated with other anomalies

Slow flow	CM VM LM	With limb overgrowth Klippel Trenaunay syndrome
Fast flow	CM AVF	With limb overgrowth Parkes weber syndrome
Slow flow	Limb VM	With limb overgrowth Servelle Martorell syndrome
Slow flow	Limb VM	With congenital limb hypertrophy
Slow flow	VM	With /without spindle cell hemangioma and encondroma (maffucci syndrome)
Slow and fast flow	LM VM CM. AVM	With lipomatous overgrowth Sindrome di Cloves
Slow flow	CM VM LM	With asymmetric somatic overgrowth (Proteus)
Fast Flow	AVM VM	With macrocephaly and lipomatous overgrowth (PTEN hamartoma syndrome

Table 5. ISSVA genetic classification of vascular anomalies (2014)

Vascular anomaly	**Gene/locus**	**Location**	**Inheritance**
Capillary/venulocapillary malformation			
Sturge-Weber syndrome (leptomeningeal and cutaneous venulocapillary malformation, aka "port-wine stain")	a. GNAQ	9q21	Somatic
Non-syndromic port-wine stain	b. GNAQ	9q21	Somatic
Arteriovenous malformations			
Capillary malformation-arteriovenous malformation (CM-AVM)	*RASA1	5q14.3	AD
Parkes Weber syndrome	*RASA1 (in subset)	5q14.3	AD
Hereditary hemorrhagic telangiectasia			
HHT1	*ENG	9q34.11	AD
HHT2	ACVRL1/ALK1	12q13.13	AD
HHT3	Unknown	5q31.3-q32	AD
HHT4	Unknown	7p14	AD
Juvenile polyposis/HHT syndrome (JP/HHT)	*SMAD4	18q21.2	AD
HHT5/atypical HTT	*BMP9/GDF2	10q11.22	Association only
HBT	Unknown	CMC1/5q14	Association only
Angiokeratoma Fabry disease	*GLA	Xq22.1	XD
Progressive patchy capillary malformations Angioma serpiginosum	Unknown	Xp11.3-Xq12	Association only
Familial cerebral cavernous malformations (CCM)			
CCM1	*KRIT1	7q21.2	AD

CCM2	*Malcavernin/CCM2	7p13	AD
CCM3	*PDCD10	3q26.1	AD
CCM4	Unknown	3q26.3-27.2	
Venous malformations			
Sporadic Venous malformations (VM)	*TEK/TIE2	9p21.2	Somatic
Familial venous malformations cutaneous-mucosal (VMCM)	TEK/TIE2	9p21.2	AD
Glomuvenous malformation (GVM)	*Glomulin/GLMN	1p22.1	AD
Verrucous venous malformation (VVM)/verrucous hemangioma	MAP3K3	17q23.3	Somatic
Lymphatic malformations, lymphedemas, and complex syndromes			
CLOVES	*PIK3CA	3q26.32	Somatic
Klippel-Trenaunay syndrome (KTS)	PIK3CA	3q26.32	Somatic
Fibro-adipose vascular anomaly (FAVA)	*PIK3CA	3q26.32	Somatic
Macrocephaly-capillary malformation	PIK3CA	3q26.32	Somatic
Microcephaly-capillary malformation (MICCAP)	*STAMBP	2p13.1	AR
Nonne-Milroy syndrome	*FLT4/VEGFR3	5q34-35	AD/AR
Primary hereditary lymphedema (Nonne-Milroy-like syndrome)	*VEGFC	4q34	AD
Hypotrichosis lymphedema telangiectasia (HLT)	SOX18	20q13.33	AD/AR
Primary hereditary lymphedema	GJC2/Connexin 47	1q41-42, 4q34	AD
Lymphedema distichiasis	FOXC2	16q24.1	AD
Primary lymphedema with myelodysplasia (Emberger syndrome)	GATA2	3q21.3	AD
Primary generalized lymphatic anomaly (Hennekam syndrome)	CCBE1	18q21.32	AR
Microcephaly with or without chorioretinopathy, lymphedema, or mental retardation syndrome	KIF11	10q23.33	AD
Lymphedema-choanal atresia	PTPN14	1q41	AR
Proteus syndrome	AKT1	14q32.3	Somatic
PTEN hamartoma tumor syndrome (PHTS) Bannayan-Riley-Ruvalcaba syndrome (BRRS)	PTEN	10q23.3	AD
Cowden syndrome (CS)/Cowden-like syndrome	*PTEN, *SDHB, *SDHD, KLLN	10q23.3	AD
“Proteus-like” syndrome	*PTEN	10q23.3	AD
PTEN-related Proteus syndrome (PS)	*PTEN	10q23.3	AD

Vascular tumors (distinguished by endothelial hyperplasia) tend to regress as the patient ages, while vascular malformations (distinguished by dysmorphogenesis and abnormal cellular turnover) increase in size with the progression time. The latter are divided into capillary, venous, lymphatic, arterio-venous and combined malformations, depending on their dominant vasculature.

According to their aspect, venous malformations are the most common representative of vascular anomalies (70%), followed by lymphatic malformations (12%), arterio-venous malformations (8%), combined malformation syndromes (6%) and capillary malformations (4%) [38].

Based on their flow characteristics, vascular malformations can be divided into four main categories: those with slow-flow (i. capillary malformation, ii. venous malformation, iii. lymphatic malformation) and those with fast-flow (iv. arteriovenous malformation) [39].

Vascular malformations are present from birth, having the same endothelial lineage. They result from errors in the signaling of apoptosis, rather than in the growth and maturation of endothelial cells at the time of embryogenesis [40], [41] according to the presence or absence of endothelial mitotic activity. Vascular malformation derive from errors in the first weeks of development of the embryo (angiogenesis) and in later phase of the vessel formation (vasculologenesis).

Many times the vascular malformations are mixed, making the already complicated nomenclature and the formulation of diagnosis even more difficult. In these cases, it is very useful the investigation through the acquisition of images such as ultrasound (US), rather than color Doppler or magnetic resonance imaging (MRI) [42].

Generally, the treatment of vascular malformations may require both invasive and non-invasive procedures and may be different depending on the type of vascular malformation. The venous malformations are managed with laser therapy, sclerotherapy, and surgery, the hemangioma with systemic or intralesional corticosteroids, chemotherapeutic agents such as vincristine, alpha-interferon, surgery, lasers, or a combination of these therapies or the arteriovenous malformations are treated with arteriogram and embolization using varying substances, such as alcohol glue, and coils [43]. However, these procedures are invasive, painful, and risky.

According to the evolution of the therapy of vascular anomalies which is progressively becoming more endovascular than surgical we presumed that the examination of a blood specimen taken during vascular catheterism might give some information which could replace biopsies. In cases of huge a-v shunts, intraosseous malformations, biopsies might be dangerous.

But would it work? The most involved cells are endothelial cells and supportive cells, which all are in contact with blood flow. We can assume that the death rate of these cell should be lower than that of neoplastic cells and for this reason we have chosen to take blood specimen as close as possible to the vascular lesion.

The use of liquid biopsy helps us to overcome the obstacle of the invasiveness of tissue biopsies that are still needed for the molecular diagnosis of Vascular Malformations.

1.6 ***Aim's project***

The aim of my work project was to assess a new approach as the non-invasive method such as the liquid biopsy. The rationale consists of taking a blood sample from a peripheral vein in cancer patients and, thanks to the easy performance of the technique, repeating the analysis during the time in order to follow the clonal evolution over time.

Regarding the vascular malformations' patients, the blood withdrawal is taken from the efferent vein of the vascular lesion and from the peripheral vein. By comparing the data obtained from both samples, we expect to find mutations with a higher allelic frequency percentage from the sample coming from the vascular malformation site compared to that of the peripheral vein. The liquid biopsy allows us to detect the presence of a very low frequency of somatic mosaic mutations, not easily identifiable with the classic tissue biopsy.

2 Materials and methods

2.1 ***Patient samples collection***

During these three years, we collected 69 patients with different solid tumors, who experienced disease progression after standard therapy; in the last academic year, we also investigated 37 patients suffering from different vascular malformations. Blood samples were collected in 10 mL Cell-Free DNA BCT® Streck tubes (Streck, La Vista, NE, USA) (Fig.1). The tubes hold formaldehyde-free preservatives useful to stabilize nucleated blood cells preventing the release of genomic DNA from cells and allowing the cell-free DNA stabilization. These conditions guarantee the preservation and isolation of high-quality cell-free DNA. Streck tubes keep stable the Cell-free DNA for up to 14 days at 6 °C to 37 °C *Figure 4.*

Figure 4. Cell-Free DNA BCT® Streck tubes

Ion Torrent sequencing

2.2 ***Cell-free Plasma Isolation***

The plasma was obtained by double centrifugation at RT (room temperature): the first centrifugation at 1900 rcf for 15 minutes, and the second one at 1900rcf for 10 minutes to remove eventual cells and cellular debris from the plasma. After that, the plasma was stored at -80 °C or directly processed for cf-DNA extraction.

2.3 ***Cell-free Nucleic Acid Isolation***

Cf-DNA was extracted from 4.0 mL of plasma manually using MagMAX™ Cell-Free Total Nucleic Acid Isolation Kit according to the manufacturer's instructions.

First, the sample plasma was digested using Proteinase K combining 4.0 mL of plasma with 60 µL of MagMAX™ Cell-Free Total Nucleic Acid Proteinase K (20 mg/mL) and 2mL of MagMAX™ Cell-Free Total Nucleic Acid Lysis/Binding Solution in 50mL falcon tubes. The sample was incubated in the shaking at 1000 rpm for 30 minutes at 65°C.

After Proteinase K incubation, the samples were cooled on ice until they reached RT. Then 3.0 mL of MagMAX™ Cell-Free Total Nucleic Acid Lysis/Binding Solution plus 120 µL of MagMAX™ Cell-Free Total Nucleic Acid Magnetic Beads (Fig.2) were added to the digested plasma. Later, the samples were placed on an RT shaker at 1000 rpm for 10 minutes that allow binding the nucleic acid to the beads.

Then, the 50ml tubes were placed on the DynaMag™–50 Magnet stand, when the supernatant was clear it was removed and discarded without disturbing the beads. The latter were resuspended in 1 mL of Wash Solution 1. The bead slurry was recovered and transferred to a new 1.5 mL microcentrifuge tube, placed on the DynaMag™–2 Magnet stand for 20 seconds, and washed two times with 1 mL of freshly prepared 80% ethanol. The beads were air-dried and resuspended in 400 µL of Elution Solution vortexing for 5 minutes. The supernatant containing cfDNA was transferred to a new 1.5 mL microcentrifuge tube.

The next step was to concentrate the cfDNA combining 500 µL Lysis/Binding Solution with 10 µL of well-vortexed Magnetic Beads following the same procedure previously explained. Finally, were obtained 15 µL of cfDNA ready for quantity and quality check.

2.4 ***cfDNA quantity check***

The cell-free DNA quantity was asses using the Qubit™ dsDNA HS Assay Kits on Qubit 2.0 fluorometer (Invitrogen, Carlsbad, CA, USA) according to the Qubit dsDNA HS Assay user guide. The working solution was prepared by diluting the Qubit® dsDNA HS Reagent 1:200 in Qubit® dsDNA HS Buffer. After, were prepared two standards combining 190 µL of the working solution with 10 µL of each standard. For sample preparation, 1 µL was combined with 199 µL of the working solution. After an RT incubation of 3 minutes the standards and the samples were read. The Qubit can evaluate only the quantity and not the quality for which is necessary to perform an Agilent High Sensitivity DNA analysis.

2.5 ***cfDNA quality check***

The cfDNA quality was evaluated with Agilent™ High Sensitivity DNA Kit (Agilent Technologies, Palo Alto, CA) on Agilent2100 Bioanalyzer (Agilent Technologies) according to the manufacture's protocol. The Gel-Dye mix (9µL) was loaded in the DNA chip, followed by 1µL of the ladder 1 µL of the sample. Before starting the run on Agilent 2100 Bioanalyzer, the chip was vortexed for 60 seconds at 2400 rpm. The fragmented cfDNA is characterized by 150-170 bp peaks *Figure 5*.

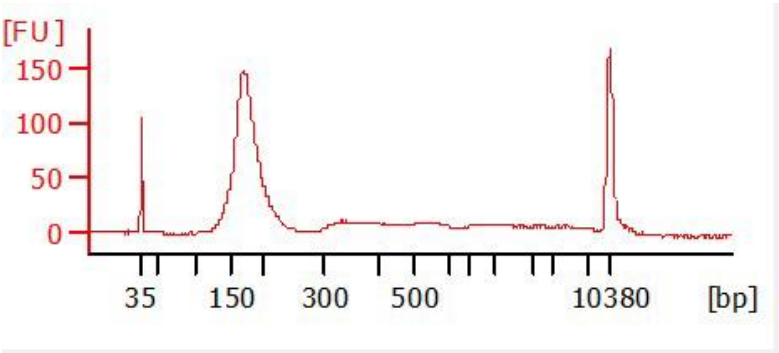

Figure 5. Typical profile of the cfDNA (150-170bp) extracted from plasma (my own data).

2.6 ***Library preparation***

The libraries were performed using the Oncomine™ Pan-Cancer Cell-Free Assay (ThermoFisher Scientific, Carlsbad, CA, USA), according to the manual instructions. Optimal libraries can be prepared from 20− 50 ng of cfDNA using a maximum volume of 10.4 µL. The libraries were generated performing three PCR reactions in the Veriti™ 96-well Thermal Cycler (Applied Biosystem, Thermo Fisher) *Figure 6*.

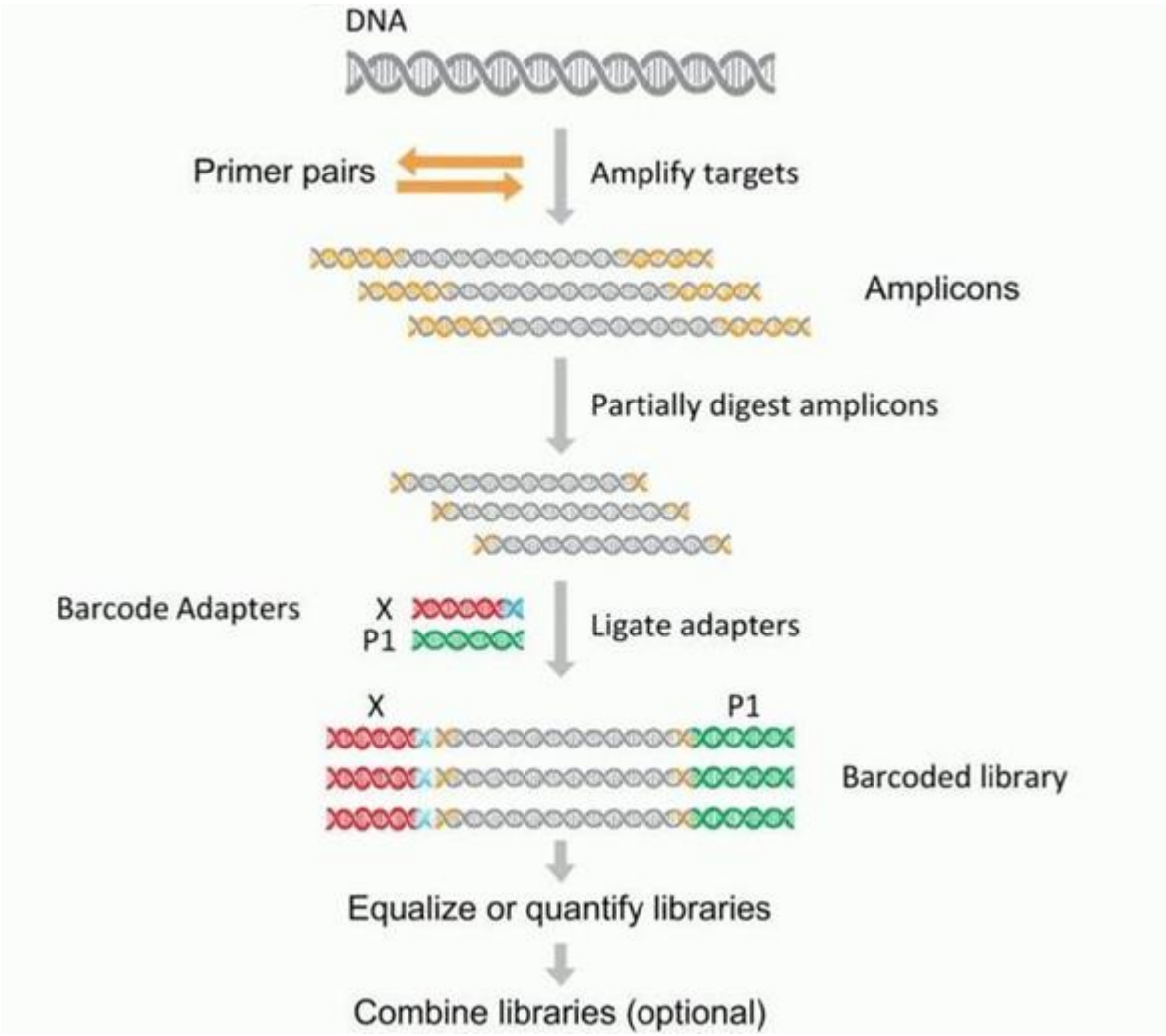

Figure 6. Library preparation (ThermoFisher Scientific).

To make unique fragments belonging to the same sample, we used different Tag Sequencing BC# (Set 1-24) allowing us to sequence a sample pool on the same chip. At the end of the PCR amplification and purifications, 28 µL of the library were recovered. The final library can be stored for long term at -20°C or the library can be qualified and quantify by qPCR.

2.7 ***Library quality check***

The quality check was performed following the same procedures used for the cfDNA quality check with the use of Agilent™ High Sensitivity DNA Kit on Agilent™ 2100 Bioanalyzer™ *Figure 7.*

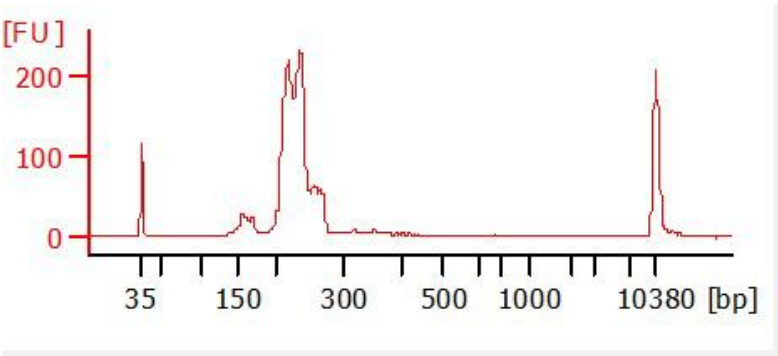

Figure 7. Shows the library profile, with a good library peak around 200bp and minimal presence of primer-dimers (150bp) (my own data).

2.8 ***Library qPCR quantification***

The library concentration of each sample was determined by qPCR with the Ion Library TaqMan® Quantitation Kit following the manufactures instruction.

In real-time PCR, DNA is amplified by DNA-polymerase chain reactions. After each round of amplification, the DNA is quantified. Higher is the number of the nucleic acid target, the sooner is the fluorescence observed. The qPCR is a compound of the following steps.

1. An oligonucleotide probe contains a reporter (R) fluorescent dye on the 5´ end and a quencher dye (Q) on the 3´ end. While the probe is entire, the closeness of the Q reduces

the fluorescence emitted by the R by fluorescence resonance energy transfer (FRET) through space.

2. When the probe anneals to the target sequence downstream from one of the primer sites the Taq DNA polymerase cleaves the probe as the primer is extended. This cleavage moves away from the R from the Q, increasing the reporter dye signal and allowing primer extension. At each cycle, other probes will be cleave increasing the fluorescence signal which is directly proportional to the amplified quantity.

The E. coli DH10B Control Library was used and diluted serially to generate a set of standards: 10-fold serial dilution was prepared at 6.8 pM, 0.68 pM, 0.068 pM. Also, the library was diluted and for each sample, a 1:100 and 1:1000 dilution were prepared.

Then, 11 µL of the PCR master mix was aliquoted for a single reaction. The PCR reactions were set in an Optical 96-well plate by adding 11 µL of PCR Master Mix and 9 µL of the E. coli control dilutions, sample dilutions, and nuclease-free water for NTC. Finally, the plate was loaded in the 7900HT Fast Real-Time PCR Instrument and the run program of the user guide was performed. Once the standard curve is generated, the libraries' concentration is calculated.

2.9 ***Ion Proton™ Sequencing***

Before proceeding to the sequencing on Ion Proton™ Sequencer, the libraries are loaded as a pool in the Ion PI™ Hi-Q™ Chef System to prepare the templates and to load the sequences on the chip. The pool libraries are diluted according to the protocol and loaded in the appropriate Ion Chef™ Library Sample Tube. Once the Ion Chef™ Instrument was completely loaded with all the consumables and 2 chips (Ion PI™ Chip v3), it is ready to set up the emulsion PCRs and load the sequences onto the chips.

Indeed, the Ion Chef System performs an emulsion PCR creating a template-positive Ion Sphere™ Particles (ISPs). Finally, the templates are loaded into the chip. In the end, the Ion Chef™ Instrument was unloaded and cleaned with UV rays. Each chip contains 4 libraries samples which will be sequenced on the Ion Proton™ Sequencer.

After the cleaning and initialization of the Ion Proton™ Sequencer with the Ion PI™ Hi-Q™ Sequencing 200 Kit, the chip was loaded and the sequencing process started.

Ion Proton technology is based on the detection of the PH variation by the instrument's ionic sensor. The value of PH change when a nucleotide is incorporated into a strand of DNA by a polymerase and a hydrogen ion is released as a byproduct. This signal is transformed from chemical information to digital information *Figure 8*.

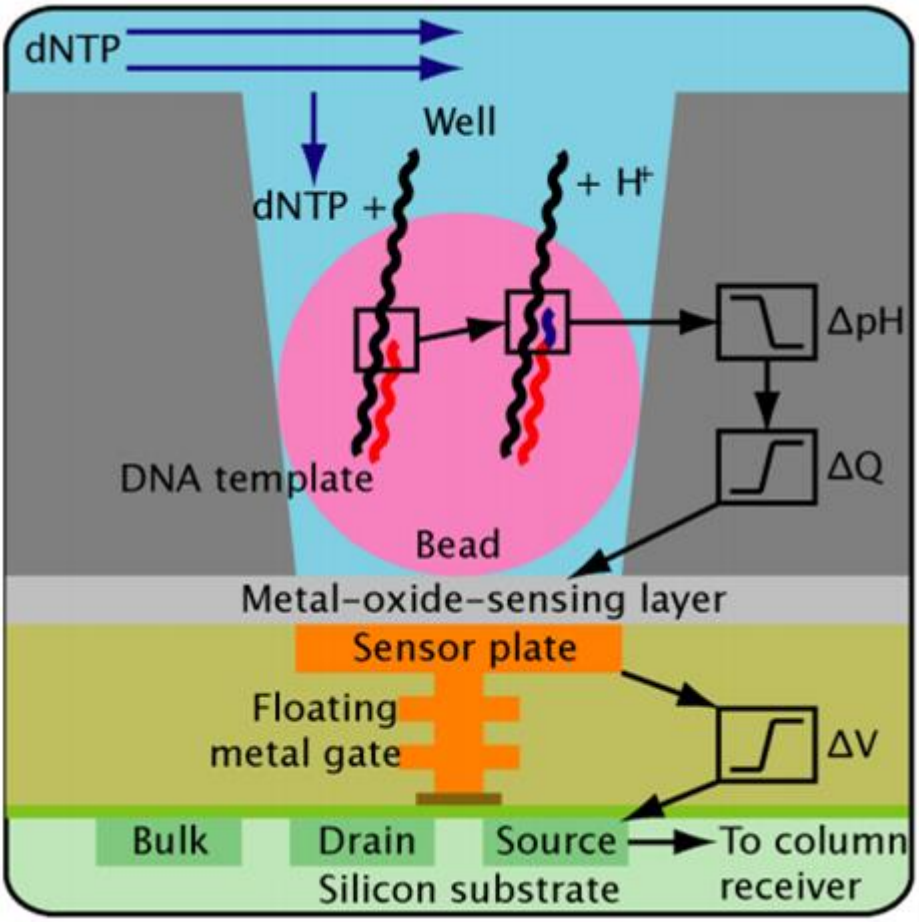

Figure 8. Incorporation of nucleotide and H^+ release [44].

2.10 ***Sequencing Analysis***

The sequencing analysis was performed with the Ion Reporter Server System (Thermo Fisher Scientific). The quality of the run is dictated by the unaligned section, reviewing Total Bases, Total Reads, Mean, and Median read lengths *Figure 9.*

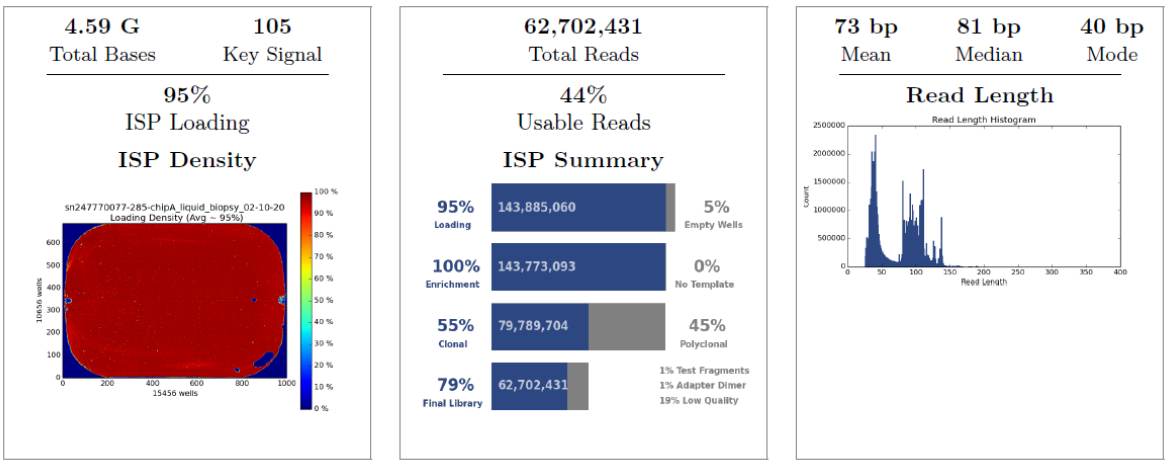

Figure 9. Unaligned metrics (my own data).

IPS Density: The ISP Density includes the Total Bases (Number of filtered and trimmed base pairs reported in the output BAM file) and the Bead Loading (Percentage of chip wells that contain a live ISP).

IPS Summary: In this section, several metrics are found including Usable Sequences (The percentage of library ISPs that pass the polyclonal, low quality, and primer-dimer filters), the percentage of Clonal and Polyclonal ISPs, the Final Library (Percentage of reads which pass all filters and which are recorded in the output BAM file) and Percentage of ISPs with a low or unrecognizable signal.

Read Length: This section includes the read length histogram (a histogram of the trimmed lengths of all reads present in the output files) and the following metrics: Mean Read Length (average length, in base pairs, of called reads) and the Median length of called reads.

As a metric, it was considered also the Total Alignment Bases to the reference genome (Hg19), the Reference Coverage, the percentage of Aligned and Unaligned bases, and the Raw Accuracy, which is reported in a graph that plots percent accuracy for each position in an aligned sequence. The alignment quality reports different scores referred to as AQ17, AQ20, and Perfect with an error rate of 2% (or less), 1% (or less), and (the longest perfectly aligned

segment) respectively. The quality level is also reported with the Total number of bases, the Mean length, and the mean coverage depth *Figure 10.*

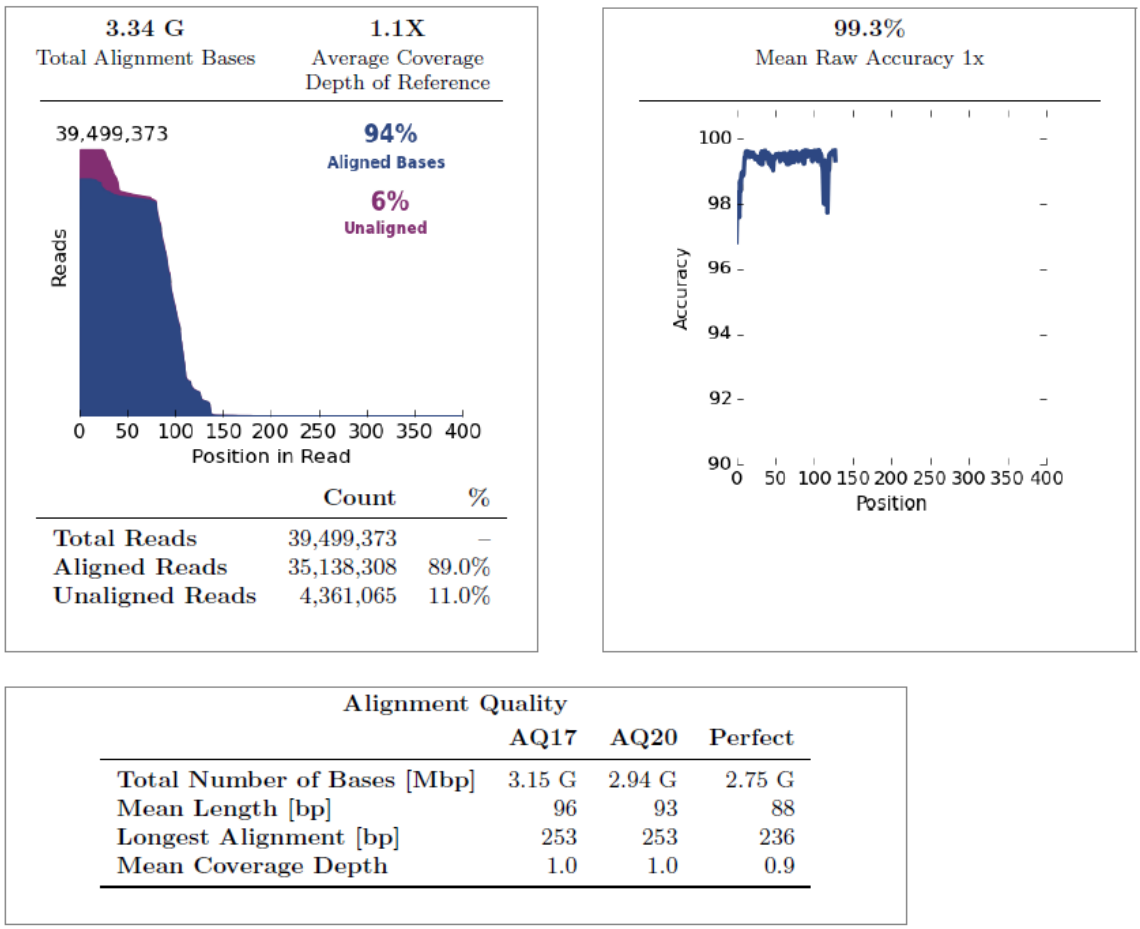

Figure 10. Sequence alignment to Homo sapiens (my own data). Number of filtered and trimmed aligned base pairs reported in the output BAM file. Total number of bases aligned to the reference sequence. Excludes the library key, barcodes, and 3' adapter sequences.

The Ion Reporter™ software calls all the identified variants reported as:

- SNV (single-nucleotide polymorphism)
- Indel (insertion or deletion of bases)
- CNV (copy number variation)
- Fusion (joining parts of two different genes)
- MET Exon 14 Skipping

For each variant, listed by chromosomal location, exon, a reference sequence, amino acid variation, and so on, it indicates several annotations, which include:

- The coverage (the number of base positions covered by at least one read)
- The Median Read Coverage (median number of individual interrogated DNA molecules across targets)
- The Molecular Depth (number of interrogated DNA molecules containing target)
- The Molecular Counts (the number of detected DNA molecules containing variant allele)
- The LOD % (Limit of detection determined by the minimum amplicon coverage and input of DNA used for library preparation.
- The frequency % (frequency of mutant allele)
- The variant type (Missense, Synonymous, etc.)
- The DrugBank (list of drugs known to target the gene)
- The Phred quality score (base-calling error probabilities).

Illumina sequencing

2.11 ***Cell-free Nucleic Acid Isolation***

After the sample collection and plasma isolation (see above), the cfDNA isolation start combining in a 15ml canonical tube, 4ml of plasma with 500 µL of reconstituted Proteinase K incubated at RT for 5 minutes. A second incubation of 30 minutes took place after the addition of 4 mL of DNA PBB. After that, 1000 µL of isopropanol was added and the sample was transferred to the High Pure Extender Assembly Unit (HPEA). The HPEA was centrifuged at 3270x g for 5 minutes, the filter tube recovered and two washing of 500 µL with Wash Buffer I and subsequently Wash Buffer II were performed. The cfDNA was eluted in 65 µL of Elution Solution, 60 µL were recovered to proceed to the Quantity, and Quality control step using the Qubit™ dsDNA HS Assay Kits and Agilent2100 Bioanalyzer respectively (see 2.4 and 2.5 sections).

2.12 ***Preparation of sequencing libraries***

The library preparation protocol (AVENIO ctDNA Analysis Kits), supports 10 to 50 ng cfDNA input ranges with a maximum of 50 µL. A first PCR to prepare the cfDNA sample for the ligation was performed mixing DNA preparation buffer, DNA preparation enzyme, and

cfDNA sample. Then, to perform the sample Adapter ligation, a second overnight (o.n.) PCR was run adding the sample adapter and ligation master mix to each sample. A clean with fresh 80% ethanol and cleanup beads was performed to the post-ligation sample, followed by PCR amplification. After the PCR, the samples were washed and prepared for the target enrichment step. The amplified samples were prepared for the hybridization combining the hybridization supplemented with the hybridization master mix, Enhancing Oligo that must match the corresponding Sample Adapter used in the ligation step, and the appropriate AVENIO Expanded genes panel. The hybridization program lasted o.n. Once the hybridization finish, the hybridization cleanup was performed and a post-hybridization enrichment followed combining a PCR master mix with the sample which is amplified for 30 minutes in the thermocycler. After, the last wash for post-capture PCR was performed. The libraries so created are ready for the quantity and quality check using Qubit™ dsDNA HS Assay Kits and Agilent2100 Bioanalyzer respectively (see 2.4 and 2.7 sections).

2.13 ***Illumina NextSeq 550 Sequencing***

Based on the libraries' concentration, the final pool concentration is calculated. The NextSeq 550 instrument was loaded with NextSeq 500/550 High Output Kit v2.5 (300 Cycles, Illumina) included High Output Reagent Cartridge, High Output Flow Cell Cartridge, and Buffer Cartridge. The Illumina NextSeq 550 technology is based on the bridge amplification; the DNA fragments bind the complementary sequences on the flowcell. The strand attaches to a second stand forming a bridge and the reverse strand is synthesized by the enzyme DNA polymerase. The two strands release and straighten and each of them forms a new bridge resulting in a cluster of forward and reverse strand clones. Each time a tagged nucleotide is incorporated into the DNA filament, a wavelength is emitted, recorded, and transformed in bioinformatic information.

2.14 ***Sequencing Analysis***

At the end of the run, the sequencing data was analyzed using AVENIO Oncology Analysis Software (Software Version 2.0.0). For each sample, several files were generated like sample metrics, variant reports, BAM, and BAI files. The information obtained concerns:

-Gene (indicates the mutated gene)

-Genomic Position (chromosomal positions of the variant found)

-Variant Depth (depth of reading, number of reads at that locus)

-Allele Fraction (allelic frequency)

-Number of mutant molecules per mL

-Transcript (transcript of the exon)

-Coding Change (variant detected respecting the reference sequence)

-Aminoacid Change (any amino acid changed on the mutated protein compared to wild-type protein)

-Variant Description (effect of the variant, missense, nonsense, silent, etc.)

-Exon Number Over Total Exon (exons involved in the variants)

-ExAC Overall Frequency (database to detect rare gene variants for specific population)

-1000 Genomes Frequency (database to establish a detailed catalog of human genetic variant)

-COSMIC (database annotations for somatic variants in human cancers)

-TCGA (The Cancer Genome Atlas, the database for genetic mutations involved in cancer).

3 Results

3.2 ***PIK3CA-CDKN2A clonal evolution in metastatic breast cancer and multiple points cell-free DNA analysis***

Palmieri *et al. Cancer Cell Int* (2019) 19:274
https://doi.org/10.1186/s12935-019-0991-y

Cancer Cell International

COMMENTARY Open Access

PIK3CA-CDKN2A clonal evolution in metastatic breast cancer and multiple points cell-free DNA analysis

Maria Palmieri[1], Margherita Baldassarri[2], Francesca Fava[1], Alessandra Fabbiani[1], Giuseppe Maria Campennì[3], Maria Antonietta Mencarelli[2], Rossella Tita[2], Stefania Marsili[4], Alessandra Renieri[1,2*] and Elisa Frullanti[1]

Abstract

Background: Daily experience tells us that breast cancer can be controlled using standard protocols up to the advent of a relapse. Now new frontiers in precision medicine like liquid biopsy of cell free DNA (cfDNA) give us the possibility to understand cancer evolution and pick up the key mutation on specific cancer driver gene. However, tight schedule of standardized protocol may impair the use of personalized experimental drugs in a timely therapeutic window.

Main body: Here, using a combination of deep next generation sequencing and cfDNA liquid biopsy, we demonstrated that it is possible to monitor cancer relapse over time. We showed for the first time the exact correspondence from the increasing clonal expansion and clinical worsening of metastatic breast cancer.

Conclusion: Thanks to liquid biopsy may be possible to introduce new experimental drugs in the correct therapeutic window which would lead in the near future to an effective treatment which otherwise remains challenging.

Keywords: PIK3CA-CDKN2A, cfDNA, Liquid biopsy, Deep-next generation sequencing, Targeted-therapy

Background

Melchardt et al. 2018 demonstrated that clones in distant relapse of head and neck cancer are different in respect to those identified at the beginning in tumor biopsy [1]. Classically, haematological malignancies have taught us that, within the dynamic clonal evolution, a subclonal expansion of a pre-existing mutated clone leads often to relapse [2, 3]. Expanding clones may be selected by treatment acquiring drug resistance and patients who relapse after an effective therapy usually have a poor prognosis [4, 5]. While at the beginning of tumor expansion there is a consistent, although variable, mutational burden from ten to hundred clones, at relapse the leading clone is usually only one [5]. Liquid biopsy of cell free DNA (cfDNA) has now the potential to follow the temporal evolution and to inform us about the driver mutation of the expanded clone. Among solid tumors, breast cancer is one of the most facing a high risk of recurrence after curative surgery and therapeutic treatment. *PIK3CA* mutations are found in 27% of cases of disease progression in breast cancer [6]. Free survival was demonstrated to be inversely correlated with *PIK3CA* mutations at liquid biopsy [7] but longitudinal analysis of clonal evolution and disease progression was missed.

Main text

Using a combination of deep next generation sequencing and cfDNA liquid biopsy (Oncomine pan-cancer cell free assay and tissues/blood custom panels on ion proton platform, life technologies), we showed for the first time the exact correspondence between the increasing clonal expansion and the clinical worsening of metastatic breast cancer in a 44-year-old female with disease recurrence after 4 years and half of disease control. At 38 years she presented a poorly differentiated ductal carcinoma of the right breast, pT1cN1mi(1/3) G3, estrogen receptor (ER)

*Correspondence: alessandra.renieri@unisi.it
[1] Medical Genetics Unit, Policlinico "Santa Maria alle Scotte", University of Siena, Viale Bracci, 2, 53100 Siena, Italy
Full list of author information is available at the end of the article

BMC

© The Author(s) 2019. This article is distributed under the terms of the Creative Commons Attribution 4.0 International License (http://creativecommons.org/licenses/by/4.0/), which permits unrestricted use, distribution, and reproduction in any medium, provided you give appropriate credit to the original author(s) and the source, provide a link to the Creative Commons license, and indicate if changes were made. The Creative Commons Public Domain Dedication waiver (http://creativecommons.org/publicdomain/zero/1.0/) applies to the data made available in this article, unless otherwise stated.

positive 90%, progesterone receptor (PgR) positive 40%, HER2 negative, KI67 40%. She underwent quadrantectomy and subsequent chemotherapy with Epirubicin Ciclofosfamide (EC) for four cycles and Decapeptyl every 28 days. After 7 months, she added tamoxifen for 1 year, then replaced by Exemestrane for 2 years. Radiotherapy was also performed. Family history was positive for breast cancer in the paternal side although exome analysis failed to reveal germline mutation in known cancer driver genes.

After 4 years and half from the diagnosis, liver and bone metastasis were detected. Biopsy of the VIII hepatic segment showed metastasis of breast carcinoma, ER negative, PgR negative, HER2 negative, Ki67 17%. Subsequently, therapy with Paclitaxel was undertaken weekly. Three months later from the previous evidence of metastasis, numerical and dimensional increase in liver lesions was demonstrated. Monotherapy with cisplatin was started and then in association with capecitabine and epirubicin (ECX scheme) with dose of 80% for seven consecutive cycles. Afterwards, she had treatment with Capecitabine and metronomic cyclophosphamide for 3 months, then three cycles of eribuline were performed. Therapy with carboplatin and gemcitabine was subsequently administered. One month later, since there was an increase of liver enzymes, monotherapy with carboplatin was undertaken. No other treatment options were available given the disease progression.

After about 1 year from the evidence of bones and liver metastasis, we performed a first cfDNA analysis, which revealed pathogenic mutations in *PIK3CA* gene [c.1633G>A; p.(Glu545Lys)] and *CDKN2A* [c.1904T>G; p.(Leu635Arg)]. Five months later, a second cfDNA analysis highlighted an exponential increase of clones with the same pathogenic mutations (Fig. 1). In comparison with the mutational burden identified at primary tumor biopsy, the expanding clone has a simplified architecture (Fig. 1).

We demonstrated here that multiple points cfDNA analysis give now the possibility to understand the overall cancer dynamics and pick up the key mutation leading to cancer recurrence, separating them from not expanding

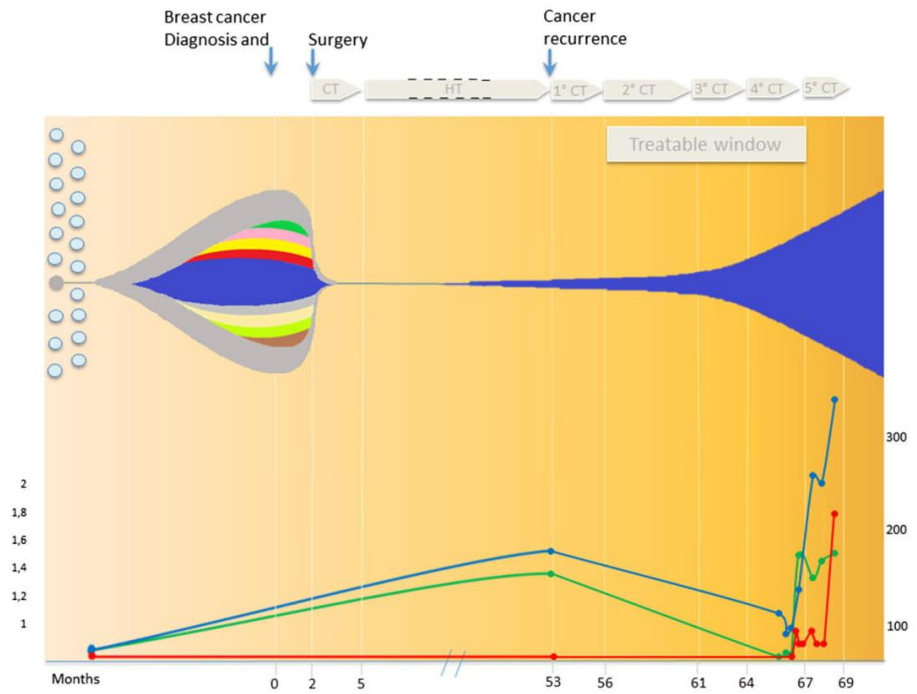

Fig. 1 Outline of clonal and subclonal architecture and clinical outcome. Upper panel: fish plot of clonal evolution and timing. At the primary tumor biopsy, 10 different distinctive clones with different mutational load (ranging from 0.3 to 25%) were identified: IDH1 (green), CTNNB1 (pink), FBXW7 (yellow), APC (red), EGFR (beige), PIK3CA (blue), PTEN (brown), SMAD4 (grey), CDKN2A (blu), GNAS (light green). Among these, the clone-bearing PIK3CA/CDKN2A mutations (blue) increases from 25% at the time of primary tumor biopsy to around 50% at 180 days' post-recurrence. Bottom panel: liver enzymes (AST = blue line; ALT = green line; values in U/L on the right) and bilirubin (red line; values in mg/dL on the left) whose values increase according to disease progression. *CT* chemotherapy; *HT* hormone therapy

occasional clones. Large comprehensive analysis of haematological malignancies indicates a complex temporal dynamic landing although in few (from one to six) driver mutations at late relapse [8]. Likewise, in breast cancer one (or few) is the driver mutation leading to cancer recurrence and it is of pivotal importance to target this driver mutation(s) on time. However, stick too tightly to standardised protocol may impair the use of personalised experimental drugs in a timely therapeutic window.

Data reported here indicate that there is a tight therapeutic window useful for counteract final clonal expansion and that the minimally invasive cfDNA analysis allows a close and dynamic monitoring of clonal evolution. This is also supported by the mathematical model developed by Khan et al. [9]. In our case, an innovative and more effective therapy could be CDK4/6 inhibitors in combination with PI3 K-specific inhibitor initiated at the beginning of the clonal expansion [10]. Introducing of experimental drug in the correct therapeutic window would lead in the near future to effective treatment which otherwise remain challenging.

Conclusions

In conclusion, we demonstrated that multiple points cfDNA analysis reflects clonal evolution and allows track the evolving molecular landscapes of growing cancer cells by capturing broader molecular alterations that could hinder targeted treatments efficacy. The shorter turnaround time of cfDNA analysis and its high sensitivity and specificity are key factors to provide novel opportunities for adaptive personalised therapies, optimizing healthcare resources and enabling higher treatment efficacy and lower side-effects.

Abbreviations

CDKN2A: cyclin dependent kinase inhibitor 2A; CDK: cyclin dependent kinase; cfDNA: cell-free DNA; EC: epirubicin ciclofosfamide; ECX: epirubicin cisplatin and capecitabine; ER: estrogen receptors; HER2: human epidermal growth factor receptor 2; PgR: progesterone receptor; PIK3CA: phosphoinositide-3-kinase, catalytic, alpha polypeptide.

Acknowledgements

The cell lines and DNA bank of Rett Syndrome, X-linked mental retardation and other genetic diseases, member of the Telethon Network of Genetic Biobanks (project no. GTB12001), funded by Telethon Italy, and the Euro-BioBank network, provided us with specimens. Authors also thank the ERN-EURACAN (European network for Rare adult solid Cancer). We thank SienaGenTest srl, a Spin-off of the University of Siena (www.sienagentest.dbm.unisi.it) for bioinformatic analysis of genetic data.

Authors' contributions

MP performed experiments on cfDNA and analysed the data and wrote the paper, FF, AF, took care of the clinical part of the study and wrote the paper, RT performed experiments on blood, tumoral tissue and metastasis, AR designed the research strategy, analysed the data and wrote the paper, EF analysed the data and wrote the paper, MB and MAM performed genetic counselling and provided patient samples, SM and GMC followed the patient as oncologist. All authors read and approved the final manuscript.

Funding

Authors would thank for support Regione Toscana - Istituto Toscano Tumori (ITT) (Project "Identification of genetic bases of individual predisposition to lung cancer in non-smokers") and from ASSO (Associazione per lo Sviluppo della Scienza Oncologica) onlus.

Availability of data and materials

The datasets used and/or analyzed during the current study are available from the corresponding author on reasonable request.

Ethics approval and consent to participate

This study was consistent with Institutional guidelines and approved by the ethical committees of Azienda Ospedaliera Universitaria Senese, Siena, Italy. Informed consent was obtained from the patient.

Consent for publication

Consent was obtained from the patient.

Competing interests

The authors declare that they have no competing interests.

Author details

[1] Medical Genetics Unit, Policlinico "Santa Maria alle Scotte", University of Siena, Viale Bracci, 2, 53100 Siena, Italy. [2] Genetica Medica, Azienda Ospedaliera Universitaria Senese, Siena, Italy. [3] European Institute of Oncology, Milan, Italy. [4] Oncology, Azienda Ospedaliera Universitaria Senese, Siena, Italy.

Received: 27 May 2019 Accepted: 12 October 2019
Published online: 28 October 2019

References

1. Melchardt T, Magnes T, Hufnagl C, Thorner AR, Ducar M, Neureiter D, et al. Clonal evolution and heterogeneity in metastatic head and neck cancer-an analysis of the Austrian Study Group of Medical Tumour Therapy study group. Eur J Cancer. 2018. https://doi.org/10.1016/j.ejca.2018.01.064.
2. Fouillet L, Daguenet E, Schein F, Tavernier E, Flandrin-Gresta P, Cornillon J. Clonal evolution of myelofibrosis treated with hematopoietic transplantation, using RUXOLITINIB for chronic GvHD: a case report. Curr Res Transl Med. 2018. https://doi.org/10.1016/j.retram.2018.07.001.
3. Pinto AM, Papa FT, Frullanti E, Meloni I, Tita R, Caselli R, et al. Low-level TP53 mutational load antecedes clonal expansion in chronic lymphocytic leukaemia. Br J Haematol. 2019. https://doi.org/10.1111/bjh.15147.
4. Ghatalia P, Smith CH, Winer A, Gou J, Kiedrowski LA, Slifker M, et al. Clinical utilization pattern of liquid biopsies (LB) to detect actionable driver mutations, guide treatment decisions and monitor disease burden during treatment of 33 metastatic colorectal cancer (mCRC) patients (pts) at a Fox Chase Cancer Center GI Oncology Subspecialty Clinic. Front Oncol. 2019. https://doi.org/10.3389/fonc.2018.00652.
5. Jacoby MA, Duncavage EJ, Chang GS, Miller CA, Shao J, Elliott K, et al. Subclones dominate at MDS progression following allogeneic hematopoietic cell transplant. JCI Insight. 2018. https://doi.org/10.1172/jci.insight.98962.
6. Lee JH, Jeong H, Choi JW, Oh HE, Kim YS. Liquid biopsy prediction of axillary lymph node metastasis, cancer recurrence, and patient survival in breast cancer. Medicine. 2018. https://doi.org/10.1097/MD.0000000000012862.
7. Nakauchi C, Kagara N, Shimazu K, Shimomura A, Naoi Y, Shimoda M, et al. Detection of TP53/PIK3CA mutations in cell-free plasma DNA from metastatic breast cancer patients using next generation sequencing. Clin Breast Cancer. 2016. https://doi.org/10.1016/j.clbc.2016.05.004.
8. Spinella JF, Richer C, Cassart P, Ouimet M, Healy J, Sinnett D. Mutational dynamics of early and late relapsed childhood ALL: rapid clonal expansion and long-term dormancy. Blood Advances. 2018. https://doi.org/10.1182/bloodadvances.2017011510.
9. Khan KH, Cunningham D, Werner B, Vlachogiannis G, Spiteri I, Heide T, et al. Longitudinal liquid biopsy and mathematical modeling of clonal evolution forecast time to treatment failure in the PROSPECT-C

phase II colorectal cancer clinical trial. Cancer Discov. 2018. https://doi.org/10.1158/2159-8290.CD-17-0891.
10. Gul A, Leyland-Jones B, Dey N, De P. A combination of the PI3 K pathway inhibitor plus cell cycle pathway inhibitor to combat endocrine resistance in hormone receptor-positive breast cancer: a genomic algorithm-based treatment approach. Am J Cancer Res. 2018;8:2359–76.

Publisher's Note

Springer Nature remains neutral with regard to jurisdictional claims in published maps and institutional affiliations.

Ready to submit your research? Choose BMC and benefit from:

- fast, convenient online submission
- thorough peer review by experienced researchers in your field
- rapid publication on acceptance
- support for research data, including large and complex data types
- gold Open Access which fosters wider collaboration and increased citations
- maximum visibility for your research: over 100M website views per year

At BMC, research is always in progress.

Learn more biomedcentral.com/submissions

BMC

3.3 *Two-point-NGS analysis of cancer genes in cell-free DNA of metastatic cancer patients*

Received: 20 August 2019 | Revised: 18 November 2019 | Accepted: 2 December 2019

DOI: 10.1002/cam4.2782

ORIGINAL RESEARCH

Cancer Medicine Open Access WILEY

Two-point-NGS analysis of cancer genes in cell-free DNA of metastatic cancer patients

Maria Palmieri[1] | Margherita Baldassarri[2] | Francesca Fava[1,2] | Alessandra Fabbiani[1,2] | Elisa Gelli[1] | Rossella Tita[2] | Pamela Torre[3] | Roberto Petrioli[3] | Theodora Hadijstilianou[4] | Daniela Galimberti[4] | Elisa Cinotti[5] | Carmelo Bengala[6] | Marco Mandalà[7] | Pietro Piu[8] | Salvatora Tindara Miano[3] | Ignazio Martellucci[3] | Agnese Vannini[3] | Anna Maria Pinto[2] | Maria Antonietta Mencarelli[2] | Stefania Marsili[3] | Alessandra Renieri[1,2] | Elisa Frullanti[1]

[1]Medical Genetics, University of Siena, Siena, Italy

[2]Genetica Medica, Azienda Ospedaliera Universitaria Senese, Siena, Italy

[3]Oncology, Azienda Ospedaliera Universitaria Senese, Siena, Italy

[4]Department of Ophthalmology, Referral Center for Retinoblastoma, Azienda Ospedaliera Universitaria Senese, Siena, Italy

[5]Department of Medical, Surgical and Neurosciences, Dermatology Unit, University of Siena, Siena, Italy

[6]Medical Oncology, Ospedale Misericordia, Azienda Toscana Sud-Est, Grosseto, Italy

[7]Department of Otology and Skull Base Surgery, University of Siena, Siena, Italy

[8]VisMederi s.r.l, Strada del Petriccio e Belriguardo, Siena, Italy

Correspondence
Alessandra Renieri, Medical Genetics Unit - University of Siena, Policlinico "Santa Maria alle Scotte", Viale Bracci, 2 -53100 Siena, Italy.
Email: alessandra.renieri@unisi.it

Funding information
Istituto Toscano Tumori; ASSO (Associazione per lo Sviluppo della Scienza Oncologica)

Abstract

Background: Although the efficacy of molecularly target agents in vitro, their use in routine setting is limited mainly to the use of anti-HER2 and antiEGFR agents in vivo. Moreover, core biopsy of a single cancer site may not be representative of the whole expanding clones and cancer molecular profile at relapse may differ with respect to the primary tumor.

Methods: We assessed the status of a large panel of cancer driver genes by cell-free DNA (cfDNA) analysis in a cohort of 68 patients with 13 different solid tumors at disease progression. Whenever possible, a second cfDNA analysis was performed after a mean of 2.5 months, in order to confirm the identified clone(s) and to check the correlation with clinical evolution.

Results: The approach was able to identify clones plausibly involved in the disease progression mechanism in about 65% of cases. A mean of 1.4 mutated genes (range 1-3) for each tumor was found. Point mutations in *TP53*, *PIK3CA*, and *KRAS* and copy number variations in *FGFR3* were the gene alterations more commonly observed, with a rate of 48%, 20%, 16%, and 20%, respectively. Two-points-Next-Generation Sequencing (NGS) analysis demonstrated statistically significant correlation between allele frequency variation and clinical outcome ($P = .026$).

Conclusions: Irrespective of the primary tumor mutational burden, few mutated genes are present at disease progression. Clinical outcome is consistent with variation of allele frequency of specific clones indicating that cfDNA two-point-NGS analysis of cancer driver genes could be an efficacy tool for precision oncology.

KEYWORDS

cell-free DNA, liquid biopsy, next-generation sequencing, solid tumors, targeted-therapy

This is an open access article under the terms of the Creative Commons Attribution License, which permits use, distribution and reproduction in any medium, provided the original work is properly cited.

© 2019 The Authors. *Cancer Medicine* published by John Wiley & Sons Ltd.

1 | INTRODUCTION

Cancer cells continuously acquire new mutations due to genomic instability and/or selective pressure from the tissue microenvironmental and clinical treatment. During anti-cancer drug treatment, subclones survive and multiply, contributing to further evolution of metastases into diverse tumor cell phenotypes. Several studies demonstrated that at disease progression, expanding clones are different with respect to those identified at the beginning in tumor biopsy and that expanding clones may be selected by progresses therapies[1] and have differential sensitivities to therapy.[2] This was extensively shown for both hematological[3-5] and solid tumors.[1]

Large-scale studies demonstrated a limited usefulness of molecular profiling obtained from Formalin-Fixed and Paraffin-Embedded tumor specimen of primary tumor, relapse, or metastasis.[6] Tumor biopsies normally accomplish the sampling of only a part of the tumor and may only capture a fraction of its heterogeneity, consequently not being totally informative about the levels of genetic variability of a patient's cancer. Moreover, it is unlikely for a patient to undergo sequential biopsies of primary and metastatic lesions along tumor progression.[7]

During the last years, to answer the need of a more accessible approach for tumor genetic analysis, "liquid biopsy" is emerging as an innovative, minimally invasive and efficient alternative to investigate cancer cells being able to take multiple blood samples over time informing on what type of molecular changes are taking place in a tumor.[8-10] Now the cell-free DNA (cfDNA) analysis has the possibility to overcome the space-time profile constraint of physical biopsies and opens a new scenario for personalized treatment. The usefulness of cfDNA sequencing for identifying markers of disease progression is well established.[11,12] The European Medicines Agency (EMA) in 2015, and the Food and Drug Administration (FDA) in 2016 approved the use of cfDNA extracted from plasma for detection of *EGFR* mutations in non-small-cell lung cancer (NSCLC) patients without tissue available or after resistance to a first or second generation TKIs.[13] Notwithstanding the potential game-changing role of cfDNA assessments, its clinical utility is still under investigation and translational trials focused on the impact of its integration in the therapeutic algorithm are pivotal and of great impact to further develop precision medicine approaches.

In the present study, we investigated whether combined cfDNA analysis may detect emerging clones and track the patterns of clonal dynamics in a case series of 68 metastatic cancer patients. We revealed that two-point-NGS (next-generation sequencing) analysis in cfDNA is able to distinguish evanishing from expanding clones. Furthermore, we found that mutations in *TP53*, *PIK3CA*, *KRAS,* and *FGFR3* were the most commonly observed in solid tumor irrespective to the primary tumor type, opening the way to a history or-free new era. This in turn could result in an innovative trial design. Finally, we showed that only by combining cfDNA analysis with genomic analysis, it is possible to distinguish the germline mutation/somatic mosaicism from the true expanding clones eventually responsible for disease progression.

2 | MATERIALS AND METHODS

2.1 | Patients

This is a 12-months prospective study from March 2018 to March 2019, conducted at Medical Genetics Unit of the Azienda Ospedaliera Universitaria Senese (AOUS), Siena, Italy, for diagnostic purposes. Sixty-eight patients with different solid tumors who experienced disease progression after standard therapy were enrolled in both pediatric and adult Oncology Clinics of AOUS and Azienda Toscana Sud-Est, Italy. Patients were previously treated in advanced/metastatic setting and most of them were not eligible for a curative treatment. This study was consistent with Institutional guidelines and approved by the ethical committees of Azienda Ospedaliera Senese, Siena. Informed consent was obtained from the patient. Written informed consent for genetic analysis was obtained for all patients at the Medical Genetics Unit of the Azienda Ospedaliera Universitaria Senese, Siena, Italy.

2.2 | Study subject

Inclusion criteria included patients with either locally advanced or metastatic solid tumor independently from the primary tumor site. Patients were excluded if they had early-stage solid tumors. The main information collected for each patient includes, in addition to oncological data, genealogic tree and cancer family history on a genetic consultation setting.

2.3 | cfDNA and genomic DNA sampling

A first peripheral blood sample for cfDNA analysis was either taken from medical oncology or during the genetic counseling visit at the stage of disease progression (R1). Plasma was used for cfDNA extraction while cell containing phase (buffy coat) was used for genomic DNA (gDNA) extraction using MagCore HF16 (Diatech Lab Line, Jesi, Ancona, Italy). A second sample (R2) for cfDNA analysis was taken at the follow-up visit. For a part of patients, the second sampling

was not possible either because they died or because they entered at the end of the study time period.

2.4 | CfDNA extraction

Peripheral blood samples (10 mL) were collected from each patient and placed into PAXgene blood ccfDNA tubes (Qiagen, Hilden, Germany). The plasma was obtained from a double centrifuge at 1900 g for 15 and 10 minutes and cfDNA was extracted from 4 mL of plasma using MagMAX cell-free Total Nucleic Acid Isolation Kit (ThermoFisher Scientific), according to manufacturer's instructions. cfDNA quality and quantity was verified, respectively, using the Agilent™ High Sensitivity DNA Kit (Agilent Technologies) on Agilent2100 Bioanalyzer (Agilent Technologies) and Qubit™ dsDNA HS Assay Kits on Qubit 2.0 fluorometer (Invitrogen).

2.5 | NGS sequencing on cfDNA

CfDNA sequencing was performed using Oncomine™ Pan-Cancer Cell-Free Assay (ThermoFisher Scientific) on Life Technologies Ion Proton sequencer (Life Technologies). This technology is able to identify various types of alterations, including single-nucleotide variants, insertions/deletions, gene fusions, and copy number variations (CNV) present in genes linked to cancer (clinical actionable mutations) with a reportable range up to 0.05%. The sequencing analysis was performed using Ion Reporter Server System (Thermo Fisher Scientific).

2.6 | NGS sequencing on genomic DNA

gDNA library preparation was performed according to the protocol of Life Technologies for individual germline mutation. The NGS sequencing was performed on Life Technologies Ion S5 sequencer (Life Technologies) and postrun analysis was conducted using the "coverageAnalysis" and "variantCaller" plug-in on Torrent Server Suite (Life Technologies). Tissue analysed was mainly blood. In cases of suspected mosaicism additional tissues such as urine and salivary fluid were used.

2.7 | Statistical analyses

Statistical analysis was carried out with R statistical software, version 3.6.0.[12] Overall survival (OS) was performed using the Kaplan-Meier method and the Cox proportional hazards analysis using the "survival" package in R.[14,15] The proportional hazards assumption was satisfied through Schoenfeld residuals ($\rho = 0.1016042$, $\chi^2 = 0.1041084$ and $P = .7469541$).

TABLE 1 Characteristics of patients

Subject characteristics	Total (N = 68)	%
Median age (years-range)	58 (1-82)	—
Median follow-up (years-range)	4.5 (0.5-14.4)	
Gender		
Male	25	36.8
Female	43	63.2
Primary site		
Breast	19	28
Lung	15	22.1
Glioblastoma	6	8.8
Ovarian	5	7.4
Pancreatic	4	5.9
Uterine	3	4.4
Retinoblastoma	3	4.4
Oral	3	4.4
Gastric	3	4.4
Cholangiocarcinoma	2	2.9
Colorectal	2	2.9
Sezary	2	2.9
Sarcoma	1	1.5
Metastatic site		
Bone	4	5.9
Visceral	22	32.4
Both (Bone and Visceral)	13	19.1
Local invasion	29	42.6
Median follow-up (years-range)	4.5 (0.5-14.4)	
No. alive patients	56	82.4
No. dead patients	12	17.6

Median cfDNA plasma level as variable was used as the middle value for survival analysis. An increase of 20% from R1 to R2 was used as the cut-off point for survival analysis. OS was defined as the time between the date of enrollment and the date of death or the date of last follow-up. A P value < .05 was used as threshold for statistical significance.

Differences in clonal evolution (increased/ decreased mutational load) between patients at relapse phase (R) and patients at regression (G) or stationary (S) phase were tested by the Fisher's exact test.

3 | RESULTS

3.1 | Patients' characteristics

From March 2018 to March 2019, a total of 68 patients with either locally advanced or metastatic solid tumor were considered eligible and included in the study (Table 1). The mean

age at the first circulating tumor DNA (ctDNA) analysis was 58 years (range 1-82 years); 63.2% of patients were females. Out of 68 patients harboring advanced cancer, 19 had breast cancer, 15 non-small-cell lung cancer, 6 patients had glioblastoma; 5 ovarian cancer; 4 patients had pancreatic cancer; 3 patients uterine, retinoblastoma, oral or gastric cancer; 2 patients had cholangiocarcinoma, colorectal cancer or Sezary syndrome (cutaneous lymphoma) and 1 soft tissue sarcoma of right infratemporal fossa. Six patients had microsatellite stable tumors and all other patients were not tested for microsatellite instability on the tumor. Among patients with distant metastatic disease, the visceral metastasis was the most common metastatic site (32.4%) followed by coexistence of both bone and visceral (19.1%) (Table 1). The median follow-up of OS for all patients was 3.2 months (range 1-15). At the time of survival analysis, death by tumor progression occurred in 12/68 (17.6%) patients.

3.2 | cfDNA load

Relative amount of cfDNA differs from patient to patient and from tumor to tumor, having lung cancer and glioblastoma the higher concentration (Figure 1A). In our case series of 68 metastatic cancer patients, the median cfDNA level at baseline (R1) was 27.2 ng (range 5.1-1092) for 4 mL of plasma while the median cfDNA level at second liquid biopsy (R2) of 30.3 ng (range 5.91-1128). The time span between R1 and R2 was an average of 2.4 month (range 1-5 months, with only an out-layer of 12 months).

In our case series, median OS was 3.2 months in the overall population. Use of Cox proportional hazard models for survival (adjusted for age) to evaluate the association between cfDNA levels and OS, showed that the risk of death was significantly higher for patients with high cfDNA amount [Hazard Ratio (HR): 4.81; 95% confidence interval (CI), 1.10-21.09; $P = .0372$]. Kaplan-Meier curves showed a statistically significant association between the cfDNA levels and OS ($P = .043$, Figure 1B).

3.3 | Next-generation sequencing analysis on cfDNA

NGS analysis of 52 cancer genes of cfDNA samples of 68 patients allowed for picking up clones likely involved in the mechanism of disease progression in 65% of cases. The median follow-up for positive cases was 2.9 months (range 0.3-14.4). A mean of 1.4 mutated genes (range 1-3) for each tumor was found. The percentage of positive cases was almost the same irrespective to primary tumor type (Figure 2).

The comprehensive summary of mutations, including single-nucleotide variants (SNVs) and copy number variants (CNVs), identified through cfDNA sequencing in each patient of our case series as well as treatments was represented in Figure 3. Clonal likely driver mutations in *TP53* were the most commonly observed along all patients regardless of the primary tumor type. A major Variant Allele Frequencies (VAFs) were observed for *TP53* and *PIK3CA* in breast and ovarian cancers (Figure 3).

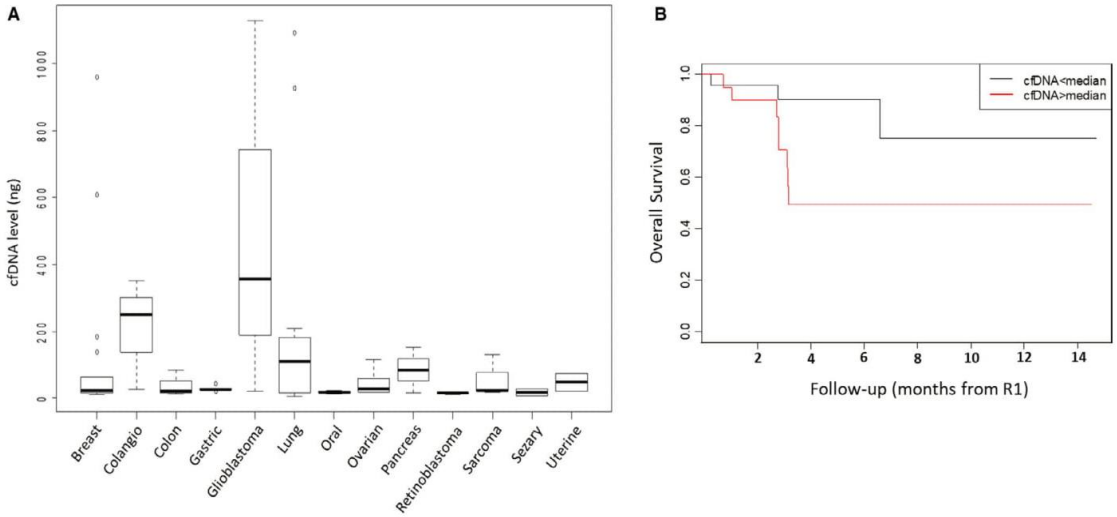

FIGURE 1 Plasma cfDNA levels according to primary tumor type and Kaplan-Meier survival analysis. A, Box plot of cfDNA level (*y*-axis) by primary tumor type (*x*-axis). The line within each box represents the median fold-change value. Upper and lower edges of each box, 75th and 25th percentile, respectively. Upper and lower bars, highest and lowest values determined, respectively. B, Kaplan-Meier curve of OS according to cfDNA plasma level. CfDNA, circulating free DNA; OS, overall survival

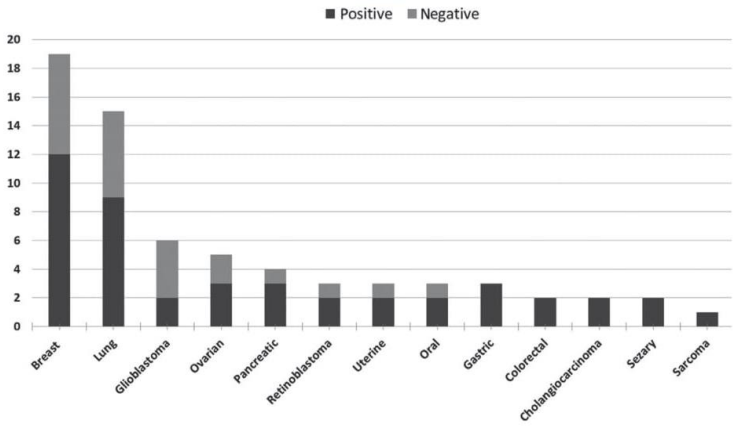

FIGURE 2 Distribution of 13 different tumor type in our cohort of 68 patients. Bar plot representing number of patients (y-axis) grouped for primary tumor type (*x*-axis). Number of positive cases (in dark gray) and negative cases (in light gray)

The distribution of all genomic alterations that were identified in the entire case series is shown in Figure 4. Point mutations in *TP53*, *PIK3CA*, and *KRAS* and CNVs in *FGFR3* were among the most commonly observed identified and persisting/growing clones, with a rate of 48%, 20%, 16% and 20%, respectively (Figure 4A). Overall mutations were detected in 22 different genes among 13 different solid tumors without specific prevalence (Figure 4B,C).

3.4 | Germline next-generation sequencing analysis

All those patients having a mutated clone close to 50% of mutational load were tested on DNA extracted from blood white cells. In 4 cases, one retinoblastoma, one glioblastoma, one breast cancer, and one oral cavity tumor, a germline mutation was identified; this was *RB1*, *TP53*, *MET*, and *MET*, respectively (Figure 3). In another case (ovary cancer), a *TP53* mutation in the mosaic state was identified (Figure 3).

3.5 | Two-point-NGS analysis

In the majority of cases, the second cfDNA analysis confirmed the clone identified in the first analysis (14/23, 61%) and among these, often (10/14, 71%) the variant allele frequency was increased (Figure 3). In other cases, the clones were stationary (Figures 3 and 5A). In few cases, additional emerging clones (4/35, 11.4%) were identified in the second analysis (R2-R1 3.1 months), pinpointing to a minimal but still present clonal evolution (Figure 5A). In some cases, the clone identified in the first analysis (8/35, 23%) was not present anymore in the second (R2-R1 2.5) and just in 2 cases the allele frequency was decreased with a mean time lapse R2-R1 of 1.1 months (Figure 5A). Notably, the variant allele frequency increased in parallel with worsening of disease (Figure 5B). Overall, statistically significant association with clonal evolution was observed according to tumor burden. Patients with an increased or persistent mutational load at R2 reported significantly worse clinical outcomes compared with patients with decreased mutational load ($P = .026$, Figure 5B and Supplementary Table. 1).

FIGURE 3 Clonal driver mutations identified in 68 patients with different solid tumors at disease progression. Driver mutations identified in 68 patients grouped for primary tumor type. Genes are represented on the top. Both CNVs (in pink) and SNVs (in blue) are indicated. Color scale indicates the variant allele frequency (VAF) of SNVs: from light [VAF ≤ 1%] to dark blue [VAF up to 50%]. The CNV ratio: from light [RATIO 1-2] to dark pink [RATIO 10-20]. *TP53*, *PIK3CA*, and *KRAS* and (CNV) in *FGFR3* were among the most commonly observed identified and persisting/growing clones, with a rate of 48%, 20%, 16% and 20%, respectively. Red boxes showed growing clones, fuchsia boxes showed stable clones and green boxes represented regression clones. In the event column R (relapse), G (regression), and S (stationary). In the metastasis site/local invasion column L (local), V (visceral), B (Bone) e T (both visceral e bone); Among 29 patients who received two-point-cfDNA analysis only 5 cases clearly showed growing clones (red outline). Most of them were mutation in 2 genes with parallel increasing of mutational load, suggesting double mutation of a single clone. For example, case 6 with *FGFR1/CCND1* clonal expansion in ER + HER2- breast cancer was treated by Ribociclib and Fulvestrant; case 40 with *ERBB2/TP53* clonal expansion in gastric cancer, in addition to chemotherapy, would benefit of Transtuzumab, which was not used due to advanced cardiopathy of the patient; case 36 with *FGFR2/TP53* clonal expansion in cholangiocarcinoma and case 42 with *BRAF/AKT1* clonal expansion in colorectal cancer are in the process to be treated by Erdafitinib and by Everolimus, respectively; and case 1 with *PIK3CA* clonal expansion in breast cancer was treated by Ipatasertib. Interestingly, retinoblastomas resistant to intra ocular Melphalan showed mutated clones in *PTEN* or *SMAD4* which disappeared after enucleation. One of the 2 tumors, the early onset with germline *RB1* mutation, started to grow a *FGFR3* clone after surgery indicating a incomplete disease remission

	PATIENT (code)	AGE	Germline mutation	Molecular biology PT	Quantity (ng TOT)	EVENT	Metastasis site/local invasion	R2 - R1 Time lapse (mo + w)	ESR1	CTNNB1	KRAS	PIK3CA	ERBB2	TP53	FGFR2	FGFR1	CCND1	CCND2	CCND3	FGFR3	EGFR	PTEN	SMAD4	BRAF	AKT1	SF3B1	MET	GNAS	MAP2K1	MYC	Treatment	DS (mo + w)	Follow-up (mo + w)
BREAST CANCER	1 (1084/18-2947/19)	44		ER+ HER2-	11,76	R1	T																								Chemotherapy (Eribuline)	6 + 3	
					609	R2	T	5																							Ipatasertib	1 + 2	
	2 (3197/18)	57		ER- HER2-	137,7	R1	T																								chemotherapy (Paclitaxel)	2 + 3	
	3 (3201/18)	38		ER+ HER2- ^	21,9	R1	T																								chemotherapy (doxorubicin)	2	
	4 (3756/18)	44		ER+ HER2- ^	183	R1	T																								chemotherapy (Paclitaxel)	0 + 3	
	5 (658/18-1142/19)	47		ER+ HER2+	16,65	R1	T																								Trastuzumab, Pertuzumab	A	15
					35,7	S	T	12 + 2																							Trastuzumab, Pertuzumab		
	6 (406/19-1447/19)	67	MET	ER+ HER2-	34,2	R1	T																								Ribociclib+ Fulvestrant	A	3 + 3
					63,9	R2	T	2																							ribociclib+ Fulvestrant		
	7 (189/19-1402/19)	64		ER+ HER2+ ^	16,65	R1	V																								chemotherapy (Eribuline)	A	4 + 1
					16,77	R2	V	2 + 2																							chemotherapy(Eribuline)		
	8 (653/19-1400/19)	65		ER+ HER2	11,37	R1	B																								chemotherapy (Cyclophosphamide) +	A	3 + 1
					9,6	R2	B	1 + 2																							chemotherapy (Cyclophosphamide) +		
	9 (771/19-1272/19)	50		ER+ HER2+ ^	24,18	R1	T																								chemotherapy (Nab-Paclitaxel) + Trastuzumab	A	3
					30,3	R2	T	1																							chemotherapy (Nab-Paclitaxel) + Trastuzumab		
	10 (931/19)	52		ER+ HER2+	960	R1	T																								chemotherapy (Docetaxel)	A	2 + 3
	11 (1062/19)	47		ER+ HER2	9,87	R1	T																								Chemotherapy (Eribuline+ HT Letrozole)	A	2 + 2
	12 (1540/19)	47		ER- HER2- ^	13,38	R1	V																								Chemoterapy (Paclitaxel)	A	1 + 2
LUNG CANCER	13 (864/18-2375/18)	71		p40+ TTF1-	6,9	R1	B																								Chemotherapy (Doxorubicin)	A	14 + 2
					36,6	R2	B	4																									
	14 (3433/18)	79			1092	R1	T																								chemotherapy (Cisplatin)	2 + 3	
	15 (3430/18)	65		CK7+ TTF1.*	78,3	R1	T																								Nivolumab	3 + 1	
	16 (53/19-1324/19)	56		ALK - EGFR- KRAS+ BRAF-	927	R1	V																								Carboplatin + Paclitaxel	A	4 + 3
					109,5	R2	V	2 + 3																							none		
	17 (174/19)	52		TTF1- CK7-*	182	R1	V																								none	1 + 7	
	18 (175/19)	45		EGFR- BRAF-¥	208,8	R1	V																								Crizotinib	3 + 1	
	19 (623/19-1403/19)	53		CK7- CK20- P40- TTF1-¤	113,1	R1	T																								chemotherapy (etoposide + cisplatin)	A	3 + 1
					110,1	R2	T	1 + 2																							chemotherapy (etoposide + cisplatin)		
	20 (1070/19-1628/19)	66		EGFR- ALK- KRAS- BRAF+§	15,15	R1	T																								chemotherapy [Docetaxel]	A	2 + 2
					5,91	R2	T	1																							chemotherapy (Docetaxel)		
	21 (1448/19)	71		ALK - KRAS+₹	14,7	R1	V																								chemotherapy (Vinorelbine)	A	1 + 3
GLIOBLASTOMA	22 (627/18)	49	TP53	MIB1+ p53+ ₹	20,22	R1	L																								none	2 + 3	
	23 (3872/18-55/19)	76		GFAP+ p53 15%	357	R1	L																								Everolimus	A	6 + 1
					1128	R2	L	1 + 3																							Everolimus		
OVARIAN CANCER	24 (3195/18-1290/19)	45		PAX8+ CK7+ CK20- CDX2- $	18,84	R1	V																								chemotherapy (Nab- Paclitaxel)	A	8
					22,2	G	V	5 + 3																							chemotherapy (Nab- Paclitaxel)		
	25 (3262/18-1235/19)	70	TP53 mosaic	CA125+ CK8-18+ CK7+ WT1+ £	36,9	R1	L																								chemotherapy (Cyclophosphamide)	A	7 + 3
					60	S	L	5 + 2																							chemotherapy (Cyclophosphamide)		
	26 (1007/19-1704/19)	58		WT1+ CK7+ CK20- ESA+ £	17,73	R1	L																								chemotherapy (Carboplatin)	A	2 + 3
					114,3	S	L	1 + 2																							chemotherapy (Carboplatin)		
UTERINE CANCER	27 (3259/18)	51		ER- PR- p53-	21,33	R1	V																								none	A	7 + 3
	28 (3290/18)	41		ER+ PR+ &	75,6	R1	V																								chemotherapy (Carboplatin + Paclitaxel)	A	7 + 2
SEZARY	29 (2943/18)	59			8,16	R1	L																								ECP+ Bexarotene	A	8 + 2
	30 (3060/18)	67			29,1	R1	L																								ECP+ Bexarotene	A	8 + 1
PANCREATIC CANCER	31 (3069/18)	63			84,6	R1	V																								chemotherapy (Paclitaxel + Gemcitabine)	3 + 1	
	32 (1464/19)	35			153	R1	V																								chemoterapy (Nab- paclitaxel + Gemcitabine)	A	1 + 3
	33 (1659/19)	59			16,14	R1	L																								Chemotherapy (nab-paclitaxel + Gemcitabine)	A	1 + 1
RETINOBLASTOMA	34 (3753/18-728/19)	1	RB1	MIB1 2-3%	17,61	R1	L																								Enucleation	A	6 + 1
					16,14	S	L	1 + 1																							Chemotherapy(cyclophosphamide, epirubicin,fluorouracil)		
	35 (4292-18 /509-19)	8		MIB1 >90%	12,09	R1	L																								Enucleation	A	5 + 2
					29,79	S	L	1 + 3																							Chemotherapy		
CHOLANGIOCARCINOMA	36 (52/19-1289/19)	71		CK7- CK20+ CDX2+ CEA+ ?	250,5	R1	V																								chemotherapy [Cisplatin + Gemcitabine]	A	4 + 3
					25,65	R2	V	1 + 3																									
	37 (1077/19)	40		HSA- CK7+ #	351	R1	V																								chemotherapy (Cisplatin + Gemcitabine)	A	2 + 1
GASTRIC CANCER	38 (3664/18)	46		BerEp4+ HER2+ \	28,92	R1	V																								Ipilimumab and Nivolumab + chemotherapy	2 + 3	
	39 (51/19-1445/19)	82		HER2-	44,7	R1	V																								chemotherapy (Folinic acid, fluorouracil and irinotecan	A	4 + 3
					21,3	R2	V	3																							chemotherapy (Folinic acid, fluorouracil and irinotecan		
	40 (686/19-1446/19)	76		PSA- TTF1- CK7- CDX2+ =	27,24	R1	V																								chemotherapy (Docetaxel)	A	3 + 1
					27,18	R2		1 + 2																							chemotherapy (Docetaxel)		
SARCOMA	41 (211/19-875/19 - 1539/19)	54		MDM2+ AE1/AE3 - EMA- SMA- S100- CD34-]	23,67	R1	L																								Pazopanib	A	4 + 1
					19,23	R2		1 + 1																							Pazopanib		
					130,8	G		1 + 2																									
COLORECTAL CANCER	42 (558/19-1520/19)	69		BRAF+ KRAS- NRAS-	21,18	R1	V																								chemotherapy (Oxaliplatin +Capecitabine (XELOX))	A	3 + 2
					84,3	R2		2																									
	43 (656/19-1401/19)	68		KRAS- NRAS- BRAF-	20,88	R1	V																								Chemotherapy (Capecitabine) + Panitumumab	A	3 + 1
					12,57	S		1 + 2																									
ORAL CANCER	44 (834/19-1543/19)	57	MET	p16+	13,29	R1	L																								none	A	3
					18,39	R2		1 + 3																									
	45 (1681/19)	65			23,46	R1	L																								none	A	1 + 1

Note: Molecoular Biology PT: ^PgR-; *p40- EGFR- ALK- PD-L1+; °Sinaptofisine+ , ¥KRAS+, ¤CK5/6- sinaptofisine+ cromogranine- PDL1 5%; §PDL13%; ₹ EGFR-; $ WT1+ p16+ p53- Vimentin - PR ER + focal; £ p53+ calretinin- CK20- EMA-; £ Calretinin- MIB1+; & vimentine+; ? HSA- Ck8- Ck18+ Synaptophysin+; # CK20- CDX2- CD56- TTF1- GATA3- Sinaptofisine-; \ Calretinine-; =CK20+; | STAT6- desmin- myogenin- caldesmon-;

Interestingly, among the disappearing clones, 62.5% were *TP53* mutated. In these cases, the variant allele frequency was sometimes not negligible, being around 5% to 13%.

4 | DISCUSSION

More than 50% of solid cancers sooner or later escape control of standard treatments. Those tumors with high mutational burden are easily treated with immunotherapy, which is almost ineffective in another half of cases in which specific driver genes are supposed to lead therapy resistance.[16] However, molecular-based recommended therapies have almost unfulfilled expectation. In the majority of studies the molecular profiling is inferred from either primary tumor or metastases, none of them representing the evolving expanding clone at disease progression.[6] ccfDNA is one tool capable to represent at once every metastasis and to follow them during the time showing clonal evolution of cancer driver genes which may play a major role in the therapy escaping mechanism.[11]

Previous studies indicate the amount of cfDNA as a prognostic factor.[17] Results presented here confirmed the prognostic role of cfDNA plasma level demonstrating that the detection of more than 27.2 ng (per 4 mL of plasma) allowed to stratify the patient's' overall survival. In our prospective case series, we observed a higher rate of death in the group of patients with cfDNA level > 27.2 at R1 compared with the group with cfDNA level < 27.2 (24% vs 11.8%). This difference became more evident when we observed only the subgroup of mutated patients (40% vs 12%).

Regarding the frequency of mutation in cfDNA, our data confirmed the literature evidences with SNVs in *TP53*, *PIK3CA* and *KRAS* and CNVs in *FGFR3* as the most commonly observed in breast and lung.[18,19] Our data demonstrate the absence of a correlation with mutation type and primary tumor organ since we identified mutation in 22 different genes among 13 different solid tumors without specific prevalence (Figure 4). The sniper clones leading to disease progression can be distinguished by cfDNA two-point-NGS analysis pinpointing the needs of grouping patients on truly growing clones instead of on primary tumor organ in clinical trials.

The results of our study showed that irrespective of the primary tumor mutational burden[20] and subsequent complex clonal evolution, a simplified mutational load, in term of mutated clones, is present at disease progression (Figure 5). One or few "sniper" clones drive progression and the molecular profile of metastatic tumor has a weak correlation with the primary tumor. True snipers clones can be distinguished by cfDNA two-point-NGS analysis (Figure 5), highlighting the possibility to develop a specific therapy. For example gastric cancer with growing *TP53*/*ERBB2* mutated clone will benefit of Transtuzumab plus chemotherapy.[21] Breast cancer with *CCND1*/*FGFR1* mutated clone will benefit of combined erdafitinib plus ribociclib and fulvestrant.[22]

In the majority of cases, the second cfDNA analysis confirmed the clone identified in the first analysis (Figure 3). However, not 100% of mutated clones were still present at the second liquid biopsy. For example *PIK3CA* clone in patient 1 is clearly progressive within 4 per months and correspond to clinical worsening. On the contrary, *TP53* in patient 5 disappeared and the patient is still alive after 12 months. In some cases (example case 6) one subclone expands faster than other, pinpointing as a possible main target. Therefore, the second cfDNA time point evaluation is mandatory to identified true targets for personalized medicine.

In this study, the time span between the first and the second liquid biopsy was an average of 2.5 months. Considering that 80% of clones has evolved at R2 and those not evolving had a time lapse about 1.5, this observation may suggest that a mean of 2.5 months could be the appropriate time lapse could be used in the clinical practice.

Driver mutations in *TP53* remain the main target of a not yet developed specific therapy in a wide range of progressing tumor such as breast, ovarian, uterine, lung, gastric cancers, oral, glioblastoma, and sarcoma (Figure 3). In many cases, the *TP53* mutations were accompanied by another mutation and 100% of *TP53* disappearing clones were alone. Overall, these data may suggest that *TP53* may act at "disease progression" as a main co-driver gene, reducing apoptosis and cooperating with another cancer driver gene determining the growing of metastasis/local expansion. Indeed, clones with *TP53* mutation seems to be either stationary/disappearing when alone or growing with a second mutation.

Among the actionable mutations, *PIK3CA* were found not only in the very well known breast cancers but in a number of other cancers from like uterine carcinoma, Sezary syndrome, oral cancers, and glioblastoma, with the exception of lung. At the same time, increased CNV of *FGF* receptors were identified in patients with non-small-cell lung, pancreatic, and gastric cancer, and cholangiocarcinoma. These observations pinpoint the needs of trials grouping cancer patients on growing clones instead of primary tumor tissue/organ. Therefore, what we want to point out in this paper is that different histological tumors manifest the mutations onset in the same gene and sometimes the same variant. This new approach based on molecular features of cancer at disease progression, irrespective of the primary tumor origin, may be the keystone that directs towards a real personalized medicine.

Using a comparable number of tested genes the study of Rossi et al identified, in advanced breast cancer, the same average number of mutation per patient (3) but with a more wide variability (0-27).[18] One possible explanation of this discrepancy is the different cut off in considering variant as likely pathogenic. A second likely explanation could be

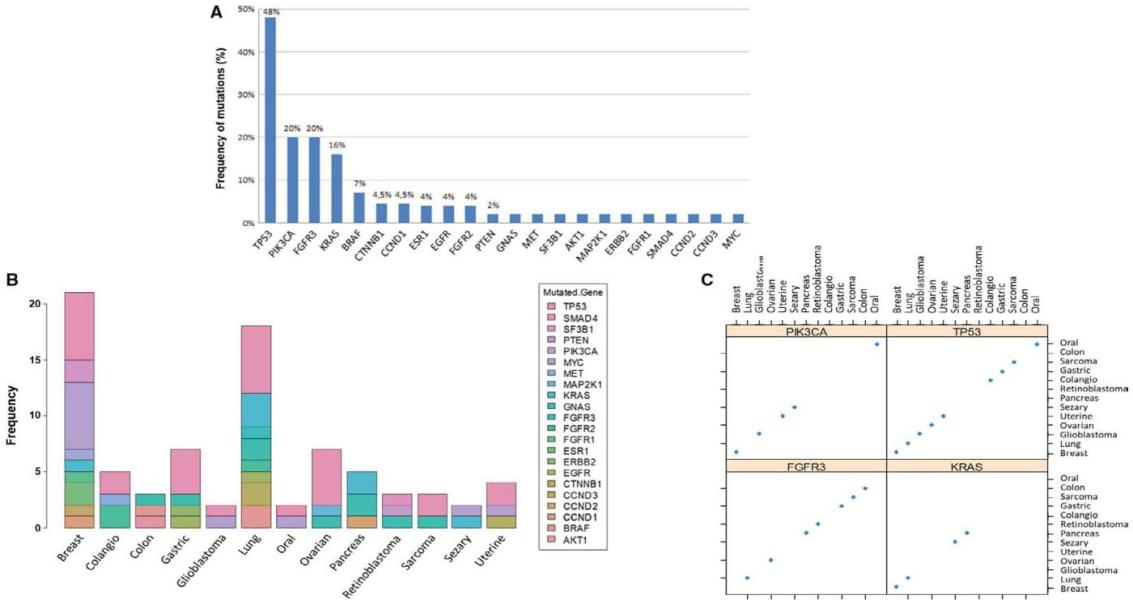

FIGURE 4 Distribution of the main alterations in mutated patients among the 68 included in the study. A, To establish the frequency of alterations within a gene, we considered the total number of alterations of that gene in the 45 positive patients, identified in the first analysis for these patients evaluated once (R1), in the second analysis in those evaluated twice (R2), because in the majority of cases, in particular 23/35, the second cfDNA analysis confirmed the clone identified in the first analysis. *TP53* is the most frequently observed clone (48%), followed by *PIK3CA* and *FGFR3* (20%). B, Bar plot showing the presence of mutated genes in frequency (*y*-axis) accordingly to the primary tumor site (*x*-axis). C, Scatter plot of mutations in the most frequently altered genes (*PIK3CA*, *TP53*, *FGFR3*, and *KRAS*) according to the tumor type

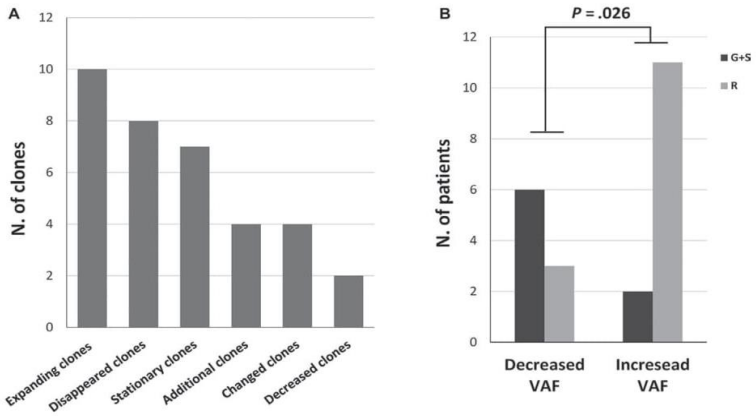

FIGURE 5 Clonal driver mutations evolution between first (R1) and second sample for cfDNA analysis (R2). A, Bar plot showing number of clones (*y*-axis) according to clonal evolution of cancer driver genes between first (R1) and second sample for cfDNA analysis (R2) (*x*-axis). If a sample showed different clones, each of them was counted. We see that the mutational load of ten clones was increased in the second sample with a mean time lapse R2-R1 of 2.5 months while seven clones were stationary (R2-R1: 2.2 months). Eight clones identified in the first analysis disappeared in the second one (R2-R1 3.2) and just for two clones the mutational load was decreased with a mean time lapse R2-R1 of 1.1 months. Four additional (R2-R1 3.1 months) or changed (R2-R1 1.9 months) emerging clones were identified in the second analysis. (B) The histograms show the distribution of the patients with decreased or increased variant allele frequency (VAF) between R1 and R2 according to clinical disease course (R, relapse; G, regression; S, stationary)

assigned to lack of subtraction of germline mutation and somatic mosaicism, which are not tested in the Rossi's study. Now we know that germline mutations could be identified even in unsuspected sporadic cases as demonstrated here by the *TP53*-mutated 76-aged sporadic glioblastoma case, and *MET*-mutated oral and breast cancer case. Somatic mosaicism is even more challenging to be identified and it can be testified only by multiple tissue analysis. One of the message that can be retrieved is that liquid biopsy could be always done in a setting in which comparison with genomic DNA is possible, which is usually genetic consultation.

Misinterpreting a germline mutation (which could appear in a percentage around 50 or more) or a somatic mosaicism (which could appear in any percentage below 50%) for a clonal mutation has serious practical consequences within personalized medicine. Germline mutation could be a useful target in early phase of the disease but somatic growing mutated clones are the main targets at disease progression. Targeting the germline mutation, although not dangerous itself, could not generate effect on outcome; hence somatic/germline misinterpretation could have fatal consequences for the patient leading in turn to underestimation of personalized medicine power.

To our knowledge, this is the first manuscript focusing on specific clonal evolution using at least two points of consecutive ctDNA analysis in a histotype unselected cohort of metastatic cancer patients. Figure 3 clearly shows that not 100% of mutated clones are still there at the second liquid biopsy. Failed personalized treatment toward those clones not persisting/not growing could be misinterpreted as failure of personalized medicine. Therefore, the second main take of message of this paper is to pay attention to start a personalized treatment only after a second cfDNA check confirming the presence/growing of targeted mutated clones.

5 | CONCLUSIONS

In conclusion, our results indicate that cfDNA two-point-NGS analysis of cancer driver genes could be an efficacy tool for precision oncology. Indeed, the identification of key mutations that are responsible for tumor growth allows optimizing the therapeutic choice by addressing targeted therapy against specific driver mutation(s) of growing clones. This strategy may be the only one needed to win the war on individual patient.

ACKNOWLEDGMENTS

The authors thank the Regione Toscana - Istituto Toscano Tumori (ITT) for their support (Project "Identification of genetic bases of individual predisposition to lung cancer in non-smokers") and from ASSO (Associazione per lo Sviluppo della Scienza Oncologica) onlus. This work is generated within the ERN-EURACAN (European network for Rare adult solid Cancer). We thank SienaGenTest srl, a Spin-off of the University of Siena (www.sienagentest.dbm.unisi.it) for bioinformatic analysis of genetic data.

CONFLICT OF INTERESTS

The authors declare that they have no competing interests.

AUTHORS' CONTRIBUTIONS

MP performed the experiments, analyzed the data, and wrote the paper, FF and AF took care of the clinical part of the study and wrote the paper, RT and EG performed experiments on blood, tumoral tissue, and metastasis. AR designed the research strategy, analysed the data, and wrote the paper, EF analysed the data and wrote the paper, MB, AMP, and MAM performed genetic counselling and provided patient samples. TH, DG, EC, and MM took care of the patients at first need. SM, CB, STM, IM, PT, RP, and AV were the oncologists.

DATA AVAILABILITY STATEMENT

The data that support the findings of this study are available from the corresponding author upon reasonable request.

ORCID

Alessandra Renieri https://orcid.org/0000-0002-0846-9220

REFERENCES

1. Ghatalia P, Smith CH, Winer A, et al. Clinical utilization pattern of Liquid Biopsies (LB) to detect actionable driver mutations, guide treatment decisions and monitor disease burden during treatment of 33 metastatic colorectal cancer (mCRC) patients (pts) at a Fox Chase Cancer Center GI Oncology Subspecialty Clinic. *Front Oncol*. 2019;17(8):652.
2. Mossner M, Jann JC, Wittig J, et al. Mutational hierarchies in myelodysplastic syndromes dynamically adapt and evolve upon therapy response and failure. *Blood*. 2016;128:1246-1259.
3. Fouillet L, Daguenet E, Schein F, Tavernier E, Flandrin-Gresta P, Cornillon J. Clonal evolution of myelofibrosis treated with hematopoietic transplantation, using RUXOLITINIB for chronic GvHD: a case report. *Current Research in Translational Medicine*. 2018;66:111-113.
4. Pinto AM, Papa FT, Frullanti E, et al. Low-level TP53 mutational load antecedes clonal expansion in chronic lymphocytic leukaemia. *Br J Haematol*. 2019;184(4):657-659.
5. Jacoby MA, Duncavage EJ, Chang GS, et al. Subclones dominate at MDS progression following allogeneic hematopoietic cell transplant. JCI. *Insight*. 2018;3(5):e98962.
6. Trédan O, Wang Q, Pissaloux D, et al. Molecular screening program to select molecular-based recommended therapies for metastatic cancer patients: analysis from the ProfiLER trial. *Ann Oncol*. 2019;30(5):757-765.
7. Castro-Giner F, Gkountela S, Donato C, et al. Cancer diagnosis using a liquid biopsy: challenges and expectations. *Diagnostics*. 2018;8(2):31.

8. Adalsteinsson VA, Ha G, Freeman SS, et al. Scalable whole-exome sequencing of cell-free DNA reveals high concordance with metastatic tumors. *Nat Commun*. 2017;8(1):1324.
9. Koeppel F, Blanchard S, Jovelet C, et al. Whole exome sequencing for determination of tumor mutation load in liquid biopsy from advanced cancer patients. *PLoS ONE*. 2017;12(11):e0188174.
10. Shu Y, Wu X, Tong X, et al. Circulating tumor DNA mutation profiling by targeted next generation sequencing provides guidance for personalized treatments in multiple cancer types. *Sci Rep*. 2017;7(1):583.
11. Corcoran RB, Chabner BA. Application of cell-free DNA analysis to cancer treatment. *N Engl J Med*. 2018;379(18):1754-1765.
12. Buono G, Gerratana L, Bulfoni M, et al. Circulating tumor DNA analysis in breast cancer: is it ready for prime-time? *Cancer Treat Rev*. 2019;73:73-83.
13. US Food & Drug Administration. Cobas EGFR Mutation Test v2. 2016. http://www.fda.gov/Drugs/InformationOnDrugs/ApprovedDrugs/ucm504540.htm.
14. R Core Team. R: A language and environment for statistical computing. Vienna, Austria: *R Foundation for Statistical Computing*; 2016. http://www.R-project.org/.
15. Therneau T. A Package for Survival Analysis in S. version 2.38. 2015. https://CRAN.R-project.org/package=survival.
16. Chan TA, Yarchoan M, Jaffee E, et al. Development of tumor mutation burden as an immunotherapy biomarker: utility for the oncology clinic. *Ann Oncol*. 2019;30(1):44-56.
17. De Mattos-Arruda L, Caldas C. Cell-free circulating tumour DNA as a liquid biopsy in breast cancer. *Mol Oncol*. 2016;10:464-474.
18. Rossi G, Mu Z, Rademaker AW, et al. Cell-free DNA and circulating tumor cells: comprehensive liquid biopsy analysis in advanced breast. *Cancer. Clin Cancer Res*. 2017;24(3):560-568.
19. Li BT, Janku F, Jung B, et al. Ultra-deep next-generation sequencing of plasma cell-free DNA in patients with advanced lung cancers: results from the Actionable Genome Consortium. *Ann Oncol*. 2019;00:1-7.
20. Sun P, Chen C, Xia Y, et al. Mutation profiling of malignant lymphoma by next-generation sequencing of circulating cell-free DNA. *J Cancer*. 2019;10(2):323-331.
21. Lee J, Franovic A, Shiotsu Y, et al. Detection of ERBB2 (HER2) gene amplification events in cell-free DNA and response to anti-HER2 agents in a large asian cancer patient cohort. *Front. Oncol*. 2019;9:212.
22. Formisano L, Lu Y, Servetto A, et al. Aberrant FGFR signaling mediates resistance to CDK4/6 inhibitors in ER+ breast cancer. *Nature Communication*. 2019;10:1373.

SUPPORTING INFORMATION

Additional supporting information may be found online in the Supporting Information section.

How to cite this article: Palmieri M, Baldassarri M, Fava F, et al. Two-point-NGS analysis of cancer genes in cell-free DNA of metastatic cancer patients. *Cancer Med*. 2020;9:2052–2061. https://doi.org/10.1002/cam4.2782

3.4 *A pilot study of next generation sequencing-liquid biopsy on cell-free DNA as a novel non-invasive diagnostic tool for Klippel-Trenaunay syndrome*

eck for updates

Original Article

Vascular

Vascular
0(0) 1–7
© The Author(s) 2020
Article reuse guidelines:
sagepub.com/journals-permissions
DOI: 10.1177/1708538120936421
journals.sagepub.com/home/vas
SAGE

A pilot study of next generation sequencing–liquid biopsy on cell-free DNA as a novel non-invasive diagnostic tool for Klippel–Trenaunay syndrome

Maria Palmieri[1], Anna Maria Pinto[2], Laura di Blasio[3,4], Aurora Currò[1,2], Valentina Monica[3,4], Laura Di Sarno[1], Gabriella Doddato[1,2], Margherita Baldassarri[2], Elisa Frullanti[1], Annarita Giliberti[1,2], Benedetta Mussolin[3], Chiara Fallerini[1,2], Francesco Molinaro[5], Massimo Vaghi[6], Alessandra Renieri[1,2] and Luca Primo[3,4]

Abstract

Objectives: Somatic mosaicism of *PIK3CA* gene is currently recognized as the molecular driver of Klippel–Trenaunay syndrome. However, given the limitation of the current technologies, *PIK3CA* somatic mutations are detected only in a limited proportion of Klippel–Trenaunay syndrome cases and tissue biopsy remains an invasive high risky, sometimes life-threatening, diagnostic procedure. Next generation sequencing liquid biopsy using cell-free DNA has emerged as an innovative non-invasive approach for early detection and monitoring of cancer. This approach, overcoming the space-time profile constraint of tissue biopsies, opens a new scenario also for others diseases caused by somatic mutations.

Methods: In the present study, we performed a comprehensive analysis of seven patients (four females and three males) with Klippel–Trenaunay syndrome. Blood samples from both peripheral and efferent vein from malformation were collected and cell-free DNA was extracted from plasma. Tissue biopsies from vascular lesions were also collected when available. Cell-free DNA libraries were performed using Oncomine™ Pan-Cancer Cell-Free Assay. Ion Proton for sequencing and Ion Reporter Software for analysis were used (Life Technologies, Carlsbad, CA, USA).

Results: Cell-free circulating DNA analysis revealed pathogenic mutations in *PIK3CA* gene in all patients. The mutational load was higher in plasma obtained from the efferent vein at lesional site (0.81%) than in the peripheral vein (0.64%) leading to conclude for a causative role of the identified variants. Tissue analysis, available for one amputated patient, confirmed the presence of the mutation at the malformation site at a high molecular frequency (14–25%), confirming its causative role.

Conclusions: Our data prove for the first time that the cell-free DNA-next generation sequencing–liquid biopsy, which is currently used exclusively in an oncologic setting, is indeed the most effective tool for Klippel–Trenaunay syndrome diagnosis and tailored personalized treatment.

Keywords

Slow-flow vascular malformations, *PIK3CA* mutation, non-invasive technique, vascular system injuries, cell-free DNA-next generation sequencing–liquid biopsy, Klippel–Trenaunay syndrome

[1]Medical Genetics, University of Siena, Siena, Italy
[2]Genetica Medica, Azienda Ospedaliera Universitaria Senese, Siena, Italia
[3]Candiolo Cancer Institute FPO-IRCCS, Candiolo, Italy
[4]Department of Oncology, University of Torino, Torino, Italy
[5]Chirurgia Pediatrica, Azienda Ospedaliera Universitaria Senese, Siena, Italia
[6]Chirurgia Vascolare, Ospedale Maggiore di Crema, Largo Ugo Dossena, Italy

Corresponding author:
Alessandra Renieri, Medical Genetics Unit, University of Siena, Policlinico "Santa Maria alle Scotte", Viale Bracci, 2, 53100 Siena, Italy.
Email: alessandra.renieri@unisi.it

Introduction

Klippel–Trenaunay syndrome (KTS) is a sporadic congenital disorder characterized by slow-flow vascular malformations mainly involving lower extremities and often accompanied by localized overgrowth.[1,2] The three diagnostic criteria of KTS are capillary nevus, early onset of varicosities, and hypertrophy of soft tissue and bones.[3] KTS has been previously associated with missense activating mutations in a *VG5Q* susceptibility gene, a powerful angiogenic factor involved in vessels formation.[4] However, Luks et al.[5] have recently reported that up to 90% of patients with classic Klippel–Trenaunay–Weber syndrome carry *PIK3CA* somatic activating mutations in pathological lesions.[5] These *PIK3CA* variants have been previously described as gain-of-function mutations in cancer.

PIK3CA encodes the 110-kD catalytic subunit of PI3K (p110a), which, in response to tyrosine kinase receptor-ligand binding, is activated and converts phosphatidylinositol (4,5)-bisphosphate to phosphatidylinositol phosphatidylinositol (3,5)-triphosphate. This leads to AKT activation, which increases cell proliferation through mTOR1, with tissue overgrowth.[6] E542K and E545K are the most frequent mutations in patients with KTS.[7,8] During the last years, next generation sequencing (NGS)–liquid biopsy has emerged as an innovative non-invasive technique for the identification of key mutations that are responsible for tumor growth allowing to optimize diagnosis, monitoring, and therapeutic choice.[9–11] Therefore, cell-free DNA (cfDNA) analysis overcomes the space-time profile constraint of physical biopsies and opens a new scenario for vascular malformations where tissue biopsy represents an invasive high risky, sometimes life-threatening, diagnostic procedure. The use of liquid biopsy would also improve the opportunities to check illness evolution on a molecular basis.

In the present study, we performed a comprehensive analysis of seven patients with KTS to determine if non-invasive NGS–liquid biopsy from the efferent vein at the lesional site could detect the key variant bypassing the need for a highly risky life-threatening tissue biopsy. NGS–liquid biopsy from the efferent vein at the vascular malformation site detected pathogenic mutations in *PIK3CA* gene in each patient. All of the identified mutations have already been described as responsible of KTS.[5] The mutational load was higher at the lesional level leading to conclude for a causative role of the identified variants.

Material and methods

Patients' enrollment and samples collection

Seven patients affected by KTS were enrolled at the Medical Genetics Unit of the Azienda Ospedaliera Universitaria Senese, Siena, Italy, for a new diagnostic approach. This study was consistent with Institutional guidelines and approved by the ethical committees of Azienda Ospedaliera Senese, Siena (Ethics Committee, Prot Name GeVaMa_2015, v.4_21-02–2020). Written informed consent for genetic analysis was obtained from all patients. Clinical information as well as genealogic trees and cancer family history were collected on a genetic consultation setting. The collection of samples from peripheral vein was carried out in Siena, while liquid biopsy from the lesion efferent vein was performed by Vascular Surgery of Ospedale Maggiore di Crema. For patient 2, different specimens from the stump were archived as FFPE (Formalin Fixed Paraffin Embedded) tissues as well as frozen in OCT (Optimal Cutting Temperature) compound.

Patient's characteristics. This is a two-year study in which patients were enrolled based on Klippel–Trenaunay diagnosis. Gender and age were not considered as exclusion criteria. The diagnostic features shared by all patients are congenital low-flow vascular malformation of lower, upper limb, or facial region; congenital "port wine stain" angioma; and hypertrophy. Patient 3 presented with splenectomy and referred small dilated vessels at the lung level, patient 4 lymphangitis and intestinal lymphangiomatosis.

Genomic DNA extraction from tissues

For patient 2, gDNA (genomic DNA) and total RNA were extracted from slices of different tissues frozen in OCT compound with AllPrep DNA/RNA Mini Kit (Qiagen, Hilden, Germany) following manufacturer's instructions.

cfDNA extraction from plasma

Blood samples (10 ml) were collected and placed into cfDNA BCT® blood collection tube (Streck, La Vista, NE, USA). cfDNA was extracted from 4 ml of plasma using MagMAX cell-free Total Nucleic Acid Isolation Kit (Thermo Fisher Scientific, Waltham, MA, USA), according to manufacturer's instructions. cfDNA quality and quantity was verified respectively using the Agilent™ High Sensitivity DNA Kit (Agilent Technologies, Palo Alto, CA) on Agilent2100 Bioanalyzer (Agilent Technologies) and Qubit™ dsDNA HS Assay Kits on Qubit 2.0 fluorometer (Invitrogen, Carlsbad, CA, USA).

Plasma sample from patient 2 was obtained as described in Palmieri et al.[9] Briefly, at least 10 ml of whole blood was collected in EDTA tubes. Plasma was separated within 5 h through two different centrifugation steps (10' × 1600 *g* and 10' × 3000 *g* at RT),

obtaining at least 3 ml of plasma. cfDNA was extracted from 1 ml plasma using the Maxwell RSC ccfDNA Plasma Kit (Promega, Madison, WI, USA) with the automated Maxwell RSC Instrument (Promega) according to the manufacturer's instructions.

NGS sequencing on cfDNA

The library was set up through two polymerase chain reaction (PCR) cycles in accordance with the manufacturer's instructions in order to increase the number of target amplicons and to allow binding of specific barcodes. Each cfDNA amplified fragments of a single pool has a unique barcode type.

CfDNA sequencing was performed using Oncomine™ Pan-Cancer Cell-Free Assay (Thermo Fisher Scientific) on Ion Proton sequencer (Life Technologies, Carlsbad, CA, USA). This technology is able to identify single nucleotide variants, insertions/deletions, gene fusions, and copy number variations in cancer-related genes (clinical actionable mutations) with a reportable range up to 0.05%. Sequencing analysis was performed using Ion Reporter Server System (Thermo Fisher Scientific). Study design is shown in Figure 1.

PCR and droplet digital PCR

Sanger sequencing was performed in all patients. The DNA was amplified by PCR on exon 3 of *VG5Q* gene (NM_0108046.4) using specific primer pairs (Forward 5'-gccagtgttttgtagttaagtc-3'; Reverse 5'-ctgttctatcggtaccagggt-3'—designed on Primer 3web; version 4.1.0) and PCR products were sequenced employing ABI PRISM3130 Genetic Analyzer (Applied Biosystems, Foster City, CA, USA) and data were analyzed with Sequencher software V.4.9 (Gene Codes, Ann Arbor, MI, USA).

cfDNA and gDNA from patient 2 were amplified using droplet digital (dd) PCR Supermix for Probes (Bio-Rad) using *PIK3CA* (PrimePCR ddPCR Mutation Assay, Bio-Rad) ddPCR assays for E542K point mutation. ddPCR was then performed according to manufacturer's protocol, and the results were reported as the percentage or fractional abundance of mutant DNA alleles to total (mutant plus wild-type) DNA alleles.[11]

Hematoxylin and eosin staining

Different specimens taken from the patient 2's stump were formalin-fixed and embedded in paraffin and then serially cut (10 μm) and rehydrated through 100% xylene and 100, 95, and 70% ethanol before immersion in H_2O. Sections were then stained with hematoxylin and eosin (H&E) and dehydrated.

Results

Patient 1, a 55-year-old female, has previously undergone several interventions of sclerotherapy. NGS–liquid biopsy analysis on cfDNA from peripheral vein revealed a pathogenic mutation in *PIK3CA* gene (c.1634A > G; p.(Glu545Gly)) with VAF (Variant Allele Frequency) of 0.23%.

Patient 2, a 34-year-old woman, reported frequent bleeding events and inability to walk because of intractable knee flexion and foot extension, which led to limb

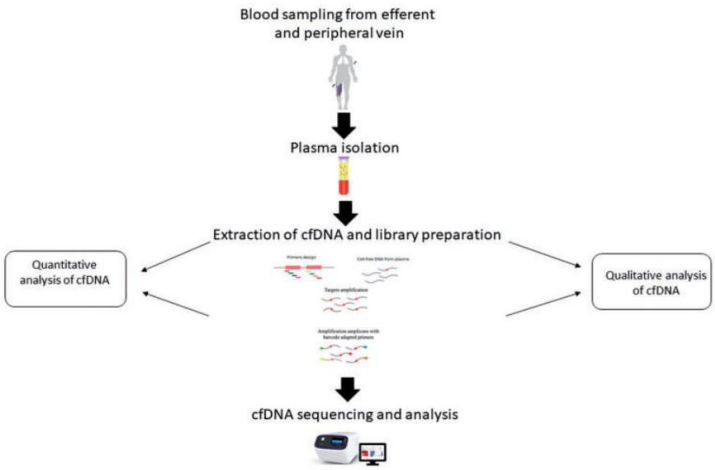

Figure 1. Study design flowchart.
cfDNA: cell-free DNA.

amputation and lower limb prosthesis. At the time of amputation surgery of patient 2, several surgical specimens were collected from the amputee leg. Figure 2(b) shows H&E staining of samples 1 ((b) I mainly adipose tissue) and 2 ((b) II adipose and connective). NGS analysis was performed on different specimens from the stump: samples 1 and 2 cited above, sample 3 (adipose and connective tissue taken from another site), and sample 4 (efferent vein). Targeted NGS analysis indicated presence of *PIK3CA* oncogenic point mutation (c.1624G > A; p.(Glu542Lys) in three out of four samples (1, 2, and 4, Figure 2(c)). These results were confirmed by ddPCR with fractional abundance as indicated in Figure 2(c). Blood of patient 2 was collected during surgery from peripheral vein and cfDNA was extracted from plasma and analyzed by ddPCR for the p.Glu542Lys mutation of *PIK3CA*. As indicated in Figure 2(c), positivity in plasma was found with low frequency (0.71%). One year after surgery, NGS–liquid biopsy analysis was performed and the same mutation in *PIK3CA* gene (c.1624G > A; (p.Glu542Lys)) was detected with VAF of 0.21% and 0.75% in the peripheral and efferent veins, respectively.

Patient 3, a 45-year-old male, underwent several debulking surgeries and sclerotherapy interventions. NGS–liquid biopsy analysis detected in *PIK3CA* gene (c.1633G > A; p.(Glu545Lys)) the mutation with a VAF of 0.18% from the efferent vein.

Patient 4, a 61-year-old male, has a *PIK3CA* c.1357G > A; p.(Glu453Lys) mutation in NGS–liquid biopsy analysis detected with a VAF of 0.36% from the peripheral vein. Due to thrombosis, the efferent vein material was not available.

Patient 5, a 58-year-old female, had congenital angiomas of the oropharyngeal and facial region, that underwent surgery, and uterine, abdominal, and left arm angiomas with slight general asymmetry between the two sides of the body. NGS–liquid biopsy analysis detected the *PIK3CA* mutation c.2176G > A; p.(Glu726Lys) with a VAF of 1.09% from the efferent vein.

Patient 6, a 26-year-old female, has congenital angiomas of the right upper limb and lymphatic anomalies

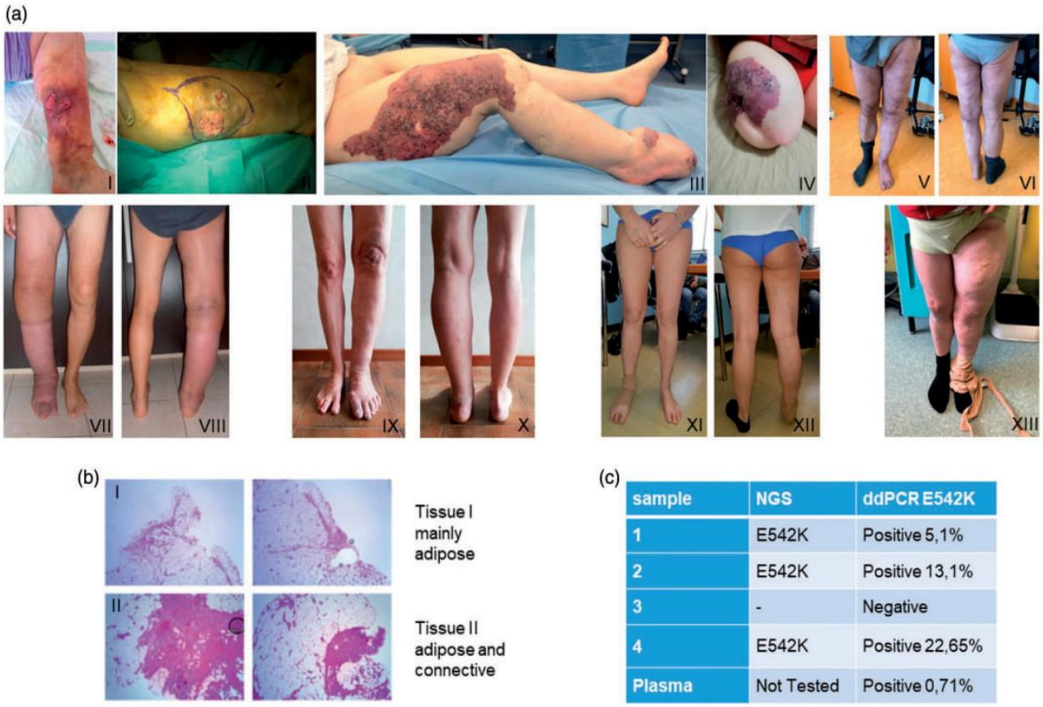

sample	NGS	ddPCR E542K
1	E542K	Positive 5,1%
2	E542K	Positive 13,1%
3	-	Negative
4	E542K	Positive 22,65%
Plasma	Not Tested	Positive 0,71%

Figure 2. (a) Clinical features of the patients. (I) and (II): Patient 1; right lower limb vascular malformation with leg ulceration; (III) and (IV): Patient 2; right low limb before intervention (c) and thigh stump (d). The amputation was performed for functional reason; (V) and (VI): Patient 3; left lower limb angioosteo hypertrophy; (VII) and (VIII): Patient 4; right lower limb angioosteo hypertrophy; (IX) and (X): Patient 5; left lower limb angioosteo hypertrophy; (XI) and (XII): Patient 6; right lower limb angioosteo hypertrophy; and (XIII): Patient 7; left lower limb angioosteo hypertrophy. (b) and (c) Hematoxylin and eosin staining and percentage of *PIK3CA*. Hematoxylin and eosin staining in four tissue biopsies of patient 2 (b). *PIK3CA* mutation analysis in different tissues from patient 2. Hematoxylin and eosin staining of mainly adipose tissue (b,I), adipose and connective (b,II). Percentage of *PIK3CA* mutation in four tissue biopsies of patient 2 (c).

of the right lower limb. The *PIK3CA* c.3129G > A; p.(Met1043Ile) mutation in NGS–liquid biopsy analysis was detected with a VAF of 1.47% from peripheral vein.

Patient 7, a 38-year-old male, has a severe asymmetry necessitating the hip prosthesis in order to reduce walking difficulty. The same pathogenic mutation in *PIK3CA* gene (c.1633G > A; p.(Glu545Lys)), previously identified in patient 3, was identified in this patient with a VAF of 0.96% and 1.23% respectively from the peripheral and efferent veins.

All patients were negative for the E133K variant in *VG5Q* gene. Clinical features and molecular findings are shown in Figure 2(a) and Table 1.

Discussion

Somatic missense mutations in *PIK3CA* are frequent in ovarian, breast, colorectal, brain, lung, and many other tumors.[12] This gene is known to be involved in the PI3 Kinase/AKT signaling pathway which plays an import role in cell growth and proliferation.[13] Gain-of-function mutations in *PIK3CA* generate an oncogene. The majority of activating *PIK3CA* mutations map to three sites: exon 9, codons 542 and 545 in the helical domain, and exon 20, codon 1047 in the kinase domain.[12] In ovarian cancer, most frequently the mutations occurred at codon 545 and 1043. For breast cancer, the mutations occurred at codon 542.[14] These well-known mutations in tumors have also been reported in vascular malformations which are a non-tumor subset of vascular anomalies probably due to a dysmorphogenesis in the developmental process. Causative genes have been identified not only for hereditary forms such as HHT[15] but also of sporadic ones such as Parkes-Weber syndrome.[16] Although molecular causes involved in the pathogenesis begin to be clarified, in most cases, the causative gene is not known. Furthermore, in the past decade, studies carried out through massive parallel sequencing techniques on DNA extracted from the lesional tissue have shown that somatic mutations localized at the malformation site may be responsible for the clinical phenotype. In particular, *PIK3CA* somatic mutations are recently being reported as the genetic cause of the overgrowth-related syndromes, now so-called PROS (*PIK3CA*-related overgrowth syndromes), including the Klippel–Trenaunay syndrome.[5] This finding highlighted the importance of carrying out targeted molecular diagnosis on biopsy specimen of affected tissues.

In view of the frequent inaccessibility of vascular tissues due to the invasiveness of solid biopsy, we evaluated the efficacy of detecting cfDNA fragments released into the bloodstream from the affected tissue. Circulating cfDNA analysis revealed pathogenic mutations in *PIK3CA* gene in all patients with two of them sharing the same mutation (c.1634A > G; p.(Glu545Gly)). Tissue analysis, available for two, confirmed the presence of the mutation at the malformation site at a high molecular frequency (14–25%), confirming its causative role.

Our data prove that in the new era of precision medicine, this novel approach, based on the combination of NGS and liquid biopsy from the efferent vein at the vascular malformation site, allows to detect even low-grade somatic mosaicism responsible for the vascular phenotype, thus bypassing the need for a highly risky tissue biopsy.

The diagnostic use of liquid biopsy for non-oncologic diseases would forward the development of

Table 1. Patient clinical features and *PIK3CA* molecular findings.

Patient	Code number	Gender	Age (years)	Phenotype	Limbs hypertrophy	Vascular nevi/ port-wine stain	Varicose vein	Peripheral NGS–liquid biopsy	Efferent vein NGS–liquid biopsy
1	2576/19	F	55	KTS monolateral	dx leg	No	Yes	(p.(E545G)) 0.23%	na
2	2968/19	F	34	KTS monolateral; pancreatic cystadenoma	dx leg	Port-wine stain	Yes	(p.(E542K)) 0.21%	(p.(E542K)) 0.75%
3	4263/19	M	45	KTS bilateral	both legs	Vascular nevi	Yes	na	(p.(E545K) 0.18%
4	5075/19	M	61	KTS monolateral with dx foot macrodactyly	dx leg	Vascular nevi	Yes	(p.(E453K)) 0.36%	na
5	4893/19	F	58	KTS monolateral	sx leg	Vascular nevi	Yes	na	(p.(E726K))1.09%
6	165/20	F	26	KTS monolateral	dx limbs	Vascular nevi	Yes	(p.(M1043I)) 1.47%	na
7	534/20	M	38	KTS monolateral	sx leg	no	Yes	(p.(E545K)) 0.96%	(p.(E545K)) 1.23%

NGS: next generation sequencing; KTS: Klippel–Trenaunay syndrome.

personalized therapeutic approach for KTS. Several preclinical and clinical studies show the efficacy of *PIK3CA* inhibitors in tumors harboring *PIK3CA* activating mutations. Presently, there are 40 studies on ClinicalTrial.gov on Alpelisib alone or in combination with other chemotherapeutics, recruiting patients with breast cancer, head and neck squamous cell cancer, colon and pancreatic cancer with promising results on safety and efficacy.[17,18] Notably, it has been recently reported that BYL719 (Alpelisib) administered at a dosage of 250 mg per day (the lowest used in clinical trials) for 540 days, is clinically effective, with a promising safety profile, in patients with overgrowth syndrome regardless of the type of *PIK3CA* mutation.[19]

Identifying KTS patients with overgrowth and vascular lesions *PIK3CA*-driven by liquid biopsy, in non-invasive manner, could open new therapeutic strategies, which could slow down or regress the disease and gives the possibility to monitor the evolution of the illness.

Acknowledgements

We thank KTS patients and ILA association (Italian association on Angiodysplasias). The EuroBioBank network provided us with specimens. We thank SienaGenTest srl, a Spin-off of the University of Siena (www.sienagentest.dbm.unisi.it) for assessment of data analysis.

Authors' contribution

AR and LP have made substantial contributions to conception and design, acquisition of data, analysis and interpretation of data, and have been involved in drafting the manuscript. MP and LDS performed the experiments, analyzed the data, and wrote the manuscript. EF analyzed the data and wrote the manuscript. MV, AC, MB, and AMP took care of the clinical part of the study and wrote the manuscript. AG, GD, and CF have made substantial contributions to data analysis. LDB and VM have made substantial contributions to histological analysis and interpretation. BM produced ddPCR and ctDNA data. FM was involved in clinical evaluation.

Declaration of conflicting interests

The author(s) declared no potential conflicts of interest with respect to the research, authorship, and/or publication of this article.

Funding

The author(s) disclosed receipt of the following financial support for the research, authorship, and/or publication of this article: This work was supported by ILA association (Italian association on Angiodysplasias). The "Cell lines and DNA bank of Rett Syndrome, X-linked mental retardation, and other genetic diseases", member of the Telethon Network of Genetic Biobanks (project no. GTB12001 and GFB18001) was funded by Telethon Italy.

ORCID iDs

Aurora Currò https://orcid.org/0000-0002-7321-9148
Alessandra Renieri https://orcid.org/0000-0002-0846-9220

References

1. Klippel M and Trénaunay P. Du naevus variqueux ostéohypertrophique. *Arch Gén Méd* 1900; 3: 641–672.
2. Sharma D, Lamba S, Pandita A, et al. Klippel–Trénaunay syndrome – a very rare and interesting syndrome. *Clin Med Insights Circ Respir Pulm Med* 2015; 9: 1–4.
3. Berry SA, Peterson C, Mize W, et al. Klippel–Trenaunay syndrome. *Am J Med Genet* 1998; 79: 319–326.
4. Tian XL, Kadaba R, You SA, et al. Identification of an angiogenic factor that when mutated causes susceptibility to Klippel–Trenaunay syndrome. *Nature* 2004; 427: 640–645.
5. Luks VL, Kamitaki N, Vivero MP, et al. Lymphatic and other vascular malformative/overgrowth disorders are caused by somatic mutations in PIK3CA. *J Pediatr* 2015; 166: 1048–1054.e1–5.
6. Vahidnezhad H, Youssefian L and Uitto J. Klippel–Trenaunay syndrome belongs to the PIK3CA-related overgrowth spectrum (PROS). *Exp Dermatol* 2016; 25: 17–19.
7. Mirzaa GM and Dobyns WB. The "megalencephaly-capillary malformation" (MCAP) syndrome: the nomenclature of a highly recognizable multiple congenital anomaly syndrome. *Am J Med Genet A* 2013; 161A: 2115–2116.
8. Keppler-Noreuil KM, Rios JJ, Parker VE, et al. PIK3CA-related overgrowth spectrum (PROS): diagnostic and testing eligibility criteria, differential diagnosis, and evaluation. *Am J Med Genet A* 2015; 167A: 287–295.
9. Palmieri M, Baldassarri M, Fava F, et al. Two point-NGS analysis of cancer genes in cell free-DNA of metastatic cancer patients. *Cancer Med* 2019; 6: 2052–2061.
10. Crowley E, Di Nicolantonio F, Loupakis F, et al. Liquid biopsy: monitoring cancer-genetics in the blood. *Nat Rev Clin Oncol* 2013; 10: 472–484.
11. Corcoran RB and Chabner BA. Application of cell-free DNA analysis to cancer treatment. *N Engl J Med* 2018; 379: 1754–1765.
12. Liao X, Morikawa T, Lochhead P, et al. Prognostic role of PIK3CA mutation in colorectal cancer: cohort study and literature review. *Clin Cancer Res* 2012; 18: 2257–2268.
13. Ma YY, Wei SJ, Lin YC, et al. PIK3CA as an oncogene in cervical cancer. *Oncogene* 2000; 19: 2739–2744.
14. Levine DA, Bogomolniy F, Yee CJ, et al. Frequent mutation of the PIK3CA gene in ovarian and breast cancers. *Clin Cancer Res* 2005; 11: 2875–2878.
15. McDonald J, Bayrak-Toydemir P and Pyeritz RE. Hereditary hemorrhagic telangiectasia: an overview of

diagnosis, management, and pathogenesis. *Genet Med* 2011; 13: 607–616.
16. Revencu N, Boon LM, Mulliken JB, et al. Parkes Weber syndrome, vein of Galen aneurysmal malformation, and other fast-flow vascular anomalies are caused by *RASA1* mutations. *Hum Mutat* 2008; 29: 959–965.
17. Dickler MN, Saura C, Richards DA, et al. Phase II study of taselisib (GDC-0032) in combination with fulvestrant in patients with HER2-negative, hormone receptor–positive advanced breast cancer. *Clin Cancer Res* 2018; 24: 4380–4387.
18. Mayer IA, Abramson VG, Formisano L, et al. Phase Ib study of alpelisib (BYL719), a PI3Kα-specific inhibitor, with letrozole in ER+/HER2-negative metastatic breast cancer. *Clin Cancer Res* 2017; 23: 26–34.
19. Venot Q, Blanc T, Rabia SH, et al. Targeted therapy in patients with PIK3CA-related overgrowth syndrome. *Nature* 2018; 558: 540–546.

3.5 *MET somatic activating mutations are responsible for lymphovenous malformation and can be identified using cell-free DNA next generation sequencing liquid biopsy*

ARTICLE IN PRESS

MET somatic activating mutations are responsible for lymphovenous malformation and can be identified using cell-free DNA next generation sequencing liquid biopsy

Maria Palmieri, MS,[a] Laura Di Sarno, MS,[a] Andrea Tommasi, MD,[a,b] Aurora Currò, MD,[a,b] Gabriella Doddato, MS,[a] Margherita Baldassarri, MD,[a] Elisa Frullanti, PhD,[a] Annarita Giliberti, MS,[a] Chiara Fallerini, PhD,[a] Aldo Arzini, MD,[c] Annamaria Pinto, MD,[b] Massimo Vaghi, MD,[c,d] *and* Alessandra Renieri, MD, PhD,[a,b] *Siena and Crema, Italy*

ABSTRACT

Objective: Germline mutations of either the endothelial cell-specific tyrosine kinase receptor TIE2 or the glomulin (*GLMN*) gene are responsible for rare inherited venous malformations. Both genes affect the hepatocyte growth factor receptor c-Met, inducing vascular smooth muscle cell migration. Germline mutations of hepatocyte growth factor are responsible for lymphatic malformations, leading to lymphedema. The molecular alteration leading to the abnormal mixed vascular anomaly defined as lymphovenous malformation has remained unknown.

Methods: A group of 4 patients with lymphovenous malformations were selected. Plasma was obtained from both peripheral and efferent vein samples at the vascular malformation site for cell-free DNA extraction. When possible, we analyzed tissue biopsy samples from the vascular lesion.

Results: We have demonstrated that in all four patients, an activating *MET* mutation was present. In three of the four patients, the same pathogenic activating mutation, T1010I, was identified. The mutation was found at the tissue level for the patient with tissue samples available, confirming its causative role in the lymphovenous malformations.

Conclusions: In the present study, we have demonstrated that cell-free DNA next generation sequencing liquid biopsy is able to identify the *MET* mutations in affected tissues. Although a wider cohort of patients is necessary to confirm its causative role in lymphovenous malformations, these data suggest that lymphovenous malformations could result from postzygotic somatic mutations in genes that are key regulators of lymphatic development. The noninvasiveness of the method avoids any risk of bleeding and can be easily performed in children. We are confident that the present pioneering results have provided a viable alternative in the future for lymphovenous malformation diagnosis, allowing for subsequent therapy tailored to the genetic defect. (J Vasc Surg: Venous and Lym Dis 2020;■:1-5.)

Keywords: cfDNA; Liquid biopsy; Lymphovenous malformation; *MET* mutation; Noninvasive technique

Among the venous anomalies, the two most represented subclasses are venous malformations (VMs) at ~95% and glomuvenous malformation at 5%.[1] Low-flow VMs result from an error in vascular morphogenesis. The TIE2 receptor tyrosine kinase was the first gene to be associated with inherited VM development. This receptor is located on chromosome 9p21 and is specific for endothelial cells.[2-5] TIE2, through action in ANGPT1 (angiopoietin 1), upregulates hepatocyte growth factor (HGF), leading to the abnormal growth of veins. Thus, mice overexpressing Angpt1 in the skin will develop more, larger, and more highly branched vessels.[6]

Loss of function mutations in the glomulin (*GLMN*) gene are responsible for the more rare hereditary glomuvenous malformations. They are mostly situated on the extremities and implicate the skin and subcutis but seldom the mucosa. Unlike other vein malformations, these multifocal, frequently hyperkeratotic, injuries will be painful on palpation and cannot be completely flattened by compression. The mode of inheritance is paradominant, with a second somatic alteration inducing the pathogenicity. Glomulin interacts with the HGF receptor c-Met, inducing vascular smooth muscle cell migration and angiogenesis.[7]

A common feature to all blood and lymphatic vessels is the presence of endothelial cells as the luminal cell layer. Dysfunction of the *LYVE1* and *VEGFR3* genes or *VEGF-C, VEGF-D, PROX1, NRP2*, and *ANGPT2* involved in lymphangiogenesis and/or lymphatic vessels could be potential candidates for lymphatic malformations.[1]

From the Medical Genetics, University of Siena,[a] and the Genetica Medica, Azienda Ospedaliera Universitaria Senese,[b] Siena; and the Chirurgia Vascolare, Ospedale Maggiore di Crema, Largo Ugo Dossena,[c] and the Radiologia interventistica, Ospedale Maggiore di Crema,[d] Crema.

The present study was supported by the Italian Association of Angiodysplasias and Childhood Hemangiomas (ILA).

Author conflict of interest: none.

Correspondence: Alessandra Renieri, MD, PhD, Medical Genetics, University of Siena, Policlinico "Santa Maria alle Scotte", Viale Bracci, 2, Siena 53100, Italy (e-mail: alessandra.renieri@unisi.it).

The editors and reviewers of this article have no relevant financial relationships to disclose per the Journal policy that requires reviewers to decline review of any manuscript for which they may have a conflict of interest.

2213-333X

Copyright © 2020 by the Society for Vascular Surgery. Published by Elsevier Inc.

https://doi.org/10.1016/j.jvsv.2020.07.015

HGF, and its receptor c-MET, previously unrecognized lymphedema genes, are attractive candidate genes for lymphedema.[8] HGF-mediated activation of cMet has promoted angiogenesis and lymphangiogenesis in cell models and in vivo.[9] Somatic-activating *MET* mutations have been identified in some cancers, including non–small-cell lung cancer and germline mutations in renal carcinoma.[10]

The mutations occur within the juxtamembrane region (T1010I and D1028N) and are known to be activating mutations identified rarely in lung cancer. Mutations occurring at *MET* exon 14, even if they do not produce juxtamembrane-missing variants, might be responsible for such neoplasms and, therefore, could be considered as exon 14 driver mutations, rather than as a polymorphism.[11] Human c-Met mutations can be studied in the nematode *Caenorhabditis elegans*, in which induction of the activating mutation p.T1010I will induce abnormal vulval development, vulval hyperplasia, and lower fecundity.[12]

Next generation sequencing (NGS)-liquid biopsy (LB) using cell-free DNA (cfDNA) is a novel approach that enables the early detection and monitoring of cancer.[13-15] The use of NGS-LB overcomes the space-time limit of tissue biopsies and represents a new possibility for diagnosing and monitoring vascular malformations due to somatic mosaicism.

Mosaic somatic mutations occur after the first zygotic divisions and exclusively affect specific cell lines. Thus, the cell lines harboring the variant will generate mutated tissues and the unmutated cell lines will develop normal tissues. Therefore, some anatomic areas will generate the disease and others will remain normal. Using NGS-LB, we identified a somatic activating mutation in p.T1010I and p.D1028N of the *MET* gene, not previously associated with VMs, although already known to be very well involved in the distrusted signalling pathway of both inherited VMs and glomuvenous malformations. The present study complied with institutional guidelines, and the ethics committees of the Azienda Ospedaliera Universitaria Senese, Siena, approved the present study (project name, GeVaMa_2015, v.4_21-02-2020).

METHODS

Patient enrollment and sample collection. At the Medical Genetics Unit of the Azienda Ospedaliera Universitaria Senese, Siena, Italy, we enrolled four patients with VM in the present study. In the context of the genetic counseling, informed consent, clinical data, genealogic trees, and family history were collected for each patient. For patient 3, the Division of Vascular Surgery, Ospedale Maggiore, Crema, collected blood samples from the efferent vein at the lesion site and different formalin-fixed paraffin-embedded (FFPE) tissue samples were stored until use.

ARTICLE HIGHLIGHTS

- **Type of Research**: Multicenter, prospective study
- **Key Findings**: Cell-free DNA next generation sequencing liquid biopsy was able to identify somatic mutations of the *MET* gene in all lymphovenous malformations investigated. The mutations were also confirmed at the tissue level when tissue samples were available.
- **Take Home Message**: Liquid biopsy applied to vascular malformations represents an innovative and effective approach capable of overcoming the limitations of tissue biopsy.

Obtaining cfDNA from plasma. For each patient, 10 mL of blood was collected in cfDNA BCT tubes (Streck, La Vista, Neb). The plasma was stored at −80°C until use. cfDNA extraction was performed from 4 mL of plasma using the MagMAX cell-free Total Nucleic Acid Isolation Kit (ThermoFisher Scientific, Waltham, Mass). The cfDNA quantity was assessed using the Qubit dsDNA High Sensitivity test kit and a Qubit 2.0 fluorometer (Invitrogen, Carlsbad, Calif). The quality was assessed using the Agilent High Sensitivity DNA kit (Agilent Technologies, Palo Alto, Calif) and an Agilent 2100 Bioanalyzer (Agilent Technologies).

NGS sequencing of cfDNA. The cfDNA library was set up using the Oncomine Pan-Cancer Cell-Free Assay gene panel (ThermoFisher Scientific), and sequencing was performed using the Ion Proton sequencer (Life Technologies, Carlsbad, Calif). The gene panel was designed to identify single nucleotide variants, insertions and deletions, gene fusions, and copy number variations to a detection limit of 0.05%. The Ion Reporter Server System (ThermoFisher Scientific) was used to perform variant analysis. The same panel was used to sequence genomic DNA (gDNA) from patient 3.

Hematoxylin and eosin staining. For patient 3, tissue samples had been taken from the right upper limb, FFPE, serially cut (10-μm sections), and rehydrated with 100% xylene and 100%, 95%, and 70% ethanol before immersion in water. The slices were then stained with hematoxylin and eosin and dehydrated.

gDNA extraction from tissues. For patient 3, gDNA was extracted from FFPE tissue samples using the MagCore Genomic DNA FFPE One-Step Kit for the MagCore System (Diatech Pharmacogenetics SRL, Ancona, Italy) following the manufacturer's instructions. gDNA was quantified using the Qubit Fluorometer and Qubit dsDNA High Sensitivity Assay (Life Technologies, Carlsbad, Calif).

Journal of Vascular Surgery: Venous and Lymphatic Disorders
Volume ■, Number ■

RESULTS

Patient 1 was a 26-year-old woman with angiomatous lesions on her forehead, perinasal and perioral regions, both hands, abdominal region, and left lower limb. Laser therapy on both upper and lower limbs was performed, with partial benefit for the hands. However, the laser therapy had caused ulcers in the lower limbs. A venous echocardiogram-color Doppler examination of the lower limbs showed mild ectasia of the great saphenous vein and insufficiency of the perforating veins, in addition to ectatic veins on the foot. The patient also reported skin fragility of the external auditory canal. The *MET* c.3029C>T p. (The1010Ile) mutation was detected with a variant allele frequency (VAF) of 0.32% from the peripheral vein using NGS-LB analysis.

Patient 2 was a 34-year-old woman with congenital angiomas of the left upper limb and left side of the chest. The patient reported congenital hypertrophy of her left upper limb, mainly at her hand and third finger. A previous spinal magnetic resonance imaging examination had revealed the presence of multiple dorsal neuromas. The patient also reported two lipomas, previous obesity, and troncular neuropathy of both median nerves. NGS-LB analysis detected the same pathogenic c.3029C>T p.(The1010Ile) mutation in the *MET* gene at a VAF of 0.97%.

Patient 3 was a 36-year-old woman with telangiectasias of the right hand. The first vascular surgery had been performed when she was 2 years old, with subsequent further interventions and progressive loss of function of the limb. Computed tomography scans showed a paravertebral mixed capillary lymphatic VM that extended along the right anterolateral chest wall and forearm. The malformation affected both the cutaneous and subcutaneous and the muscle tissues. *MET* mutation c. 3082G>A; p.(Asp1028Asn) was detected using NGS-LB analysis, with a VAF of 0.11%. For patient 3, we were also able to perform an analysis of the available tissue samples, which confirmed the existence of the mutation at the malformation site with a VAF of 0.011%, confirming its likely causative role in the lymphovenous malformations.

Patient 4 was a 61-year-old man with congenital angiodysplasia and right lower limb elephantiasis that extended up to the lumbar region. The lesion had increased in extent during adolescence, when the initial episode of lymphangitis had been reported. The patient also had intestinal lymphangiomatosis with episodes of gastrointestinal bleeding. Patient 4 also had features of Klippel-Trenaunay syndrome. *PIK3CA* c.1357G>A p.(Glu453Lys) and *MET* c.3029C>T, p.(The1010Ile) mutations were detected using NGS-LB analysis with a VAF of 0.36% and 0.09%, respectively. The clinical features and molecular results obtained for all 4 patients are shown in Fig and Table.

DISCUSSION

MET activation occurs through the binding of receptor tyrosine kinases and its ligand, HGF. This binding leads to activation of the downstream PI3K/mTOR (phosphoinositide 3-kinase/mammalian target of rapamycin), STAT (signal transducer and activator of transcription), and MAPK (mitogen-activated protein kinase) pathways. The erroneous Met/HGF regulation has been studied and demonstrated for various cancers. It leads to oncogenesis by increasing cell proliferation and survival, epithelial—mesenchymal transition, tumor invasion, and tumor angiogenesis.[16]

Several gene mutations, such as amplification, copy number variations, and dysregulation of pathways, can lead to *MET* signaling defects. Although rare, several *MET* mutations have been observed in the kinase domain, rather than in the juxtamembrane or extracellular domain, for several tumors.[17]

It is also essential to consider the alternative splicing that occurs in *MET* exon 14. Several alterations affecting exon 14 and adjacent intronic regions will induce splicing alterations, which will lead to different protein isoforms, including the isoform with exon 14 skipping.[11] Some of these aberrant RNA transcripts can, thus, modulate disease onset and progression.

The p.T1010I mutation is located in the juxtamembrane domain and causes greater cellular proliferation and less cell adhesion. Furthermore, when the domain has mutated, it will show an increase in cellular polarity and a more disordered cellular pattern and cytoarchitecture.

Previous evidence has shown the p.T1010I alteration in patients with cancer, in particular, in patients with thyroid cancer, and might reflect a *MET* exon 14 alteration rather than a polymorphism owing to its oncogenic characteristics.[17] The suspicion of a polymorphism was raised by a family history of papillary renal cell carcinoma in which the germline alteration did not segregate with the disease.[18]

The prevalence of the MET p.T1010I mutation in the population overall is 0.07% according to the Exome Aggregation Consortium and 1.1% in the European population. All 4 of our analyzed patients with a lymphovenous malformation had this mutation. Definitely, a larger cohort of patients is needed to establish with certainty the frequency of the identified variant among patients with lymphovenous malformations.

Exon 14 skipping mutations prolong *MET* oncogenic activity by inhibition of Met receptor degradation. This type of oncogenic event could have clinical effects and could provide therapeutic options for several cancer types. In mammary epithelium, the presence of p.T1010I resulted in the formation of cellular colonies, cell migration, and invasion in vitro and tumor growth and invasion in vivo.[19] Mahjoubi et al[20] reported a case of lung

Fig. Clinical features of the patients. Patient 1: angiomatosis in the hands **(A)**, abdomen **(B)**, and left lower limb **(C)**. Patient 2: diffuse venous and lymphatic malformations **(D-F)**. Patient 3: lymphatic malformation of the right forearm **(G)**. Patient 4: right lower limb angio-osteohypertrophy in Klippel-Trenaunay syndrome with prominent lymphatic involvement **(H-J)**.

adenocarcinoma with a *MET* exon 14 donor splice site mutation (D1028N) that had been treated with efficacy using crizotinib. The *MET* exon 14 skipping alteration is a pharmacological target of Met inhibitors, such as crizotinib, cabozantinib, and capmatinib, and/or another potent Met inhibitor, such as foretinib. Their use has resulted in dose-dependent inhibition of growth in c-MET–amplified cells, with concomitant induction of apoptosis. Thus, the use of Met inhibitors could be a new treatment approach for patients with cancer.[11,21]

At present, vascular malformations are treated by surgical removal or sclerotherapy. The latter involves the use of alcohol or toxic agents capable of destroying aberrant blood vessels. However, depending on the anatomic location of the malformation, both treatments can be inadequate, with regrowth occurring often. Thus, different treatment options are needed.

Given the invasiveness of performing a tissue biopsy and the inaccessibility of some vascular sites, we evaluated the efficacy of NGS-LB for detecting cfDNA fragments released by the malformation into the bloodstream. We compared the blood from the efferent venous sample with that from the peripheral venous sample. We found that the cfDNA was enriched with mutated fragments released from the cells in the vascular lesion, in line with a causative role of the identified mutation.

Therefore, this procedure allows for the detection of even low-grade mosaicism. cfDNA analysis revealed pathogenic variants in exon 14 of the *MET* gene. The tissue biopsy analysis, performed for patient 3, validated the alteration at the malformation site, confirming its likely causative role. The broad and variable phenotypic spectrum is related to the different allele frequency of the MET variant in each single. Furthermore, it is possible that the MET mutation is not the only mutation causing the disease. Also, it is likely that the concomitant presence of other mutations with different degrees of expression would contribute to and could explain the phenotypic variability.

Table. Patient clinical features and molecular findings

Pt. No.	Code No.	Gender	Age, years	Phenotype	Peripheral vein NGS-LB finding	Efferent vein NGS-LB finding
1	5410/19	Female	26	Diffuse extratroncular venous anomalies	*MET* [p.(T1010I)], 0.32%	NA
2	5543/19	Female	34	Diffuse disseminated venous cutaneous malformations associated with hypertrophy of fatty tissues	*MET* [p.(T1010I)], 0.97%	NA
3	5461/19	Female	36	Venous lymphatic malformation of upper right limb	NA	*MET* [p.(D1028N)], 0.11%
4	278/20	Male	61	Venous lymphatic malformations and Klippel-Trenaunay syndrome	*MET* [p.(T1010I)], 0.09%	NA

NA, Not applicable; *NGS-LB*, next generation sequencing liquid biopsy; *Pt. No.*, patient number.

CONCLUSIONS

From these data, we believe that the use of NGS-LB with blood samples from the efferent vein of the vascular malformation will allow for the identification of somatic mosaic mutations that have very low frequency and are the basis of the vascular phenotype. This approach overcomes the difficulty of tissue biopsy and enables the transition to precision medicine.

We thank the patients with vascular malformations who participated in the present study. The "cell lines and DNA bank of Rett syndrome, X-linked mental retardation and other genetic diseases," a member of the Telethon Network of Genetic Biobanks (project nos. GTB12001 and GFB18001), funded by Telethon Italy, and the EuroBioBank network provided us with specimens. We thank SienaGenTest SRL, a spinoff of the University of Siena (available at: www.sienagentest.dbm.unisi.it), for the assessment of the data analysis.

AUTHOR CONTRIBUTIONS

Conception and design: MV, AR
Analysis and interpretation: MP, LDS, EF, AP, MV, AR
Data collection: MP, LDS, AT, AC, GD, MB, EF, AG, CF, AA, AP, MV, AR
Writing the article: MP, LDS, AT, AC, GD, MB, EF, AG, CF, AP, MV, AR
Critical revision of the article: EF, AA, AP, MV, AR
Final approval of the article: MP, LDS, AT, AC, GD, MB, EF, AG, CF, AA, AP, MV, AR
Statistical analysis: Not applicable
Obtained funding: Not applicable
Overall responsibility: AR

REFERENCES

1. Uebelhoer M, Boon LM, Vikkula M. Vascular anomalies: from genetics toward models for therapeutic trials. Cold Spring Harb Perspect Med 2012;2:a009688.
2. Vikkula M, Boon LM, Carraway KL III, Calvert JT, Diamonti AJ, Goumnerov B, et al. Vascular dysmorphogenesis caused by an activating mutation in the receptor tyrosine kinase TIE2. Cell 1996;87:1181-90.
3. Wouters V, Limaye N, Uebelhoer M, Irrthum A, Boon LM, Mulliken JB, et al. Hereditary cutaneomucosal venous malformations are caused by TIE2 mutations with widely variable hyper-phosphorylating effects. Eur J Hum Genet 2010;18:414-20.
4. Brahami N, Subramaniam S, Al-Ddafari MS, Elkaim C, Harmand PO, Sari BE, et al. Facial cutaneo-mucosal venous malformations can develop independently of mutation of TEK gene but may be associated with excessive expression of Src and p-Src. J Negat Results Biomed 2017;16:9.
5. Natynki M, Kangas J, Miinalainen I, Sormunen R, Pietila R, Soblet J, et al. Common and specific effects of TIE2 mutations causing venous malformations. Hum Mol Genet 2015;24:6374-89.
6. Suri C, McClain J, Thurston G, McDonald DM, Zhou H, Oldmixon EH, et al. Increased vascularization in mice overexpressing angiopoietin-1. Science 1998;282:468-71.
7. Brouillard P, Vikkula M. Vascular malformations: localized defects in vascular morphogenesis. Clin Genet 2003;63:340-51.
8. Finegold DN, Schacht V, Kimak MA, Lawrence EC, Foeldi E, Karlsson JM, et al. HGF and MET mutations in primary and secondary lymphedema. Lymphat Res Biol 2008;6:65-8.
9. Nakagaw T, Sharma M, Nabeshima Y, Braun RE, Yoshida S. Functional hierarchy and reversibility within the murine spermatogenic stem cell compartment. Science 2010;328:62-7.
10. Giordano S, Maffe A, Williams TA, Artigiani S, Gual P, Bardelli A, et al. Different point mutations in the Met oncogene elicit distinct biological properties. FASEB J 2000;14:399-406.
11. Pilotto S, Gkountakos A, Carbognin L, Scarpa A, Tortora G, Bria E. MET exon 14 juxtamembrane splicing mutations: clinical and therapeutical perspectives for cancer therapy. Ann Transl Med 2017;5:2.
12. Siddiqui SS, Loganathan S, Krishnaswamy S, Faoro L, Jagadeeswaran R, Salgia RC. elegans as a model organism for in vivo screening in cancer: effects of human c-Met in lung cancer affect C. elegans vulva phenotypes. Cancer Biol Ther 2008;7:856-63.
13. Palmieri M, Baldassarri M, Fava F, Fabbiani A, Gelli E, Tita R, et al. Two point-NGS analysis of cancer genes in cell free-DNA of metastatic cancer patients. Cancer Med 2019;9:2052-61.
14. Crowley E, Di Nicolantonio F, Loupakis F, Bardelli A. Liquid biopsy: monitoring cancer-genetics in the blood. Nat Rev Clin Oncol 2013;10:472-84.
15. Corcoran RB, Chabner BA. Application of cell-free DNA analysis to cancer treatment. N Engl J Med 2018;379:1754-65.
16. Sylvester PW. Targeting met mediated epithelial-mesenchymal transition in the treatment of breast cancer. Clin Transl Med 2014;3:30.
17. Ma PC, Kijima T, Maulik G, Fox EA, Sattler M, Griffin JD, et al. c-MET mutational analysis in small cell lung cancer: novel juxtamembrane domain mutations regulating cytoskeletal functions. Cancer Res 2003;63:6272-81.
18. Schmidt L, Junker K, Nakaigawa N, Kinjerski T, Weirich G, et al. Novel mutations of the MET proto-oncogene in papillary renal carcinomas. Oncogene 1999;18:2343-50.
19. Liu S, Meric-Bernstam F, Parinyanitikul N, Wang B, Eterovic AK, Zheng X, et al. Functional consequence of the MET-T1010I polymorphism in breast cancer. Oncotarget 2015;6:2604-14.
20. Mahjoubi L, Gazzah A, Besse B, Lacroix L, Soria JC. A never-smoker lung adenocarcinoma patient with a MET exon 14 mutation (D1028N) and a rapid partial response after crizotinib. Invest New Drugs 2016;34:397-8.
21. Sohn SH, Kim B, Sul HJ, Choi BY, Kim HS, Zang DY. Foretinib inhibits cancer stemness and gastric cancer cell proliferation by decreasing CD44 and c-MET signaling. Onco Targets Ther 2020;13:1027-35.

Submitted Apr 15, 2020; accepted Jul 17, 2020.

3.6 ***Cell-free DNA next-generation sequencing liquid biopsy as a new revolutionary approach for arteriovenous malformation***

Check for updates

Cell-free DNA next-generation sequencing liquid biopsy as a new revolutionary approach for arteriovenous malformation

Maria Palmieri, MS,[a] Aurora Currò, MD,[a,b] Andrea Tommasi, MD,[a,b] Laura Di Sarno, MS,[b] Gabriella Doddato, MS,[a] Margheria Baldassarri, MD,[b] Elisa Frullanti, MS,[a] Ann Rita Giliberti, MS,[a] Chiara Fallerini, MS,[a] Angelo Spinazzola, MD,[c] Anna Maria Pinto, MD, PhD,[b] Alessandra Renieri, MD, PhD,[a,b] *and* Massimo Vaghi, MD,[c,d] *Siena and Crema, Italy*

ABSTRACT

Objective: Somatic mosaicism of *KRAS* gene is currently recognized as the only established molecular basis of arteriovenous malformations (AVM). However, given the limitations of the current technologies, *KRAS* somatic mutations are detected only in a limited proportion of AVMs and tissue biopsy remains an invasive high risky, sometimes life-threatening, diagnostic procedure. Next-generation sequencing liquid biopsy using cell-free DNA (cfDNA) has emerged as an innovative noninvasive approach for early detection and monitoring of cancer. This approach overcomes the space-time profile constraint of tissue biopsies opens a new scenario for vascular malformations owing to somatic mosaicism. Here, we propose a new approach as a fast noninvasive reliable tool in order to investigate the cfDNA coming from the AVMs.

Methods: A group of five patients suffering from AVM were selected. Blood samples from peripheral vein and efferent vein from vascular malformation were collected and cfDNA was extracted. The cfDNA libraries were performed using Oncomine Pan-Cancer Cell-Free Assay. We used Ion Proton for sequencing and Ion Reporter Software for analysis (Life Technologies, Carlsbad, Calif).

Results: In all cases, either G12D or G12V mutations in *KRAS* were identified. The mutational load was higher in the efferent vein than in peripheral blood, confirming the causative role of the identified mutation at a somatic level.

Conclusions: We demonstrate that cfDNA next-generation sequencing liquid biopsy is able to identify the *KRAS* mutation detected in affected tissues. Moreover, we have shown that blood sample withdrawal at the lesion site increases variant allele frequency with an order of magnitude above the limit of detection (usually 0.05%), decreasing the risk of a false negative. Finally, the noninvasiveness of the method avoids any risk of bleeding, being easily performed also in children. We propose this technique as the method of choice to better investigate AVMs and consequently to identify the therapy tailored to the genetic defect. (JVS—Vascular Science 2020;1:176-80.)

Clinical Relevance: This article highlights the importance of using liquid biopsy as a new method to investigate the molecular profile of AVMs. In view of the frequent inaccessibility of vascular tissues owing to the invasiveness of solid biopsy and the relative high incidence of biopsies with low diagnostic power, here we evaluated the efficacy of detecting cfDNA fragments released into the bloodstream from the affected tissue cells. Through a simple blood draw from the efferent vein at the vascular malformation site, the liquid biopsy allowed us to identify *KRAS* pathogenic mutations piloting a personalized therapeutic approach and opening a new scenario for new therapeutic strategies.

Keywords: Arteriovenous malformation; Liquid biopsy; cf-DNA; KRAS mutation; Noninvasive technique

Arteriovenous malformations (AVM) are fast-flow vascular malformations composed of tangles of abnormally developed vasculature. The absence of capillaries between arteries and veins often leads to high blood pressure and rupture. They can occur in some part of the body, including the brain.[1,2] In the majority of cases an activating *KRAS* mutation has been identified.[1-5] These *KRAS* variants have been previously described as

From the Medical Genetics, University of Siena,[a] and the Genetica Medica, Azienda Ospedaliera Universitaria Senese,[b] Siena; and the Radiologia interventistica, Ospedale Maggiore di Crema,[c] and the Chirurgia Vascolare, Ospedale Maggiore di Crema, Largo Ugo Dossena,[d] Crema.

Funded by ONG ILA.

Author conflict of interest: none.

Correspondence: Massimo Vaghi, MD, Chirurgia Vascolare, Ospedale Maggiore di Crema, Largo Ugo Dossena, Cremaa, Italy (e-mail: vaghim@yahoo.it); and Alessandra Renieri, MD, PhD, Medical Genetics Unit, University of Siena, Policlinico "Santa Maria alle Scotte", Viale Bracci, 2, 53100 Siena, Italy (e-mail: alessandra.renieri@unisi.it).

The editors and reviewers of this article have no relevant financial relationships to disclose per the JVS-Vascular Science policy that requires reviewers to decline review of any manuscript for which they may have a conflict of interest.

2666-3503

Copyright © 2020 by the Society for Vascular Surgery. Published by Elsevier Inc. This is an open access article under the CC BY-NC-ND license (http://creativecommons.org/licenses/by-nc-nd/4.0/).

https://doi.org/10.1016/j.jvssci.2020.08.002

gain-of-function mutations in cancer and Nikolaev et al[3] have recently shown that hot spot mutations in *KRAS*, namely p.G12V are associated with arteriovenous brain malformations through an increase in angiogenesis, migration and cell proliferation.[6] During the last years, next-generation sequencing (NGS) liquid biopsy has emerged as an innovative noninvasive technique for the identification of key mutations that are responsible for tumor growth allowing to optimize diagnosis, monitoring, and therapeutic choice.[7-9] Therefore, cell-free DNA (cfDNA) analysis has the possibility to overcome the space-time profile constraint of physical biopsies and it opens a new scenario for vascular malformations where tissue biopsy represents an invasive, high-risk, sometime life-threatening, diagnostic procedure. The use of liquid biopsy would also improve the opportunity to monitor illness evolution at a molecular level.

In the present study, we performed a comprehensive analysis of five patients with AVMs to determine if noninvasive NGS liquid biopsy from the efferent vein at the lesion site could detect the key variant bypassing the need for a high-risk, life-threatening tissue biopsy. The blood from the efferent vein at the vascular malformation site was sampled during embolization procedures before the injection of embolizing materials or liquids without causing further discomfort to the patient. For this reason, we define this technique as noninvasive. The NGS-liquid biopsy at the venous malformation site detected pathogenic mutations in *KRAS* gene in each patient. This study was consistent with Institutional guidelines and approved by the ethical committees of Azienda Ospedaliera Senese, Siena.

METHODS

Patient enrollment and sample collection. Five patients affected by AVM were enrolled at the Medical Genetics Unit of the Azienda Ospedaliera Universitaria Senese, Siena, Italy, for a new diagnostic approach. Written informed consent for genetic analysis was obtained from all patients. Clinical information as well as genealogic trees and cancer family history were collected on a genetic consultation setting. For all patients, liquid biopsy withdrawal from the lesion efferent vein was performed by Vascular Surgery of Ospedale Maggiore di Crema. All the blood specimens were taken during embolization procedures before the injection of embolizing materials or liquids. All the patients underwent a complete hemodynamic and radiologic evaluation including computed tomography angiography or magnetic resonance angiography. According to the Yakes Classification, these shunts belong to category II or III.

Extraction of cfDNA from plasma. Blood samples (10 mL) were collected from each patient and placed into cfDNA BCT blood collection tube (Streck, Neb). The cfDNA was extracted from 4 ml of plasma using MagMAX cell-free Total Nucleic Acid Isolation Kit (ThermoFisher Scientific, Waltham, Mass), according to the manufacturer's instructions. The quality and quantity of cfDNA were verified respectively using the Agilent High Sensitivity DNA Kit (Agilent Technologies, Palo Alto, Calif) on Agilent2100 Bioanalyzer (Agilent Technologies) and Qubit dsDNA HS Assay Kits on Qubit 2.0 fluorometer (Invitrogen, Carlsbad, Calif).

NGS sequencing on cfDNA. The cfDNA sequencing was performed using Oncomine Pan-Cancer Cell-Free Assay (ThermoFisher Scientific) on Life Technologies Ion Proton sequencer (Life Technologies, Carlsbad, Calif). This technology identifies various types of alterations, including single nucleotide variants, insertions/deletions, gene fusions and copy number variations in cancer-related genes (clinical actionable mutations) with a reportable range up to 0.05%. Sequencing analysis was performed using Ion Reporter Server System (Thermo Fisher Scientific).

ARTICLE HIGHLIGHTS

- **Type of Research:** multicenter, prospective study
- **Key Findings:** Cell-free DNA next-generation sequencing liquid biopsy is able to identify somatic KRAS mutations in 100% of investigated cases without the need of tissue biopsy. The mutational load is higher in the plasma sample collected in the efferent vein from vascular malformation than in peripheral vessel, confirming the causative role of the identified mutation.
- **Take Home Message:** We propose this noninvasive technique as the method of choice for arteriovenous malformation investigation and identification of tailored therapy.

RESULTS

Patient 1 is a 56-year-old man with a congenital port wine stain angioma on the lower right leg. He also suffers from varicose veins since the age of 18. At the age of 54, after meniscal injury, magnetic resonance imaging of the right knee showed an AVM with the presence of flow voids and enlargement of the arterial and venous vessels in the medial and lateral compartment, and bone involvement at femoral and tibial level; the morphology of the shunt is compatible with type III B according to the classification of Wayne Yakes

Patient 2 is a 40-year-old woman with a congenital port wine stain angioma on the external part of the lower right leg, associated with hypertrophy. Angiography and computed tomography angiography showed a complex angiodysplasia of the right limb, which presented with multiple arteriovenous fistulas, high-flow fistulas involving the tibial bone malformation, and abnormal communication between the common iliac

artery and vein. Over the time, the patient underwent multiple embolizations and resection of arteriovenous fistulas. Because of limb length discrepancy, the patient underwent the elongation of the contralateral limb with the Ilizarov technique. Previous molecular analysis with a targeted panel did not identify any RASA1 pathogenic mutation, excluding Parkes-Weber syndrome.

Patient 3 is a 29-year-old man with congenital angiodysplasia of the lower left limb, extending to the groin-abdominal region. Several endovascular and surgical interventions have been performed since childhood. He underwent a below-the-knee amputation at the age of 14 because of life-threatening bleeding and experienced a recurrence of AV shunts on the stump 10 years later. The patient reported episodes of nose bleeding, also present in other family members, but he did not satisfy Curacao criteria for a clinical diagnosis of hereditary hemorrhagic telangiectasia.

Patient 4 is a 45-year-old woman with congenital red vascular malformation in the upper right limb associated with limb hypermetry. The patient underwent several devascularization procedures, both surgical and endovascular, and resections over time.

Patient 5 is a 40-year-old woman who was referred for red-purple spots on the left lower limb, with hypertrophy and dysmetry. The first clinical manifestation dates back to the age of 11 years, with deep venous thrombosis in the left lower limb. The patient underwent multiple endovascular procedures, and surgical removal of an aneurysm at the level of the femoral artery. The sampling for the cfDNA analysis was taken from the extremity AVM. Magnetic resonance imaging identified an additional hepatic arteriovenous fistula. Clinical features of all patients are shown in the Fig.

In patients 1, 3, and 5, NGS-liquid biopsy analysis detected the same pathogenic mutation in *KRAS* gene c.35G>A; p.(Gly12Asp) (Table). In patients 2 and 4, NGS liquid biopsy analysis identified the mutation in *KRAS* gene c.35G>T; p.(Gly12Val). The variant allele frequency (VAF) ranged from 0,19% to 4,10%. In patient 1, who had the lowest VAF, a second blood draw from the efferent vein of AVMs of the knee was performed. The percentage of VAF in this experiment increased of one order of magnitude from 0.19% to 1.63%. Clinical features and molecular findings are shown in the Fig and the Table.

DISCUSSION

AVMs are a nontumor subset of vascular anomalies owing to a dysmorphogenesis in the developmental process.

In view of the increasing role of endovascular treatments, the frequent inaccessibility of vascular tissues, the invasiveness of solid biopsy, and the relative high incidence of nondiagnostic biopsies, we evaluated the efficacy of detecting cfDNA fragments that are released into the bloodstream from the affected tissue cells. Different cells, including normal healthy cells and hematopoietic cells, contribute to the cfDNA in the blood. However, in efferent venous blood, major cfDNA is released by cells; thus, this technique is highly sensitive for circulating cfDNA, allowing the identification of pathogenic mutations in *KRAS* genes, even with a very low VAF percentage in all patients.

In patient 1, liquid biopsy from the efferent vein detected an enrichment for the causative *KRAS* mutation, allowing a search for a causative role in the angiodysplastic process. Taken together, our data strengthen the idea that *KRAS* somatic mosaicism for gain-of-function mutations is the key genetic driver involved in the development of AVMs. Furthermore, our data suggest that our novel approach, based on the combination of NGS and liquid biopsy from the efferent vein at the vascular malformation site, allows detecting even low-grade somatic mosaicism responsible of the vascular phenotype, thus bypassing the need for a high-risk tissue biopsies.

Interestingly, the identified *KRAS* mutations (p.Gly12Asp and p.Gly12Val) are cancer hotspot mutations, which increase MAPK-ERK pathway activation, thus inducing endothelial cell proliferation[3] and enhancing their migratory behavior.[10-15] Noteworthy, although individuals who harbor *RAS* mutations at a germline level present with an increased risk of tumors such a juvenile myelomonocytic leukemia, acute leukemia, neuroblastoma, and rhabdomyosarcoma,[16] no increased risk for cancer development has so far been clearly shown for patients with AVMs who harbor somatic *KRAS* mutations. According to recent lines of evidence, drugs that specifically target a cancer driver gene represent innovative repurposing-based treatments readily available for use in different settings for hereditary conditions or somatic mosaic syndromes that carry the same driver genomic aberration.[14,17] Thus, in the new era of personalized medicine, agents that inhibit the MAP-ERK pathway commonly used in phase II clinical trials for the treatment of several solid tumors[18] could be likely considered as a therapy for sporadic brain AVMs caused by *KRAS* mutations. In conclusion, the diagnostic use of liquid biopsy for nononcologic diseases will forward the development of personalized therapeutic approach for AVMs and will open the door to new therapeutic strategies potentially able to block or slow down disease progression.

We thank AVMs patients and ILA association (Italian association of childhood angiodysplasias and hemangiomas). The "Cell lines and DNA bank of Rett Syndrome, X-linked mental retardation and other genetic diseases", member of the Telethon Network of Genetic Biobanks (project no. GTB12001 and GFB18001), funded by Telethon Italy, and of the EuroBioBank network provided us with specimens. We thank SienaGenTest srl, a Spin-off of the University of Siena (www.sienagentest.dbm.unisi.it) for assessment of data analysis.

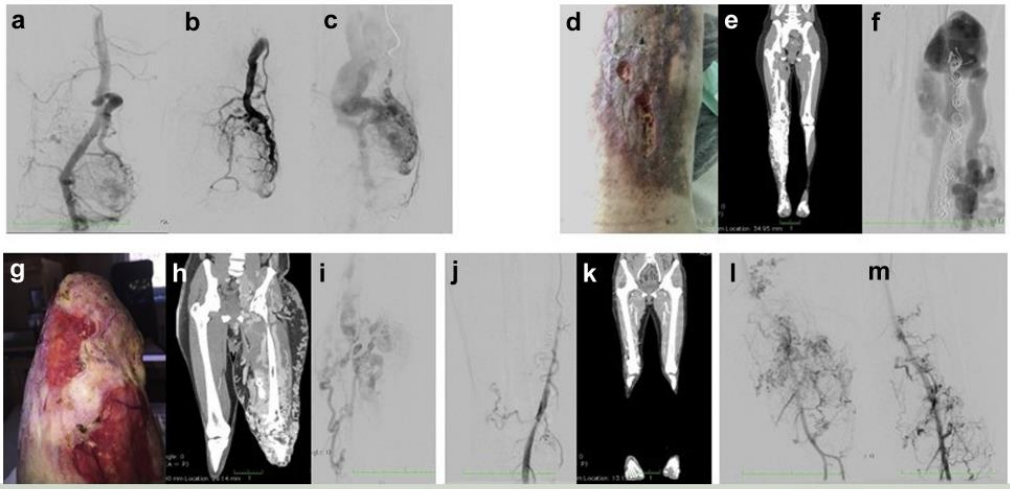

Fig. Clinical features of the patients. **A-C,** Patient 1: intra-articular arteriovenous shunt and outflow vein where the blood specimen was taken. **D-F,** Patient 2: right lower limb arteriovenous malformation (AVM) with leg ulceration **(D)**. Computed tomography (CT) scan **(E)** and angiography **(F)** of diffuse arteriovenous shunt at the tibial artery level. **G-I,** Patient 3: left lower stump AVM with leg ulceration **(G)**. CT scan **(H)** and angiography **(I)** with huge diffuse arteriovenous shunting. **J, K,** Patient 4: angiography of the right lower limb **(J)** and CT reconstruction of arteriovenous shunt at the knee level **(K)**. **L, M,** Patient 5: angiography of diffuse arteriovenous shunt.

Table. Patient clinical features and molecular findings

Patient	Code number	Gender	Age, years	Phenotype	Peripheral NGS liquid biopsy	Efferent vein NGS liquid biopsy
1	2023/19	Male	56	AVM dx leg	*KRAS* (p.(G12D)) 0.19%	*KRAS* (p.(G12D)) 1.63%
2	4417/19	Female	40	AVM dx leg	na	*KRAS* (p.(G12V)) 4.11%
3	4477/19	Male	29	AVM sx leg	na	*KRAS* (p.(G12D)) 1.18%
4	4820/19	Female	45	AVM dx leg	na	*KRAS* (p.(G12V)) 4.19%
5	3859/19	Female	40	AVM sx leg	na	*KRAS* (p.(G12D)) 1.18%

AVM, Arteriovenous malformation; *dx*, dextrum; *na*, not applicable; *NGS*, next-generation sequencing; *sx*, sinistrum.

AUTHOR CONTRIBUTIONS

Conception and design: AR, MV
Analysis and interpretation: MP, LD, EF, AS, AP, AR, MV
Data collection: MP, AC, AT, LD, GD, MB, EF, AG, CF, AP, AR, MV
Writing the article: MP, AC, AT, LD, GD, MB, EF, AG, CF, AS, AP, AR, MV
Critical revision of the article: EF, AP, AR, MV
Final approval of the article: MP, AC, AT, LD, GD, MB, EF, AG, CF, AS, AP, AR, MV
Statistical analysis: Not applicable
Obtained funding: Not applicable
Overall responsibility: AR

REFERENCES

1. Oka M, Kushamae M, Aoki T, Yamaguchi T, Kitazato K, Abekura Y, et al. KRAS G12D or G12V mutation in human brain arteriovenous malformations. World Neurosurg 2019;126:e1365-73.
2. Nikolaev SI, Vetiska S, Bonilla X, Boudreau E, Jauhiainen S, Jahromi BR, et al. Somatic activating KRAS mutations in arteriovenous malformations of the brain. N Engl J Med 2018;378:250-61.
3. Nikolaev SI, Vetiska S, Bonilla X, Boudreau E, Jauhiainen S, Rezai Jahromi B, et al. Somatic activating KRAS mutations in arteriovenous malformations of the brain. N Engl J Med 2018;378:250-61.
4. Cheng F, Nussinov R. KRAS activating signaling triggers arteriovenous malformations. Trends Biochem Sci 2018;43:481-3.
5. Priemer DS, Vortmeyer AO, Zhang S, Chang HY, Curless KL, Cheng L. Activating KRAS mutations in arteriovenous malformations of the brain: frequency and clinicopathologic correlation. Hum Pathol 2019;89:33-9.
6. Starke RM, McCarthy D, Komotar RJ, Connolly ES. Somatic KRAS mutation found in sporadic arteriovenous malformations. Neurosurgery 2018;83:e14-5.

7. Palmieri M, Baldassarri M, Fava F, Fabbiani A, Gelli E, Tita R, et al. Two point-NGS analysis of cancer genes in cell free-DNA of metastatic cancer patients. Cancer Med 2020;9:2052-61.
8. Crowley E, Di Nicolantonio F, Loupakis F, Bardelli A. Liquid biopsy: monitoring cancer-genetics in the blood. Nat Rev Clin Oncol 2013;10:472-84.
9. Corcoran RB, Chabner BA. Application of cell-free DNA analysis to cancer treatment. N Engl J Med 2018;379:1754-65.
10. McDonald J, Bayrak-Toydemir P, Pyeritz RE. Hereditary hemorrhagic telangiectasia: an overview of diagnosis, management, and pathogenesis. Genet Med 2011;13:607-16.
11. Gallione CJ, Repetto GM, Legius E, Rustgi AK, Schelley SL, Tejpar S, et al. A combined syndrome of juvenile polyposis and hereditary haemorrhagic telangiectasia associated with mutations in MADH4 (SMAD4). Lancet 2004;363:852-9.
12. Bayrak-Toydemir P, McDonald J, Markewitz B, Lewin S, Miller F, Chou LS, et al. Genotype—phenotype correlation in hereditary hemorrhagic telangiectasia: mutations and manifestations. Am J Med Genet A 2006;140:463-70.
13. Revencu N, Boon LM, Mulliken JB, Enjolras O, Cordisco MR, Burrows PE, et al. Parkes Weber syndrome, vein of Galen aneurysmal malformation, and other fast-flow vascular anomalies are caused by RASA1 mutations. Hum Mutat 2008;29:959-65.
14. Luks VL, Kamitaki N, Vivero MP, Uller W, Rab R, Bovée JVMG, et al. Lymphatic and other vascular malformative/overgrowth disorders are caused by somatic mutations in PIK3CA. J Pediatr 2015;166:1048-54.e1-5.
15. Do Prado LB, Han C, Paul Oh S, Su H. Recent advances in basic research for brain arteriovenous malformation. Int J Mol Sci 2019;20:5324.
16. Kratz CP, Franke L, Peters H, Kohlschmidt N, Kazmierczak B, Finckh U, et al. Cancer spectrum and frequency among children with Noonan, Costello, and cardio-facio-cutaneous syndromes. Br J Cancer 2015;112:1392-7.
17. Burotto M, Chiou VL, Lee JM, Kohn EC. The MAPK pathway across different malignancies: a new perspective. Cancer 2014;120:3446-56.
18. Braicu C, Buse M, Busuioc C, Drula R, Gulei D, Raduly R, et al. A comprehensive review on MAPK: a promising therapeutic target in cancer. Cancers (Basel) 2019;11:1618.

Submitted Mar 10, 2020; accepted Aug 4, 2020.

4 Discussion and Conclusion

4.1 ***Discussion***

Liquid biopsy represents a new approach for the development of non-invasive techniques targeted for personal and precision medicine [16]. In particular, cfDNA represents a valid biomarker capable to figure out the tumor heterogeneity and to monitor the clones evolutions during the progression of the disease [24].

The therapies based on molecular profiles of the primary tumor are not always efficacy because they are not representative of the evolving disease [45].

The first results that I obtained during my studies, were correlated to the clonal evolution over time in a 44-year-old female metastatic breast cancer patient. No other treatment options were available for her given the disease progression. Thanks to the two points liquid biopsy which we performed 5 months apart, we were able to capture the driver gene responsible for the disease progression. The multiple points cfDNA analysis reflects clonal evolution allowing to track the evolving molecular landscapes of growing cancer cells [46].

According to the literature evidence [47], my results obtained on a cohort of cancer patients with different tumor types shows a significant correlation between the amount of cfDNA and the disease outcome; indeed higher level of cfDNA correlates with a poor prognosis.

Regarding the allele frequency of mutated cfDNA, point mutations in *TP53*, *PIK3CA*, and *KRAS* and CNV (copy number variation) in *FGFR3* are the most commonly observed in our cohort confirming the literature evidence [48], [49]. However, we do not correlate the affected tumor organ and the mutation type.

Again, our results show how at the metastatic stage we can observe a very simplified clonal picture characterized by one or a few "snipers" clones compared to the mutational burden of the primary tumor.

Moreover, we observed that mutations in *TP53* gene are the most frequent among all mutated genes and all tumor types. Generally, mutated *TP53* was found together with another mutated gene. Furthermore, when the *TP53* gene was the only one mutated, it disappears at the second liquid biopsy. This evidence suggests that *TP53* may acts as a co-driver gene, increasing cell growth and decreasing apoptosis, and leading to tumor progression when another cancer driver gene mutates.

Moreover, some germline mutations were identified in the patient cohort and consequently confirmed on blood specimens with Sanger sequencing. However, these germline mutations have a confined significance, as although they can be considered at the early stage of the disease, they should be integrated with the analysis of growing mutated clones during disease progression. Germline mutations could be useful for therapies in the first tumor stage, but not at the metastatic stage when the somatic clones have taken over.

Among the somatic alterations, were found actionable mutations. In particular, gain-of-function *PIK3CA* mutations hyperactive the PI3K/AKT pathway, representing a target for the inhibitors of PIK3CA or kay component of the pathway, like Alpelisib or Ipatasertib respectively. Alpelisib inhibits the catalytic subunit of PI3K and it was approved by FDA the last year and it is studied in several clinical trials (https://clinicaltrials.gov/ct2/results?cond=&term=ipatasertib&cntry=&state=&city=&dist=).

Somatic mutations in *PIK3CA* are reported also in vascular malformations, and in a particular way are correlated with the overgrowth syndromes, (PROS: PIK3CA-related overgrowth syndromes), including the Klippel–Trenaunay syndrome [50].

Considering the invasiveness and the not always feasibility of tissue biopsy, our data obtained from the liquid biopsy reveals pathogenic variants in *PIK3CA* in Klippel-Trenaunay syndrome affected patients. The same mutations were found in the tissue analysis with a higher molecular frequency.

Among the slow-flow vascular malformations, I focused not only on the Klippel-Trenaunay syndrome but also on the lymphatic malformations. Our data show that patients with lymphatic malformations share variants of the *MET* gene. Comparing the allele frequency of mutated *MET* coming from the efferent vein of the lesion with that coming from the peripheral venous sample it is enriched in fragments.

Furthermore, the identification of somatic variants with low allelic frequency, impossible to see with a traditional tissue biopsy, are a valid aid in the identification of the phenotype and can explain the phenotypic variability.

Nevertheless, also the artero-venous (AVMs) fast-flow vascular anomalies patients were analyzed with the liquid biopsy. According to previous results obtained from Klippel-Trenaunay and lymphovenous malformations affected patients, also in AVMs patients the major quantity of cfDNA coming from the efferent venous blood. The pathogenic mutations found were in the *KRAS* gene, even with a very low variant allele frequency percentage. Our data reinforce the idea that mosaic gain-of-function mutations in *KRAS* are involved in the development of artero-venous malformations.

To date, 160 metastatic cancer patients have been enrolled for liquid biopsy, however the statistical significance does not change. The data are being published in a new scientific report.

4.2 ***Conclusion***

In conclusion, regarding the liquid biopsy studies conducted on cancer patients, during my Ph.D. course, the collected data indicate that patients should be grouped based on the mutated gene rather than tumor histology to provide a precision therapy targeting the evolving molecular profile. The two-point liquid biopsy is an effective tool able to follow the molecular evolution over time identifying the sniper gene responsible for the disease progression.

Moreover, the diagnostic use of liquid biopsy for non-oncologic patients could be a valid approach also for vascular malformations patients; indeed the sensitivity of the technique allowed us to identify low-grade somatic mosaic mutations useful to clarify the diagnosis that is not always easy to formulate.

Bibliography

[1] S. K. Low and Y. Nakamura, "The road map of cancer precision medicine with the innovation of advanced cancer detection technology and personalized immunotherapy," *Jpn. J. Clin. Oncol.*, vol. 49, no. 7, pp. 596–603, Jul. 2019, doi: 10.1093/jjco/hyz073.

[2] G. Méhes, "Liquid biopsy for predictive mutational profiling of solid cancer: The pathologist's perspective," *J. Biotechnol.*, vol. 297, pp. 66–70, May 2019, doi: 10.1016/j.jbiotec.2019.04.002.

[3] G. Rossi and M. Ignatiadis, "Promises and pitfalls of using liquid biopsy for precision medicine," *Cancer Research*, vol. 79, no. 11. American Association for Cancer Research Inc., pp. 2798–2804, 01-Jun-2019, doi: 10.1158/0008-5472.CAN-18-3402.

[4] G. Poulet, J. Massias, and V. Taly, "Liquid Biopsy: General Concepts," *Acta Cytologica*, vol. 63, no. 6. S. Karger AG, pp. 449–455, 01-Oct-2019, doi: 10.1159/000499337.

[5] E. Crowley, F. Di Nicolantonio, F. Loupakis, and A. Bardelli, "Liquid biopsy: Monitoring cancer-genetics in the blood," *Nature Reviews Clinical Oncology*, vol. 10, no. 8. Nat Rev Clin Oncol, pp. 472–484, Aug-2013, doi: 10.1038/nrclinonc.2013.110.

[6] R. B. Corcoran and B. A. Chabner, "Application of cell-free DNA analysis to cancer treatment," *New England Journal of Medicine*, vol. 379, no. 18. Massachussetts Medical Society, pp. 1754–1765, 01-Nov-2018, doi: 10.1056/NEJMra1706174.

[7] G. Buono *et al.*, "Circulating tumor DNA analysis in breast cancer: Is it ready for prime-time?," *Cancer Treatment Reviews*, vol. 73. W.B. Saunders Ltd, pp. 73–83, 01-Feb-2019, doi: 10.1016/j.ctrv.2019.01.004.

[8] P. and M. P. Mandel, "Les acides nucléiques du plasma sanguin chez l'Homme. Comptes Rendus des Seances de la Societe de Biologie et de ses Filiales, 142, 241-243. - References - Scientific Research Publishing," 1948. [Online]. Available: https://www.scirp.org/(S(i43dyn45teexjx455qlt3d2q))/reference/ReferencesPapers.aspx?ReferenceID=2005936. [Accessed: 17-Sep-2020].

[9] S. A. Leon, G. E. Ehrlich, B. Shapiro, and V. A. Labbate, "Free DNA in the serum of rheumatoid arthritis patients.," *J. Rheumatol.*, vol. 4, no. 2, pp. 139–143, 1977.

[10] M. Stroun, P. Anker, P. Maurice, J. Lyautey, C. Lederrey, and M. Beljanski, "Neoplastic characteristics of the DNA found in the plasma of cancer patients," *Oncology*, vol. 46, no. 5, pp. 318–322, 1989, doi: 10.1159/000226740.

[11] G. Sorenson, D. M. Pribish, F. Valone, V. Memoli, D. Bzik, and S. Yao, "Soluble normal and mutated DNA sequences from single-copy genes in human blood.," *undefined*,

1994.

[12] Y. M. Dennis Lo *et al.*, “Presence of fetal DNA in maternal plasma and serum,” *Lancet*, vol. 350, no. 9076, pp. 485–487, Aug. 1997, doi: 10.1016/S0140-6736(97)02174-0.

[13] A. Kustanovich, R. Schwartz, T. Peretz, and A. Grinshpun, “Life and death of circulating cell-free DNA,” *Cancer Biology and Therapy*, vol. 20, no. 8. Taylor and Francis Inc., pp. 1057–1067, 03-Aug-2019, doi: 10.1080/15384047.2019.1598759.

[14] I. G. Domínguez-Vigil, A. K. Moreno-Martínez, J. Y. Wang, M. H. A. Roehrl, and H. A. Barrera-Saldaña, “The dawn of the liquid biopsy in the fight against cancer,” *Oncotarget*, vol. 9, no. 2. Impact Journals LLC, pp. 2912–2922, 2018, doi: 10.18632/oncotarget.23131.

[15] T. M. Morgan, “Liquid biopsy: Where did it come from, what is it, and where is it going?,” *Investigative and Clinical Urology*, vol. 60, no. 3. Korean Urological Association, pp. 139–141, 01-May-2019, doi: 10.4111/icu.2019.60.3.139.

[16] A. J. Bronkhorst, V. Ungerer, and S. Holdenrieder, “The emerging role of cell-free DNA as a molecular marker for cancer management,” *Biomolecular Detection and Quantification*, vol. 17. Elsevier GmbH, 01-Mar-2019, doi: 10.1016/j.bdq.2019.100087.

[17] A. Bardelli and K. Pantel, “Liquid Biopsies, What We Do Not Know (Yet),” *Cancer Cell*, vol. 31, no. 2. Cell Press, pp. 172–179, 13-Feb-2017, doi: 10.1016/j.ccell.2017.01.002.

[18] A. J. Bronkhorst, J. F. Wentzel, J. Aucamp, E. van Dyk, L. du Plessis, and P. J. Pretorius, “Characterization of the cell-free DNA released by cultured cancer cells,” *Biochim. Biophys. Acta - Mol. Cell Res.*, vol. 1863, no. 1, pp. 157–165, Jan. 2016, doi: 10.1016/j.bbamcr.2015.10.022.

[19] S. Alimirzaie, M. Bagherzadeh, and M. R. Akbari, “Liquid biopsy in breast cancer: A comprehensive review,” *Clinical Genetics*, vol. 95, no. 6. Blackwell Publishing Ltd, pp. 643–660, 01-Jun-2019, doi: 10.1111/cge.13514.

[20] J. C. M. Wan *et al.*, “Liquid biopsies come of age: Towards implementation of circulating tumour DNA,” *Nature Reviews Cancer*, vol. 17, no. 4. Nature Publishing Group, pp. 223–238, 01-Apr-2017, doi: 10.1038/nrc.2017.7.

[21] A. R. Thierry, S. El Messaoudi, P. B. Gahan, P. Anker, and M. Stroun, “Origins, structures, and functions of circulating DNA in oncology,” *Cancer Metastasis Rev.*, vol. 35, no. 3, pp. 347–376, Sep. 2016, doi: 10.1007/s10555-016-9629-x.

[22] C. Bettegowda *et al.*, “Detection of circulating tumor DNA in early- and late-stage human malignancies,” *Sci. Transl. Med.*, vol. 6, no. 224, Feb. 2014, doi:

10.1126/scitranslmed.3007094.

[23] S. Khier and L. Lohan, “Kinetics of circulating cell-free DNA for biomedical applications: Critical appraisal of the literature,” *Futur. Sci. OA*, vol. 4, no. 4, 2018, doi: 10.4155/fsoa-2017-0140.

[24] L. B. Ahlborn *et al.*, “Application of cell-free DNA for genomic tumor profiling: A feasibility study,” *Oncotarget*, vol. 10, no. 14, pp. 1388–1398, Feb. 2019, doi: 10.18632/oncotarget.26642.

[25] A. Ziegler, U. Zangemeister-Wittke, and R. A. Stahel, “Circulating DNA: A new diagnostic gold mine?,” *Cancer Treat. Rev.*, vol. 28, no. 5, pp. 255–271, 2002, doi: 10.1016/S0305-7372(02)00077-4.

[26] H. Husain *et al.*, “Monitoring daily dynamics of early tumor response to targeted therapy by detecting circulating tumor DNA in urine,” *Clin. Cancer Res.*, vol. 23, no. 16, pp. 4716–4723, Aug. 2017, doi: 10.1158/1078-0432.CCR-17-0454.

[27] M. Russo *et al.*, “Tumor heterogeneity and Lesion-Specific response to targeted therapy in colorectal cancer,” *Cancer Discov.*, vol. 6, no. 2, pp. 147–153, Feb. 2016, doi: 10.1158/2159-8290.CD-15-1283.

[28] C. M. Blakely *et al.*, “Evolution and clinical impact of co-occurring genetic alterations in advanced-stage EGFR-mutant lung cancers,” *Nat. Genet.*, vol. 49, no. 12, pp. 1693–1704, Dec. 2017, doi: 10.1038/ng.3990.

[29] D. Chu and B. H. Park, “Liquid biopsy: unlocking the potentials of cell-free DNA,” *Virchows Arch.*, vol. 471, no. 2, pp. 147–154, Aug. 2017, doi: 10.1007/s00428-017-2137-8.

[30] A. A. Chaudhuri *et al.*, “Early detection of molecular residual disease in localized lung cancer by circulating tumor DNA profiling,” *Cancer Discov.*, vol. 7, no. 12, pp. 1394–1403, Dec. 2017, doi: 10.1158/2159-8290.CD-17-0716.

[31] J. Tie *et al.*, “Circulating tumor DNA analysis detects minimal residual disease and predicts recurrence in patients with stage II colon cancer,” *Sci. Transl. Med.*, vol. 8, no. 346, Jul. 2016, doi: 10.1126/scitranslmed.aaf6219.

[32] J. Abraham, S. Singh, and S. Joshi, “Liquid biopsy - emergence of a new era in personalized cancer care,” *Appl. Cancer Res.*, vol. 38, no. 1, pp. 1–17, Dec. 2018, doi: 10.1186/s41241-018-0053-0.

[33] M. Yang *et al.*, “Incorporating blood-based liquid biopsy information into cancer staging: Time for a TNMB system?,” *Annals of Oncology*, vol. 29, no. 2. Oxford University Press, pp. 311–323, 01-Feb-2018, doi: 10.1093/annonc/mdx766.

[34] F. Rothé *et al.*, “Plasma circulating tumor DNA as an alternative to metastatic biopsies for mutational analysis in breast cancer,” *Ann. Oncol.*, vol. 25, no. 10, pp. 1959–1965, Oct. 2014, doi: 10.1093/annonc/mdu288.

[35] R. Lebofsky *et al.*, “Circulating tumor DNA as a non-invasive substitute to metastasis biopsy for tumor genotyping and personalized medicine in a prospective trial across all tumor types,” *Mol. Oncol.*, vol. 9, no. 4, pp. 783–790, Apr. 2015, doi: 10.1016/j.molonc.2014.12.003.

[36] I. McCafferty, “Management of Low-Flow Vascular Malformations: Clinical Presentation, Classification, Patient Selection, Imaging and Treatment,” *Cardiovasc. Intervent. Radiol.*, vol. 38, no. 5, pp. 1082–1104, Oct. 2015, doi: 10.1007/s00270-015-1085-4.

[37] R. Dasgupta and M. Patel, “Venous malformations,” *Semin. Pediatr. Surg.*, vol. 23, no. 4, pp. 198–202, Aug. 2014, doi: 10.1053/j.sempedsurg.2014.06.019.

[38] M. Sadick *et al.*, “Interdisciplinary Management of Head and Neck Vascular Anomalies: Clinical Presentation, Diagnostic Findings and Minimalinvasive Therapies,” *European Journal of Radiology Open*, vol. 4. Elsevier Ltd, pp. 63–68, 2017, doi: 10.1016/j.ejro.2017.05.001.

[39] H. Lee *et al.*, “Clinical Exome Sequencing for Genetic Identification of Rare Mendelian Disorders,” *JAMA*, vol. 312, no. 18, pp. 1880–1887, 2014, doi: 10.1001/jama.2014.14604.

[40] J. B. Mulliken and J. Glowacki, “Hemangiomas and vascular malformations in infants and children: A classification based on endothelial characteristics,” *Plast. Reconstr. Surg.*, vol. 69, no. 3, pp. 412–420, 1982, doi: 10.1097/00006534-198203000-00002.

[41] M. M. Cohen Jr., “Vascular update: Morphogenesis, tumors, malformations, and molecular dimensions,” *Am. J. Med. Genet. Part A*, vol. 140A, no. 19, pp. 2013–2038, Oct. 2006, doi: 10.1002/ajmg.a.31333.

[42] L. H. Lowe, T. C. Marchant, D. C. Rivard, and A. J. Scherbel, “Vascular Malformations: Classification and Terminology the Radiologist Needs to Know,” *Semin. Roentgenol.*, vol. 47, no. 2, pp. 106–117, Apr. 2012, doi: 10.1053/j.ro.2011.11.002.

[43] L. M. Buckmiller, G. T. Richter, and J. Y. Suen, “Diagnosis and management of hemangiomas and vascular malformations of the head and neck,” *Oral Diseases*, vol. 16, no. 5. Blackwell Munksgaard, pp. 405–418, 2010, doi: 10.1111/j.1601-0825.2010.01661.x.

[44] J. M. Rothberg *et al.*, “An integrated semiconductor device enabling non-optical genome

sequencing," *Nature*, vol. 475, no. 7356, pp. 348–352, Jul. 2011, doi: 10.1038/nature10242.

[45] O. Trédan *et al.*, "Molecular screening program to select molecular-based recommended therapies for metastatic cancer patients: Analysis from the ProfiLER trial," *Ann. Oncol.*, vol. 30, no. 5, pp. 757–765, 2019, doi: 10.1093/annonc/mdz080.

[46] M. Palmieri *et al.*, "PIK3CA-CDKN2A clonal evolution in metastatic breast cancer and multiple points cell-free DNA analysis," *Cancer Cell International*, vol. 19, no. 1. BioMed Central Ltd., p. 274, 28-Oct-2019, doi: 10.1186/s12935-019-0991-y.

[47] L. De Mattos-Arruda and C. Caldas, "Cell-free circulating tumour DNA as a liquid biopsy in breast cancer," *Molecular Oncology*, vol. 10, no. 3. Elsevier B.V., pp. 464–474, 01-Mar-2016, doi: 10.1016/j.molonc.2015.12.001.

[48] G. Rossi *et al.*, "Cell-free DNA and circulating tumor cells: Comprehensive liquid biopsy analysis in advanced breast cancer," *Clin. Cancer Res.*, vol. 24, no. 3, pp. 560–568, Feb. 2018, doi: 10.1158/1078-0432.CCR-17-2092.

[49] B. T. Li *et al.*, "Ultra-deep next-generation sequencing of plasma cell-free DNA in patients with advanced lung cancers: Results from the actionable genome consortium," *Ann. Oncol.*, vol. 30, no. 4, pp. 597–603, 2019, doi: 10.1093/annonc/mdz046.

[50] V. L. Luks *et al.*, "Lymphatic and other vascular malformative/overgrowth disorders are caused by somatic mutations in PIK3CA," *J. Pediatr.*, vol. 166, no. 4, pp. 1048-1054.e5, 2015, doi: 10.1016/j.jpeds.2014.12.069.